AN EXPERIMENTAL INVESTIGATION OF THE PHENOMENA PRODUCED BY THE HIGHLY TURBULENT FLOW OF WATER PAST A SERIES OF SHARP OBSTACLES.

THESIS BY

RICHARD GILMAN FOLSOM

IN PARTIAL FULFILLMENT OF THE REQUIREMENTS FOR THE DEGREE OF DOCTOR OF PHILOSOPHY

CALIFORNIA INSTITUTE OF TECHNOLOGY

PASADENA, CALIFORNIA

1932

CONTENTS PAGE

ACKNOWLEDGMENT

The writer desires to express his appreciation of the valuable assistance rendered by those interested in the success of the investigation:

First; to Dr. Th. von Karman, Prof. R.L.Daugherty, and Dr. R.T.Knapp, members of the faculty of the California Institute of Technology, for their inspiration and many helpful suggestions,

Second; to Mr. R.M.Watson for assistance in the construction, installation, and testing of the small turbulence tube, and

Third; to Mr. J.S.Goodwin for the use of his personal equipment and services in making the photographic studies. (The high quality of the flow pictures is largely due to his excellent workmanship.)

INTRODUCTION

A knowledge of the resistance to flow of a body placed in a stream of fluid is necessary for many problems in hydraulics, aeronautics, and ventilation. A large amount of experimental and theoretical effort has been expended investigating the drag characteristics of single bodies and small groups of similar bodies. Only a small amount of incomplete data is available regarding the performance of a long series of similar obstacles. This latter material was obtained for air flowing past supporting timber sets in mines. Since the dimensions of the mine shafts varied at different sections, the results of the experiments merely indicated the possibilities of obtaining different pressure losses depending on the size, shape, and spacing of the timber sets. Therefore, more data are needed regarding the drag characteristics of long series of obstacles.

OBJECT

The aim of this investigation has been to supply additional experimental data regarding turbulent flow and in particular, to study the phenomena produced by a relatively long series of similar bodies forming an obstruction to flow. The problem has been treated exclusively by experimental means, since, in the present stage of development in the hydrodynamic theory, it is practically impossible to theoretically compute with any degree of reliability the characteristics of the highly complex turbulent conditions existing within the experimental apparatus.

DESCRIPTION OF APPARATUS

TURBULENCE TUBE. The experimental equipment consisted of the turbulence tube and the measuring devices necessary to obtain the required readings. The turbulence tube was the name adopted to describe the working section of the apparatus. Two 1¼ inch brass tees, each containing a 6 inch length of 1¼ extra heavy brass pipe screwed into one opening and a plug screwed into the opposite opening, a 3/8 inch brass rod fastened to the upper plug and extending through a hole drilled in the lower plug, with a 36 inch length of 1.333 inch inside diameter brass tubing placed concentric with the rod between the 6 inch lengths of pipe constitute the parts of the turbulence tube (shown digrammatically in Fig. 1.). When tension is produced in the rod by means of an external spring, all components of the apparatus become fixed. The details of construction are as follows: four piezometer connections, placed 90 deg. apart, were drilled in each 6 inch length of pipe using a No.60 drill: the inside diameter of the brass pipe was made equivalent to the inner diameter of the intermediate section of brass tubing: special care was exerted during the machining operations in order to eliminate the possibility of burs remaining around the piezometer holes: the upper pipe length was flared at the inlet in an effort to reduce detrimental entrace conditions: in putting the apparatus together, paper gaskets were used, and necessary precautions taken to insure the inside edge of the gasket being just flush with the inner surfaces of the pipe sections and tube. The apparatus was designed for the easy removal of the intermediate section of brass tubing in

order to be able to substitute a glass tube for the purpose of making visual observations. The injection tube was provided as a means of placing dye or other indicating material in the flow stream. This injection tube was only used in the apparatus when it was required, otherwise the tube was eliminated as it provided an additional source of possible trouble in the entrance conditions. A packing gland was included at the downstream end in order to make the turbulence tube completely leak-proof.

CENTRAL ASSEMBLY. The bodies forming the obstructions to flow were termed disks and the pieces separating the disks were designated as spacers. The disks and spacers were all drilled to fit the 3/8 inch diameter rod. Thus they could be strung on the rod like beads on a string, forming many different designs. This inner group of spacers and disks on the rod was called the central assembly. Several different sizes of disks and spacers were used to produce different relations between the obstructions and the enclosing tube. All disks had a uniform thickness, as they were made from 16 gage brass, but there were five different diameters varying from 0.812 inches to 1.249 inches. Two sizes of spacers were included, $\frac{1}{2}$ inch and $\frac{3}{4}$ inch outside diameter. The length of the spacers was $\frac{1}{2}$ cm. except some special ones which contained set screws and were longer. These special spacers were used to place the central assembly at different positions with respect to the piezometer groups. The diagrams given in Fig. 2 illustrate the relative sizes of the disks, spacers, and the tube for some different combinations. A large number of distributions were of course

possible, but the work was limited to studying only a given disk and spacer in any single set-up. Thus, a given disk would be combined with either one spacer or the other, but not both, in the same assembly. In addition, the ratio of spacers to disks was constant throughout the assembly for any one set-up, except in a few special cases which are carefully designated in the data.

AUXILIARY APPARATUS. The auxiliary apparatus employed included a water meter to determine the rate of flow, a centrifugal pump to produce the required head, a surge tank to eliminate the pulsations produced by the meter and pump, and a pressure gage to ascertain the magnitude of the head drop for a given length. The water was circulated by the centrifugal pump, while the regular hydraulic laboratory storage tanks served as a reservoir. Fig. 3 presents a photograph and a diagramic sketch giving the general arrangement of the experimental equipment.

Each group of four piezometers was connected to a manifold leading to one leg of a U-tube manometer. This instrument was constructed of $\frac{1}{2}$ inch inside diameter glass tubing, and mercury was used as the indicating fluid, with water filling the connections. The differential readings gave the drop in pressure between the piezometer groups. The scale consisted of a flexible steel rule graduated in mm. sliding through one and connected to the other brass slider. Each slider acted as a holder for a glass mirror with a fine line scratched on the surface. By this method, the differential mercury height could be read to the nearest 1.0 mm. and estimated to the nearest 0.2 mm. since the fine scratch provided

a method of eliminating errors due to parallax. In the glass tube, any ordinary variation in diameter might have caused a change in the differential mercury height of about 0.1 mm. due to the difference in capillary effects, but this is less than the best reading and need not be considered. The maximum reading of the manometer is about 6 feet of mercury.

PRELIMINARY TESTS OF APPARATUS

WATER METER. The water meter was a wobble plate, positive displacement type of instrument, graduated to read in pounds. As it was a commercial meter, frequent calibrations were made throughout its use. Since the apparatus was found water tight when under operation, it was then possible to calibrate the meter by weighing the discharge from the turbulence tube. The capacity of the weighing equipment was 300 pounds which was determined to the nearest quarter pound. The time required to fill the weighing system was taken with a stop watch. Fig. 4 presents the results from nine series of calibrations with temperatures varying from 63 to 92 deg. fahr. Thus not only is the calibration constant over a period of time, but reasonable temperature changes show no appreciable effect upon the rating. (The variation in the density for the temperature limits encountered is only about 0.4 per cent).

MANOMETER. A rough test was employed to determine the difference in the pressure at any piezometer as compared with the group. In general, the differences were found to be less than the variations in pressure occurring during any one run. Some damping of the oscillations was accomplished by insert-

ing sections of restricted area in the manometer connections. Since the piezometer holes were so small, it was very important that no leaks occur if accurate results were to be obtained. All piezometer and manometer connections were regularly inspected for leaks, but none were discovered during the course of the experiments. When performing experiments, precautions were taken to remove all air from the pressure measuring system and at the conclusion of each test, the zero level of the manometer was checked. In summing up the features of the manometer, it was found to be a rapid, easily manipulated, and sufficiently accurate instrument.

SURGE TANK. The pressure oscillations observed in the testing of the piezometers were mainly due to variations in flow conditions in the turbulence tube. The surge tank was equipped with a gage glass and the water level in the glass was generally very steady. The water meter pulsations were practically eliminated by the surge tank. The variations of pressure in the turbulence tube might have been due to the entrance conditions or a possible pulsating characteristic of the flow about the obstructions. However, in general, the magnitude of the oscillations was not enough to seriously effect the readings.

TURBULENCE TUBE WITH GLASS SECTION. In the preliminary work, a glass tube of approximately the same dimensions as the brass tube was used in order to visually observe the flow phenomena, and to obtain approximate data regarding the behavior of the water in the turbulence tube. Accurate results could not be expected from this glass tube since measurements showed it was not circular and the mean diameter varied throughout the length. As the head varied directly with the square of the

velocity, it was necessary that all diameters be constant within small limits. The glass tube was satisfactory for visual observations and for pictures, but the results were of little absolute value. However, the test results with this tube were sufficiently accurate for comparative purposes. Fig. 5 presents the experimental results of all points obtained at various times during the preliminary work, for a given arrangement of the central assembly with 13/16 inch disks and four ½ inch spacers. Between the runs for this arrangement, other distributions were investigated. Thus, the material of Fig. 5 indicates the general reproducibility of experimental data. This figure also indicates the relations between the head and velocity, thus, the head varies directly as the square of the velocity, this being the general relationship found throughout the investigation.

In the first runs of the preliminary work considerable vibration occurred in the central assembly particularly at high velocities. Three disks were provided with spacing prongs (spider disk of Fig. 6), thus insuring the concentric placing of the central assembly with respect to the tube, and in addition eliminating the vibrations. This procedure was necessary as distorted results were produced when the vibrations became severe. Careful centering of the central assembly was also important from the viewpoint of flow resistance. In the case of smooth annular sections, it has been shown mathematically that when the core touches one side, the quantity of flow for a given head drop was approximately two and a half times greater than when the core was concentric. Although the calculation only applied to the viscous flow condi-

tions, there was no reason to believe that non-centering would not produce a similar effect in the turbulent region although probably less in magnitude. No experimental data was obtained to determine the results on nonconcentric placing of the central assembly.

During the investigations with the glass tube, small air bubbles were introduced at the low velocity conditions and their motions were carefully observed. Although grave doubts existed regarding the indications of the bubbles, due to the large difference in density with respect to water, a study of their actions gave some ideas regarding the possibilities of different types of flow. Fig. 7 gives several sketches of the observations made upon different arrangements of the central assembly. These were obtained by watching the flow from a certain angle, where the light was reflected by the bubbles causing the eye to see a streak which indicated the path of the air bubble. Closer observation showed that the bubbles did not travel in one place between the disks, although outside the disks they apparently followed an approximately axial path. In the sections between the disks, considerable oscillatory rotation was taking place around the spacer, (in addition to the motions indicated in the sketches). In some cases as many as six revolutions around the spacer were made before the bubble was drawn out of the section. The side strip shown in Fig. 6 was used in an effort to determine the approximate magnitude of the effects due to the rotation, the strip being nothing more than an obstacle to prevent flow around the spacer. A comparison of the test results, with and without the side strips, are given in Fig. 8 for the 13/16

inch, 15/16 inch, and 17/16 inch disks, and $\frac{1}{8}$ inch spacers. Although the effect of the side strip varied throughout the different arrangements, the variation was relatively small and, in the main, the effect of the rotation did not need to be considered.

ENTRANCE CONDITIONS. It was necessary to investigate completely two important effects before the true value of the experimental work could be ascertained. The first of these was the disturbance produced by the extremely poor entrance conditions into the apparatus. The water enters in a sharp 90 deg. turn and the first piezometer group was only about four pipe diameters downstream from the entrance. Such conditions were bound to have some effect upon the measured head drop, however it was possible to determine the approximate magnitude of this effect. This approximation was obtained by placing smooth concentric cores inside of the external tube and comparing the results of the friction factor with those found by the investigators of annular flow. Fig. 9 presents the results obtained with smooth cores in the turbulence tube. The log of the head drop and the log of the velocity were used as coordinates. The work of Lonsdale gave the head varying with the 1.72 power of the velocity, and Lea and Tadros obtained 1.73. The values obtained in the turbulence tube were higher, but still decidedly less than the square. Some difference was to be expected due to the influence of the entrance flow. Work in the turbulent flow range with sections other than circular has indicated that at a given Reynolds' number, using the hydraulic radius as the linear dimension, the friction factor is approximately constant for all sections.

Fig. 12 shows the results obtained by a group of investigators of annular flow and the approximation of the friction factor with regards to Reynolds' number is thus fairly well verified for this particular section. The results in the region of viscous flow have not been considered as this condition was not reached in any of the experimental work with the turbulence tube. Fig. 10 gives the material of Fig. 9 in terms of the friction factor and Reynolds' number in order to obtain a comparison with Fig. 12. The friction factor curve for circular sections refers to the one given by Professor Daugherty in his book "Hydraulics" for the friction factor of smooth round brass tubes. This curve is an average one for a great number of experiments, including those of Stanton and Pannell from which there is little variation. Fig. 11 was obtained by considering the diameter of the annular section equal to four times the hydraulic radius, and computing the distance from the entrance to the first piezometer group on this basis. The percentage variation was taken from the curves of Fig. 10. Fig. 11 demonstrates very clearly the effects of the entrance conditions due to taking pressure measurements too close to the point where the water enters the turbulence tube. Although the error is considerable, the smallest pressure measured with the disks and spacers was several times the value for a smooth core of the same diameter as the disk, and thus the variation of the friction factor due to the entrance conditions becomes relatively small and is neglected throughout this investigation.

POSITION OF CENTRAL ASSEMBLY. The general method of locating the central assembly for the preliminary testing of

the apparatus, involved placing the first disk at a given distance from the upstream piezometers. This condition for location produced a variable distance between the last disk and the downstream piezometers depending upon the ratio of spacers to disks in the particular arrangement. In another set of preliminary experiments with the brass tube, a check run on a given arrangement of the central assembly was made by removing the last disk. The results showed a head drop per foot of length essentially identical with the original run after certain approximate corrections had been included. Rather extensive experimental work was conducted applying these approximate corrections for the end conditions before the result began to indicate a possibility of error in the correction methods. In fact, the form of all curves had been determined throughout a wide range before any apparent variation developed which tended to raise the question of the veracity of the correction procedure.

If the preliminary method of correction was satisfactory, it implied that the downstream pressure conditions were similar to the corresponding phenomenon behind an orifice plate in a pipe or in the large section when sudden expansion takes place. An investigation of the downstream pressure conditions was made by shifting the central assembly for known distances with respect to the piezometers. The relations obtained in this work are given in Fig. 13. The pressure opposite the last disk was arbitrarily taken as zero; thus the pressures plotted show the variation between any position down stream and that at the last disk. This curve is for the 65/64 inch disks with six $\frac{1}{2}$ inch spacers. The shaded isolated points

represent conditions for the different arrangements of the same size disks and spacers. Fig. 13 was included in order to demonstrate the dependence of the downstream conditions upon the distribution in the central assembly. Each point represented in the figure has been obtained for a mean velocity of 12.3 feet per second. (All velocities given in this report refer to the mean velocity between the disk and the outside tube unless otherwise specified). Any other velocity would show the same relationship, since the head drop versus the square of the velocity curve was a straight line in all distributions tested for the downstream conditions. The straight line in the figure represents the change in velocity head between the narrow section at the disk and the larger downstream section. The other curves give the corresponding pressure relations for a sharp edged orifice in a pipe, and for an example of sudden expansion, with the same area ratio of minimum and maximum cross sections. All curves refer to a mean velocity of 12.5 ft. per sec. in the narrow section. It is readily observed that there was little connection between the phenomena. The orifice pressure curve was taken from similar curves by Hodgson and Johansen. The sudden enlargement data were obtained from Archer's curves for this type of flow. The material of Fig. 13 has indicated the only position for the downstream piezometer with respect to the last disk, free from the effects of the distribution in the central assembly, was either opposite the last disk or at a distance far enough downstream to eliminate the effects of the pressure oscillations produced by the assembly. Since the tube was very limited in length the procedure of placing the last disk opposite the

downstream piezometer was adopted as standard.

HEAD LOST IN END SECTIONS. The method employed still left the correction to be applied for the head drop between the upstream piezometers and the first disk. Since the approximate pressure drop per unit of length for the spacers was known, it was then possible to calculate the pressure difference between the piezometers and the center of the first disk by applying Bernoulli's theorem and the Equation of Continuity. Values of the head drop per unit of length for corresponding central assembly arrangements, but varying in overall lengths by one disk and its related spacers, showed differences of only $\frac{1}{2}$ per cent which was well within the limits of accuracy of the experimental work. This correlation of values for the head drop was obtained with 65/64 inch disks using $\frac{1}{2}$ inch spacers. Three different arrangements of the central assembly with this disk and spacer size were used. As this correlation was obtained by always placing the last disk opposite the downstream piezometers, the procedure was then justified for use as the standard setting.

EXPERIMENTAL RESULTS

NUMERICAL AND GRAPHICAL REPRESENTATION. Table I presents the numerical values of the original readings for experimental runs with the last disk placed opposite the lower piezometer group. The run number is a designation used to indicate the particular distribution and how many times that distribution had been investigated. The disk and spacer dimensions refer to the outside diameter. The number of spacers provides a measure of the distance between successive disks. The velocity has been computed directly from the turbulence tube dia-

meter, disk diameter, and water meter reading relations. The square of the velocity has been corrected to account for the calibration values of the water meter. The total head drop has been corrected for temperature changes only, and does not include the variations introduced by the difference in effective length of the central assembly and the distance between the piezometer groups. The effective length refers to the distance between the center-lines of the first and last disks of the central assembly. The material covered by this table has been included in graphical form in Figs. 14 to 22 inclusive. The coordinates are the total head and the corrected square of the velocity. It is of particular interest to note that almost all curves are straight lines, thus the head was directly proportional to the square of the velocity.

Figs. 23 and 24 give the combined results plotted on different coordinate systems. Fig. 25 - [a] presents a table indicating the connection of the symbols used in Figs. 23, 24, and 27, with the central assembly arrangement. These later figures all refer to a constant velocity of 12.5 ft. per sec. The discontinuities in the curves represent the range where the flow changes its general characteristics. Although the disks were separated by a considerable distance in some arrangements as shown in Fig. 24, they always affected each other. Hence, there are no data available regarding the behavior of single disks.

DIMENSIONAL ANALYSIS. Although Figs. 23 and 24 present the experimental results very effectively, they provide little correlation for different sizes of disks and spacers. In the effort to develop a logical coordinate system which would include all distributions investigated, the method of dimen-

sional analysis was used. Following the method outlined by Buckingham, the equation

$$h' = \frac{v^2}{2gD} f\left[\frac{\mu}{\rho v D}, \frac{gD}{v^2}, r_1, r_2, r_3 \text{---}\right] \quad \cdots \quad [1]$$

was obtained by considering the independent quantities determining the flow conditions as

h' = head drop (feet of water per foot of length),

μ = absolute viscosity,

ρ = density,

v = velocity,

g = acceleration of gravity, and

D = a linear dimension.

The values of r represent ratios between quanities of the same dimensions. Since the experimental results of the investigations of the turbulence tube demonstrated that within certain limits the head drop was directly proportional to the square of the velocity, the effect of the first two terms of the function can be neglected without introducing any appreciable error. Then Eq. [1] is written

$$h' = \frac{v^2}{gD} f\left[r_1, r_2, r_3, \text{----}\right] \quad \cdots \quad [2]$$

For the purposes of a preliminary investigation, the ratios r of Eq. [2] were assumed to involve only linear dimensions. If these ratios were independent of the outside tube diameter, it would have been possible to apply the Laws of Similarity. Upon attempting to apply these principles, it quickly became apparent that the phenomena were not independent of the tube diameter, and thus it was impossible to have all

of the ρ terms identical at the same time with a single size of outside tube. Therefore, the only possible method to check completely the validity of the assumptions regarding the ratios of Eq. [2] , was to investigate a geometrically similar turbulence tube.

SMALL TURBULENCE TUBE. A second tube was constructed similar to the original, the ratio of inner diameter being 0.678. By using 0.688 inch diameter disks and $\frac{1}{2}$ inch spacers, it was possible to approximate closely conditions of similarity with the large tube, 65/64 inch disks, and $\frac{3}{4}$ inch spacers. The original data from the small apparatus are given in Fig. 25 - [b] . Considering the relations required by Eq. [2] and the Laws of Similitude, the values for the small tube approximately check those for the original. This correlation is considered in greater detail with the discussion of Fig. 27.

DEVELOPMENT OF DIMENSIONLESS COORDINATES. Using all information from the tests, a further investigation of Eq. [2] was made. The impossibility of deriving the ρ terms from a two dimensional flow analysis quickly became apparent; therefore it was necessary to include ratios involving the diameters. Fig. 27 was obtained by considering the 17/16 inch disk and $\frac{1}{2}$ inch spacer runs as standard and correcting the maximum point of all other sets to coincide with the standard maximum by means of arbitrary coefficients. In most cases when the maximum values coincided, the rest of the relations were very similar when considered by the coordinates of Fig. 27. An analysis of the arbitrary coefficients showed B and C to be constant for a given size of spacer and tube, while R_M depended upon the $\frac{d}{R}$ ratio. Fig. 26 gives the

relations of R_M and $\frac{d}{R}$ for two values of $\frac{D_s}{D_t}$; accordingly, the value of C is connected with the slope of the line on the R_M and $\frac{d}{R}$ plane. Eq. [2] is rewritten in the form

$$\frac{h'}{C R_M} = \frac{v^2}{2g D_t} f\left[B \frac{l}{D_D}\right] \quad \ldots\ldots\ldots [3]$$

to express the curve of Fig. 27, which has been plotted for a constant value of $\frac{v^2}{2g D_t}$, as determined by the diameter of the original turbulence tube and a velocity of 12.5 feet per second. If the conditions of Fig. 26 are substituted in Eq. [3] the expression becomes

$$\frac{h'}{1.78 C\left[\frac{d}{R} - 0.113\right]} = \frac{v^2}{2g D_t} f\left[B \frac{l}{D_D}\right], \quad \ldots\ldots [4]$$

where

$$C = f_1\left[\frac{D_s}{D_t}\right]$$
$$B = f_2\left[\frac{D_s}{D_t}\right].$$

Very little can be said regarding the functions f_1 and f_2 since only two points have been determined. At the present writing, experiments are being conducted to obtain a third point and the resulting approximate form of the functions.

LIMITS OF DIMENSIONLESS TREATMENT. The experiments have indicated the limitations of Eq. [4] . The validity of the curve of Fig. 27 has been experimentally demonstrated for the limits of $0.3 < \frac{d}{R} < 0.7$, while the minimum value of $\frac{l}{D_D}$ for the head drop being directly proportional to the square of the velocity was 0.24. At values of $\frac{d}{R} < 0.3$, the inside wall exerted an appreciable effect as shown in picture #79-A and the quadratic law was no longer valid. When $\frac{d}{R} > 0.7$, the square law applied, but the effect of the outer wall became noticeable, producing a flatter characteristic of the pressure gradient versus $\frac{l}{D_D}$. When $f_2\left[\frac{D_s}{D_t}\right]\frac{l}{D_D} < 0.9$, the flow type

approximated the conditions surrounding a smooth concentric core, and if $f_2\left[\frac{D_s}{D_t}\right]\frac{l}{D_o} > 0.9$, the flow approached the type found in the wake behind a single sharp obstruction.

PHOTOGRAPHS

INDICATING SUBSTANCES. As a means of explaining the breaks in the curves of Figs.23, 24, and 27, the flow was investigated by photographic methods. The glass tube was used with various substances injected into the flow to provide an indicating medium. Small air bubbles, potassium permanganate dye, aluminum-bronze flitters, and aluminum-bronze powder were employed as the indicating mediums. Transmitted light furnished by a 1500 watt incandescent globe was used with the first two and reflected light from an arc lamp with the aluminum-bronze. After a series of test pictures, the aluminum-bronze powder was chosen as the standard indicating medium for making the investigation.

DISTORTION. Pictures #5 and #35 were included in an effort to illustrate the effects of distortion due to the variation in the indices of refraction for air, water, and glass. The distortion was measured by taking the ratio of a horizontal measurement given by the projection of the disk from the spacer and comparing it with a vertical measurement near the center of the tube. In picture #5 this ratio is 1.37, while actual measurements gave a value of 1.11. The distortion was reduced by surrounding the tube with a box containing plate glass sides and filling the box with water. The effect of the water bath is shown in picture #35 where the level of the water surface is in the middle of the photograph. When the bath was used, the distortion ratio became

1.07, thus a variation of approximately 4 per cent still existed. Investigation of this ratio for various distributions gave a value approximately 5 per cent low for all arrangements. Although some distortions exist in all photographs, they were taken as being sufficiently correct for the purposes of this investigation.

APPARATUS FOR PHOTOGRAPHS. Fig. 28 gives the arrangement of the apparatus used in making the photographic studies. The light produced by the high intensity carbons of the arc lamp was brought to a focus on the first slit by means of a circular lens . A cylindrical lens was placed with its focus at the illuminated slit. This type of lens gave approximately parallel light in the plane of the figure and diverging light in the perpendicular plane. Thus, by changing the position of the lens system with respect to the central assembly, the vertical length of illumination was controlled. The second and third slits were used as a means of preventing any stray light striking the glass tube and spoiling the sharpness of the photograph as well as restricting the thickness of the illuminated section. The majority of the pictures were taken with the third slit 1/16 inch in width although a few were taken with 1/32 inch width. The arc lamp was used since a very intense light source was necessary to supply sufficient illumination to insure the path of the small particles being recorded on the photographic plate.

AIR BUBBLES. Studies with air bubbles were made as a means of checking the visual observation presented in Fig. 7 . Pictures #5 and #35 were taken with air as the indicating medium while #36 and #37 had a combination of very small air bubbles

and aluminum-bronze powder. In general, the photographs show the same type of flow as visually observed for the medium disks and four ½ inch spacers using air bubbles as the indicator.

DYE. Pictures #17, #19, and #21 were included in order to show typical results obtained with dye. The time of exposure for each picture was approximately 1/1000 seconds. This speed was obtained by making use of a disk rotating at about 1475 R. P. M. and having one 5 deg. sector removed. By placing this rotating disk between the light source and the camera, it was possible to use it as an auxiliary shutter when the camera shutter was adjusted to open only once per disk revolution. The pictures present different sizes of injection needles, rates and points of injections. They also clearly indicate the extremely rapid rate of dye dispersion, even at the low velocities studied, and therefore, provided very little information regarding the flow conditions. They plainly illustrate the difficulties in using dye as an indicator for complicated turbulent flow. Considering picture #19 in particular, the dye shows that there was apparently little or no transfer of water between the through particles and the particles in the wake formed by the disk. This may have been the true case, yet it is possible that the rate of dispersion increased so rapidly upon crossing the boundary of the two types of flow, that the above results are apparent only and were not the true condition. Therefore there is a question regarding dye results without considering rates of injection and detrimental effects of the injection needle upon the flow. In general, the pictures using dye as the indicating medium provide less informa-

tion than when other materials were employed for the purpose.

ALUMINUM POWDER. Picture #34 had aluminum-bronze flitters as the indicators. As seen in the photographs, the flitters tended to give a broad, blurred line, which was not desired as the path of an individual particle was then very difficult to follow.

The best photographs were taken with aluminum-bronze powder, which was of the commercial variety produced for use as a paint pigment. Since there is a difference in the density of water and aluminum, observations were made on the rate of free fall of the particles in water as a means of determining the effect of the variation in density. In a freshly made mixture, the particles settle very slowly, but if the mixture has been severely shaken for some time, the speed of settling will be increased. This behavior can be explained in the light of Professor Carmichel's observations with aluminum powder. Small air bubbles cling to the particles, thus reducing their effective density and decreasing the rate of fall. If this is the case, then severe shaking must have assisted in tearing off the air and leaving a particle of greater effective density. For the photographic work, all injection mixtures were freshly mixed for each set of pictures. The rate of free fall was so small, that the aluminum-bronze particles should have followed closely the path of the water. An inspection of the photographs of air bubbles and aluminum-bronze particles shows that they both indicate approximately the same type of flow; thus from a qualitative viewpoint, the conditions were not sensitive to reasonably small density variations.

The majority of the pictures were taken at a water

velocity between four and five feet per second. At this value, experimental data indicated the point for the head drop versus the square of the velocity was on the straight line. Some pictures were taken at a lower velocity in order to obtain a clearer photograph. #36 and #40-A refer to the same central assembly arrangement, but the velocity of the latter is approximately two and one half times the former. In spite of the difference in velocity, the photographs show the same type of flow to exist in both cases. A similar result is observed in #43-A and #80-A where the velocity of the first was over three times that of the second. The velocity with the 20/16 inch disks was approximately nine feet per second. This high value was used as the velocity in the space between the disks was considerably less than the computed value. The majority of the photographs indicated the method of computing velocities was a fair approximation, particularly for the condition of relatively few spacers per disk.

PULSATING FLOW. Comparing pictures #36-A and B, it is readily observed that the flow downstream from a disk projection was not steady with respect to time, hence the phenomenon was of a pulsating type. Standard speed motion pictures were taken in an effort to illustrate the transitory nature of the flow. The forming, the breaking down, and reforming of the whirls is definitely shown in the series of pictures presented. In the arrangements with the disks relatively close together, the whirls apparently elongated themselves until they filled the space between the disks, and then broke up. This action was decidedly different from the characteristic flow of whirls under free turbulence conditions. As the disks were separated further, the whirls elongated and tended to break away

from the projection and travel downstream similar to the whirls in free turbulence. The flow phenomena of the 20/16 inch disks with wide separations were different from these illustrated by motion pictures. Thus, in pictures #92-A, and #88A, two distinct whirl regions are shown and at no time did they elongate to interfere with each other, although varying in position in their own spheres of action. The motion pictures provided an additional check on transitory nature of the flow past different central assemblies.

TYPES OF FLOW. The photographic studies have shown the existance of at least two general types of flow. Fig. 29 presents a sketch showing typical examples of the types of flow at different stages in their development. The first of these is illustrated by pictures #53-A, #43-B, and #52-A. This type involves a surface of discontinuity which approximately coincided with the cylindrical surface enclosing the outside diameter of the disks. Under these conditions the through flow approached the characteristics shown in #84-A for a smooth annular space. The second type of flow is illustrated by photographs #68-B and #69-B. In this group the surface of discontinuity bent into the space between disks after each projection; hence the through velocity relations no longer approximated the conditions for flow in smooth annular spaces. As different types of flow existed, it is possible that a change in friction loss relations might have taken place. Table II presents the central assembly arrangements for the upper limit of the first type and the lower limit for the second as determined from the photographs. These results furnished an explanation for the breaks in the curves shown in

Figs. 23 and 24. A comparison of the table and the figure showed the break occurred when the type of flow changed; hence the factors determining the friction depended upon the type of flow existing in the spaces between the disk projections. The 20/16 inch disks were not included in this table because pictures available are not sufficient to allow an analysis, as the type of flow apparently differs from those discussed.

DISK THICKNESS. Since all disks were constructed from the same thickness of brass, picture #99-A and #98-B were taken as a means of studying the probably effects of increasing the disk width. Experimental data have shown the resistance of any arrangement of the disks and spacers to be greater than that of a smooth central core of a diameter equal to the disk diameter. The photographs show only a small variation in the velocity distribution along the long surface of the disk ($\frac{3}{4}$ inch spacers in these pictures), and the conditions with a smooth core. From an analysis of the photographs and the little experimental data available, the thinner the disk projection (limited by the thickness required for strength), the greater will be the friction drop for a given distance between disk center-lines.

Photograph #79-A gives a picture of the flow when the head drop was not proportional to the square of the velocity. With this size spacer and disk, the maximum head drop was not attained even with an arrangement of one disk per spacer. A complete analysis of these arrangements was not made as they proved to be outside the limits of application for the majority of the work.

DOWNSTREAM CONDITIONS. The downstream conditions are shown in pictures #93 to #97 inclusive. #93, #94, and #95 illustrate the complex conditions behind a single disk. The effect of the disturbance produced by the projection extended downstream further than the maximum distance between spacers used in the central assembly arrangements. Hence, the head drop per disk in the arrangements never reached the value for the head loss of a single disk. Experimentally, this is shown in Fig. 24 in which the curves never reach a constant value. Picture #96-A presents the flow conditions corresponding to the curve for the six $\frac{1}{2}$ inch spacers and 65/64 inch disks given in Fig. 13. The particles passing the projection bent around the wake until they almost reached the spacers at the point which roughly corresponded to the first maximum position in Fig. 13. After this point, a second disturbance took place which approximates the action behind a single disk. Thus, if the curve of Fig. 13 were extended, it would not form another wave, but would reach the maximum and level off similar to the orifice or sudden expansion curves. Picture #97-A illustrates the conditions of sudden enlargement when the diameter of the core is reduced. Although the curve for sudden enlargement in Fig. 13 applies to a change in circular pipe diameter when no core is present, the conditions shown in the photograph indicate the pressure relations would be approximately the same in both cases.

VALUE OF PHOTOGRAPHS. The photographs have provided an explanation for the discontinuity in the curve of Fig. 27 by illustrating the two types of flow involved in the relations. They have shown the characteristics of at least two additional types existing outside of the limitations of Eq. [4].

The motion pictures have illustrated the pulsating characteristics of the whirls formed in the wake of the disks. Although the pictures have given excellent qualitative results for the requirements of this investigation, the limits of the photographic method have not been reached, as Professor Carmichel has demonstrated the possibility of obtaining excellent pictures for quantitative purposes.

SUMMARY

The work of this investigation provides additional experimental data regarding turbulent flow, with particular reference to the phenomena associated with a long series of similar bodies forming an obstruction to the motion of water through a circular pipe. The obstacles were mounted on a rod concentric with the pipe in such a manner as to allow the space between them to be varied. Investigation of the phenomena followed two general methods; quantitative development of the relations of the pressure gradient to the mean velocity and qualitative classification of the flow by photographs of small aluminum-bronze particles in the water. The equation

$$\frac{h'}{1.78\left\{f_1\left[\frac{D_s}{D_t}\right]\right\}\left[\frac{d}{R}-0.113\right]} = \frac{v^2}{2g\,D_t} f\left[\left\{f_2\left[\frac{D_s}{D_t}\right]\right\}\frac{l}{D_o}\right]$$

expresses the relation between the pressure gradient and the velocity in terms of the dimensions of the turbulence tube. The dimensional symbols refer to the turbulence tube measurements indicated in Fig. 6. This relationship is valid within the limits $0.3 < \frac{d}{R} < 0.7$. For $f_2\left[\frac{D_s}{D_t}\right]\frac{l}{D_o} > 0.24$ the pressure gradient is directly proportional to the square of the velocity. The photographs show two general types of flow within the range of validity for the equation. At values of $f_2\left[\frac{D_s}{D_t}\right]\frac{l}{D_o} < 0.9$ the through flow approximates the conditions surrounding a smooth core and when $f_2\left[\frac{D_s}{D_t}\right]\frac{l}{D_o}$ is greater, the through flow tends to follow the characteristic conditions in the wake of a sharp obstruction. The pulsating nature of the flow is illustrated by standard speed motion pictures.

REFERENCES FOR ANNULAR FLOW.

1. Page- Introduction to Theoretical Physics. (D. Van Nostrand Co. Inc. 1929).
2. Lea and Tadros- Flow of Water Through a Circular Tube with a Central Core and Through Rectangular Tubes. (Phil. Mag. Vol.XI June 1931).
3. Atherton- Fluid Flow in Pipes of Annular Cross-Section. (Trans. A.S.M.E. 1926. p.145).
4. T. Lonsdale- The Flow of Water in the Annular Space Between Two Coaxal Cylindrical Pipes. (Phil. Mag. 46;163 1923).
5. E. Buckingham- Leakage Through Thin Clearance Spaces. (Engineering 115:225. 1923).
6. O.A. Price- Friction of Annular Pipes. (Engineering 112: 303. 1926).
7. Krantz, Macintire, Gould- Flow of Liquids in Pipes of Circular and Annular Cross-Sections. (Univ. of Ill. Engineering Experiment Station Bulletin #222. 1931).

REFERENCES FOR DOWNSTREAM PRESSURE DISTRIBUTIONS.

8. J.L. Hodgson- The Laws of Similarity for Orifice and Nozzle Flows. (Trans. A.S.M.E. Vol.51. p.303. 1929).
9. Davis and Jordan- The Orifice as a Means of Measuring Flow of Water Through a Pipe. (Univ. of Ill. Engineering Experiment Station Bulletin #109).
10. H.W. Archer- Experimental Determination of Loss of Head Due to Sudden Enlargement in Circular Pipes.(Trans. A.S.C.E. Vol.39. p.999. 1913).

11. Dr. H.C. Shutt- Losses of Pressure Head Due to Sudden Enlargement of a Flow Cross-Section. (Trans. A.S.M.E. Vol.51 Hyd.p. 83. 1929).

REFERENCES FOR DIMENSIONAL ANALYSIS.

12. Hydraulic Laboratory Practice. (A.S.M.E.).

13. R.C. Tolman- The Principle of Similitude and the Principle of Dimensional Homogeneity. (Physical Review. Second series. Vol.VI. 1915. #3 p. 219).

14. Buckingham- Model Experiments and the Forms of Empirical Equations. (Trans. A.S.M.E. Vol.37 1915. p.263).

REFERENCES FOR FRICTION HEAD DUE TO A SERIES OF OBSTACLES.

15. P.v. Mathes- Zur Abschirmwirkung von Widerstandskörpern. (Luftfahrtforschung 2. Band S.75 Heft 3. 1928).

16. Cloyde M. Smith- The Measurement of Air Quantities and Energy Losses in Mine Entries. (Univ. of Ill. Engineering Experiment Station Bulletin #199. 1929).

17. McElroy and Richardson- Resistance of Metal-Mine Airways. (U.S. Dept. of Commerce. Bureau of Mines. Bulletin #261. 1927).

18. Greenwald and McElroy- Coal-Mine Ventilation Factors. (U.S. Dept. of Commerce. Bureau of Mines. Bulletin #285. 1929).

REFERENCES FOR PHOTOGRAPHIC PROCEDURE.

19. M. Camichel- Applications des Lois de Similitude à l'Étude des Phénomènes qui se Produisent à l'Aval d'un Corps Immergé dans un Fluide Visqueux en Mouvement. (1925).

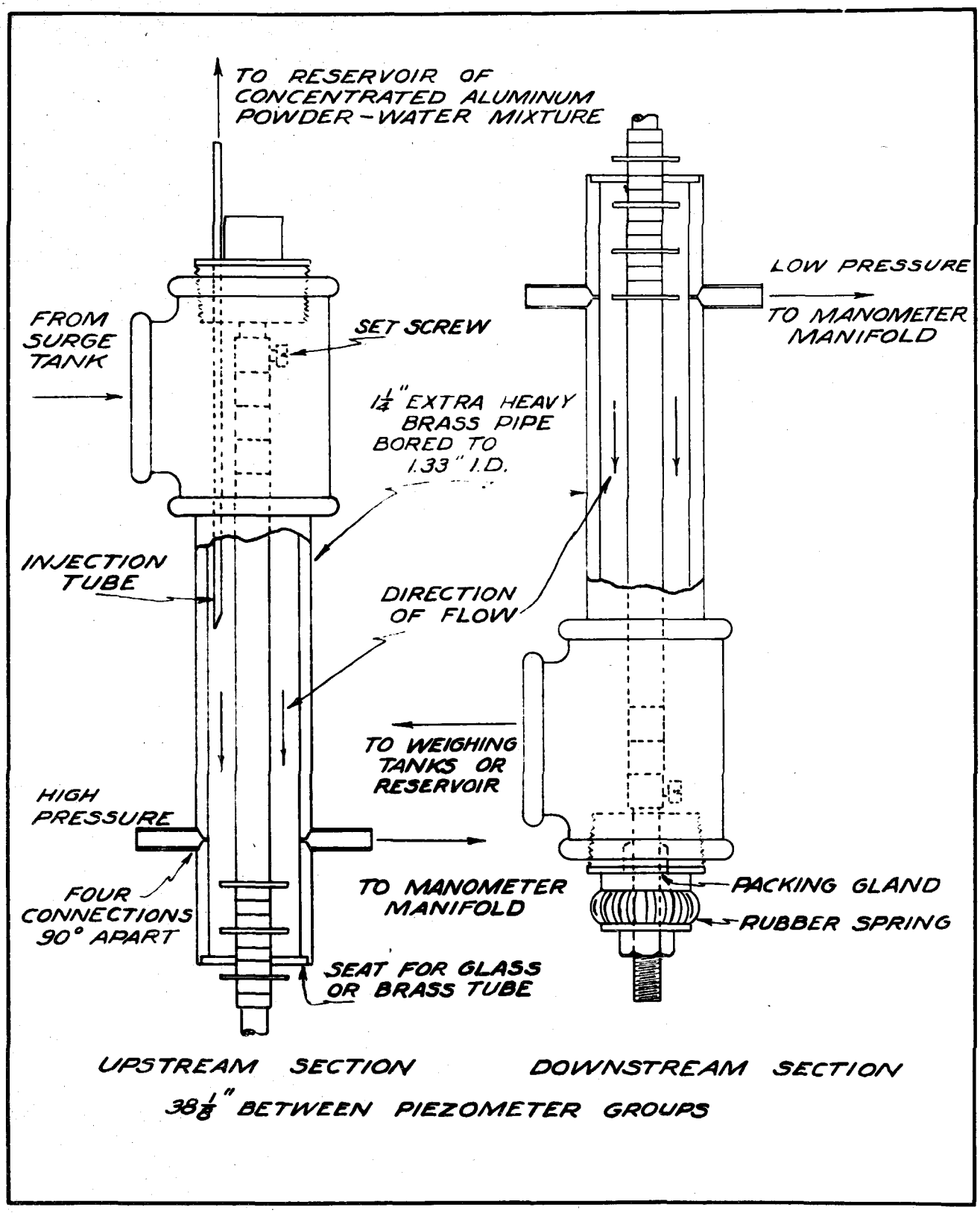

FIG. 1. DIAGRAM OF TURBULENCE TUBE.

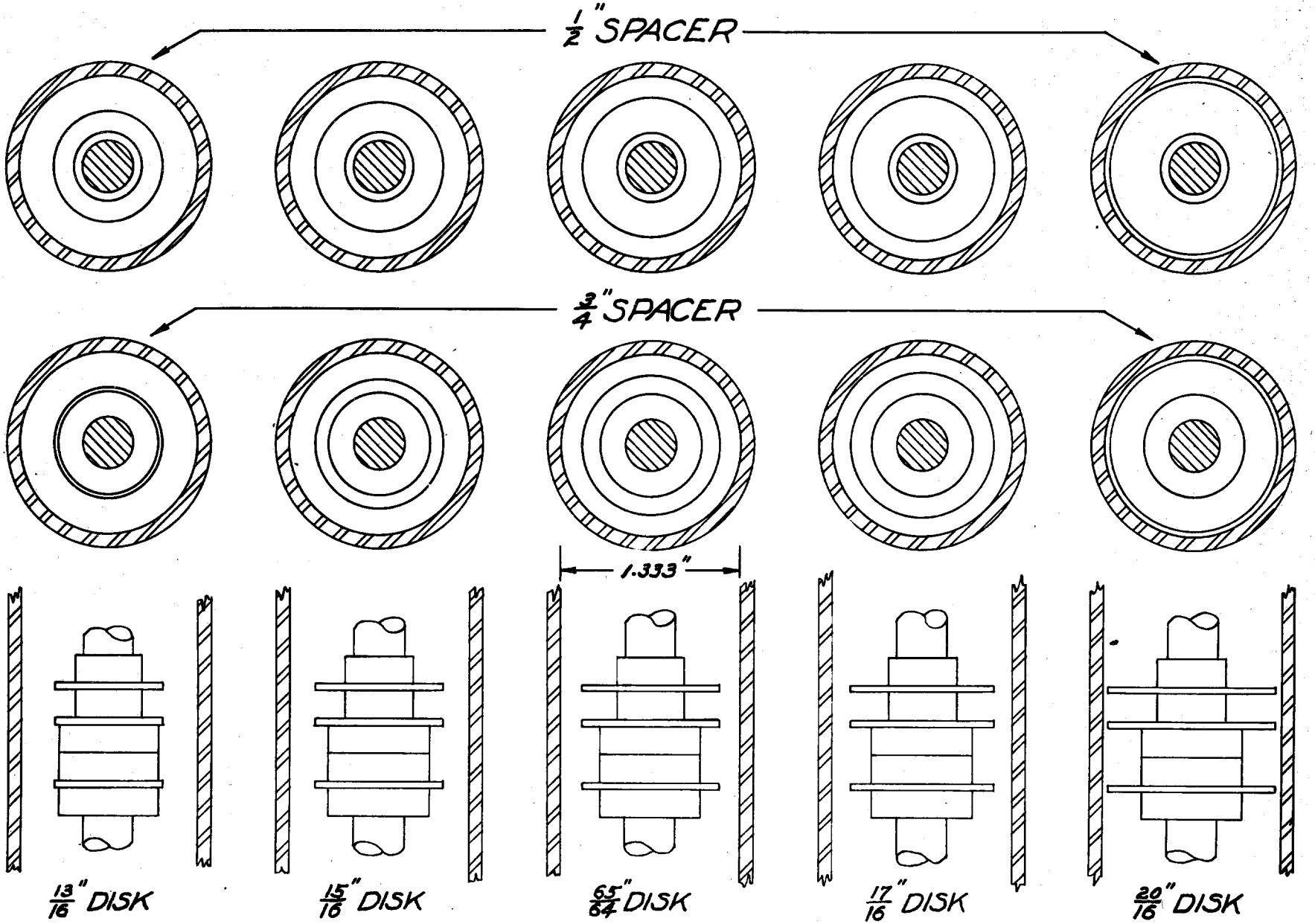

FIG. 2. COMPARATIVE SIZES OF SPACERS, DISKS, AND TUBE.

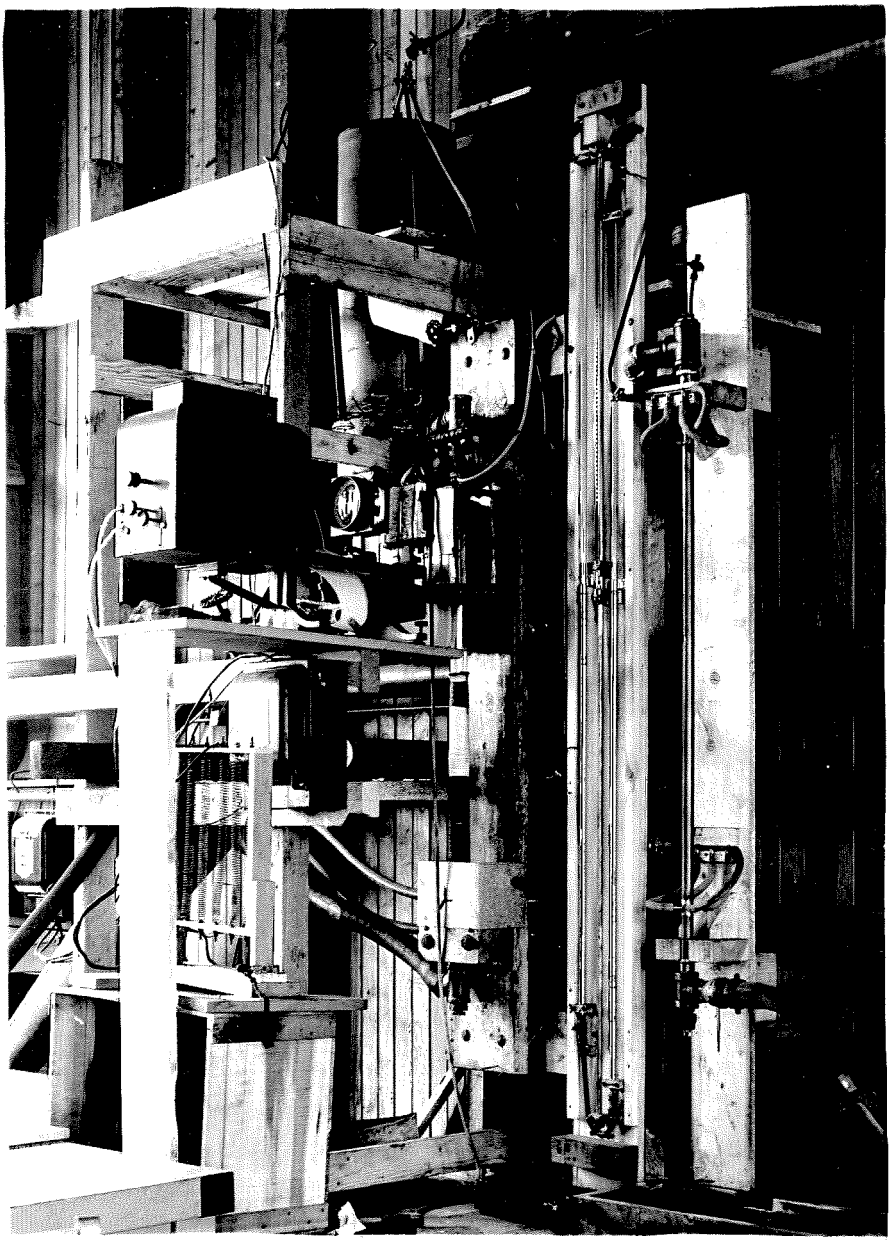

(a) PHOTOGRAPH

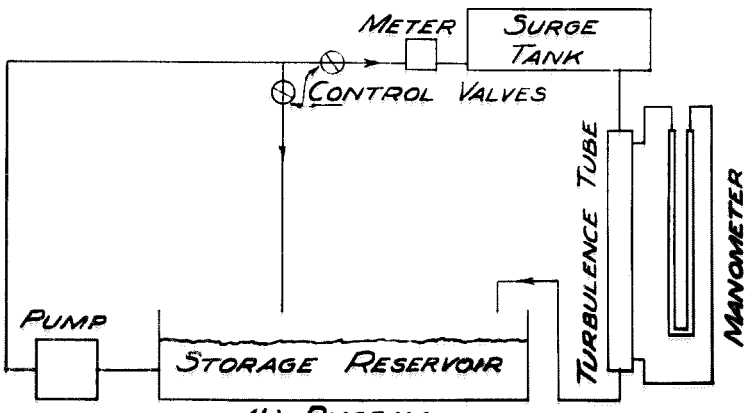

(b) DIAGRAM

FIG. 3. EXPERIMENTAL APPARATUS.

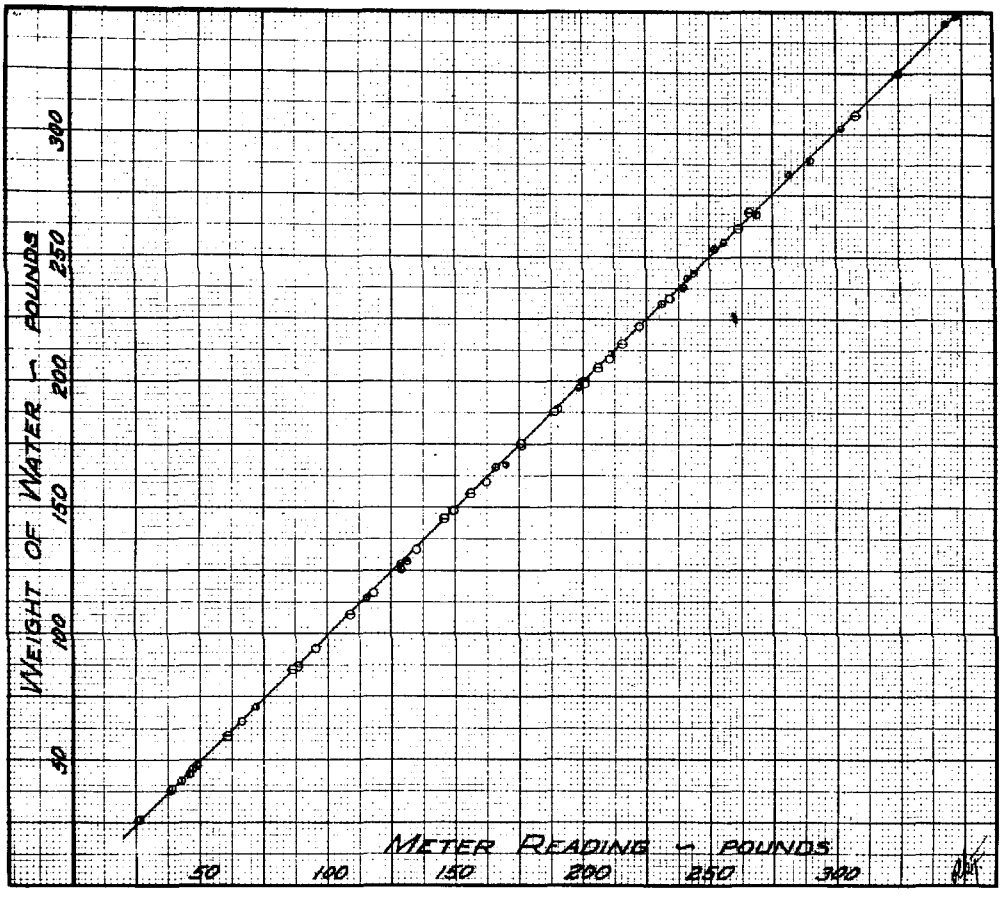

FIG. 4. WATER METER CALIBRATION.

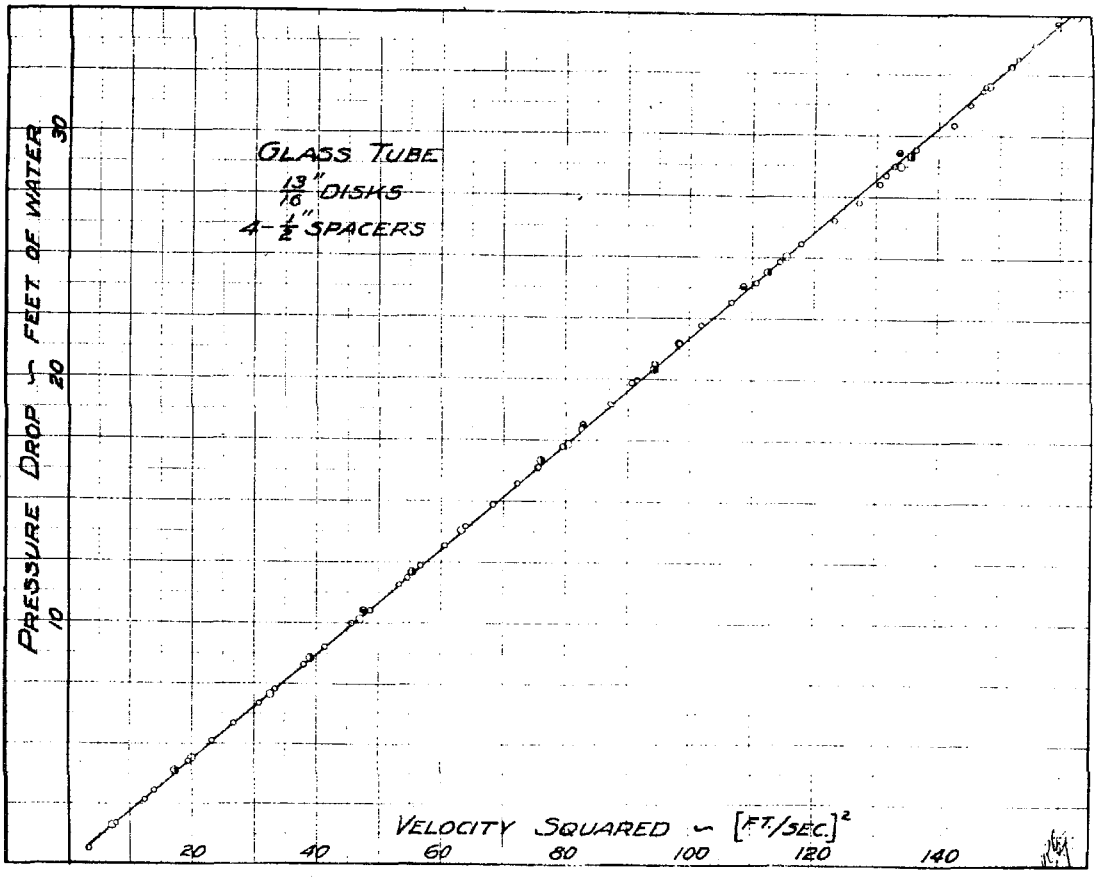

FIG. 5. TOTAL HEAD LOSS VERSUS VELOCITY SQUARED.

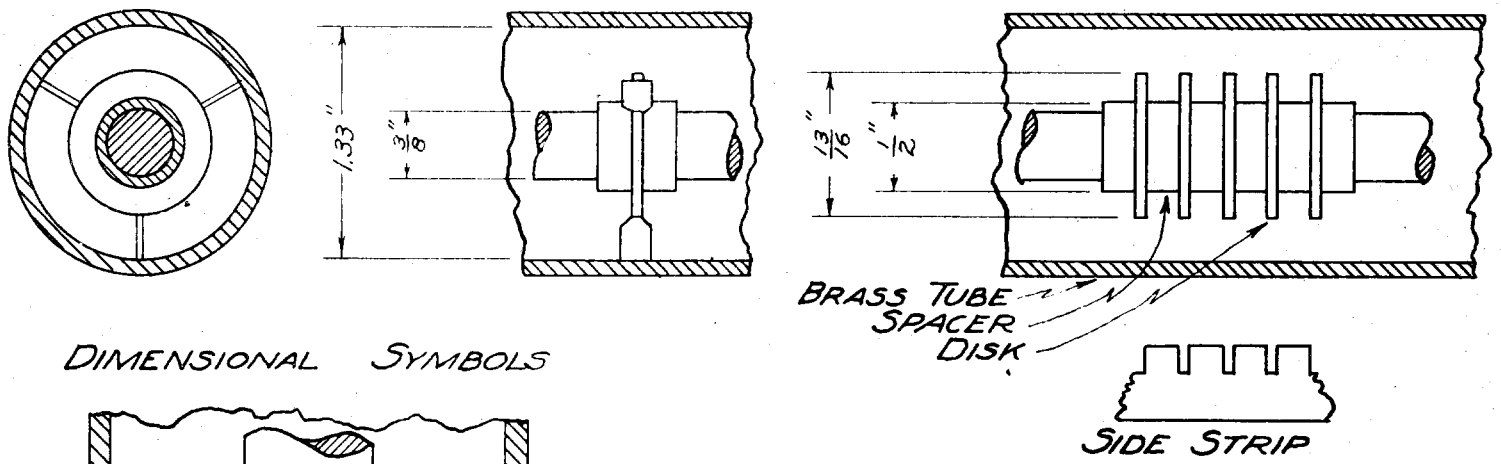

DIMENSIONAL SYMBOLS

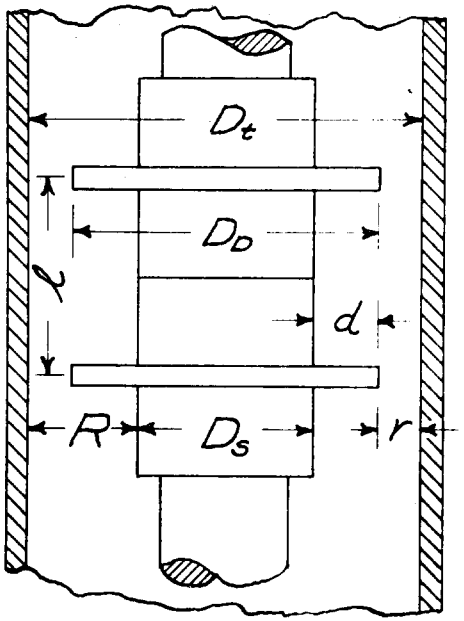

SIDE STRIP MADE FROM 20 GAUGE BRASS
DISKS MADE FROM 16 GAUGE BRASS
SPACERS ARE $\frac{1}{2}$ CM. LONG

FIG. 6. TURBULENCE TUBE PARTS AND SYMBOLS.

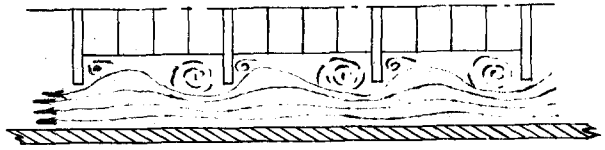

$\frac{13}{16}$" DISKS 4-$\frac{1}{2}$" SPACERS

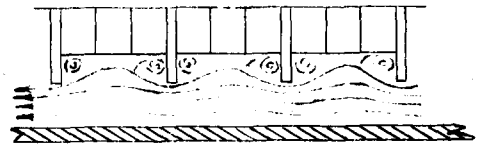

$\frac{13}{16}$" DISKS 3-$\frac{1}{2}$" SPACERS

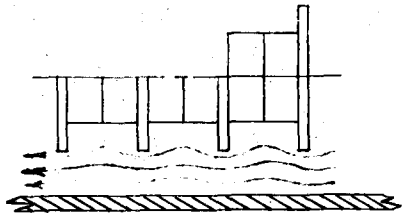

$\frac{13}{16}$" DISKS 2-$\frac{1}{2}$" SPACERS

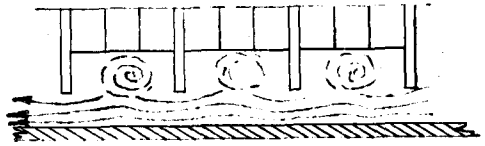

$\frac{15}{16}$" DISKS 3-$\frac{1}{2}$" SPACERS

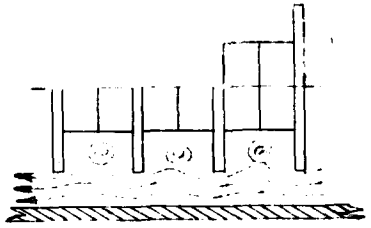

$\frac{15}{16}$" DISKS 2-$\frac{1}{2}$ SPACERS

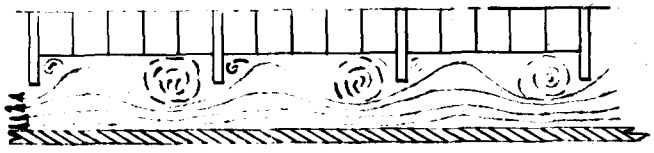

$\frac{13}{16}$" DISKS 5-$\frac{1}{2}$" SPACERS

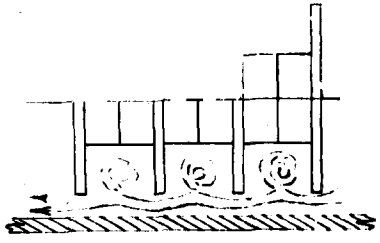

$\frac{17}{16}$" DISKS 2-$\frac{1}{2}$" SPACERS

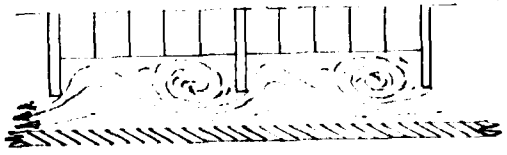

$\frac{15}{16}$" DISKS 5-$\frac{1}{2}$" SPACERS

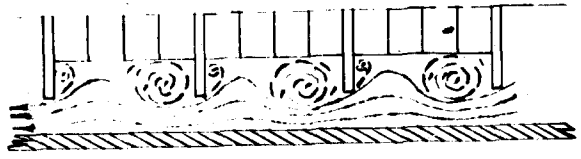

$\frac{15}{16}$" DISKS 4-$\frac{1}{2}$" SPACERS

FIG. 7. SKETCHES OF AIR BUBBLE PATHS

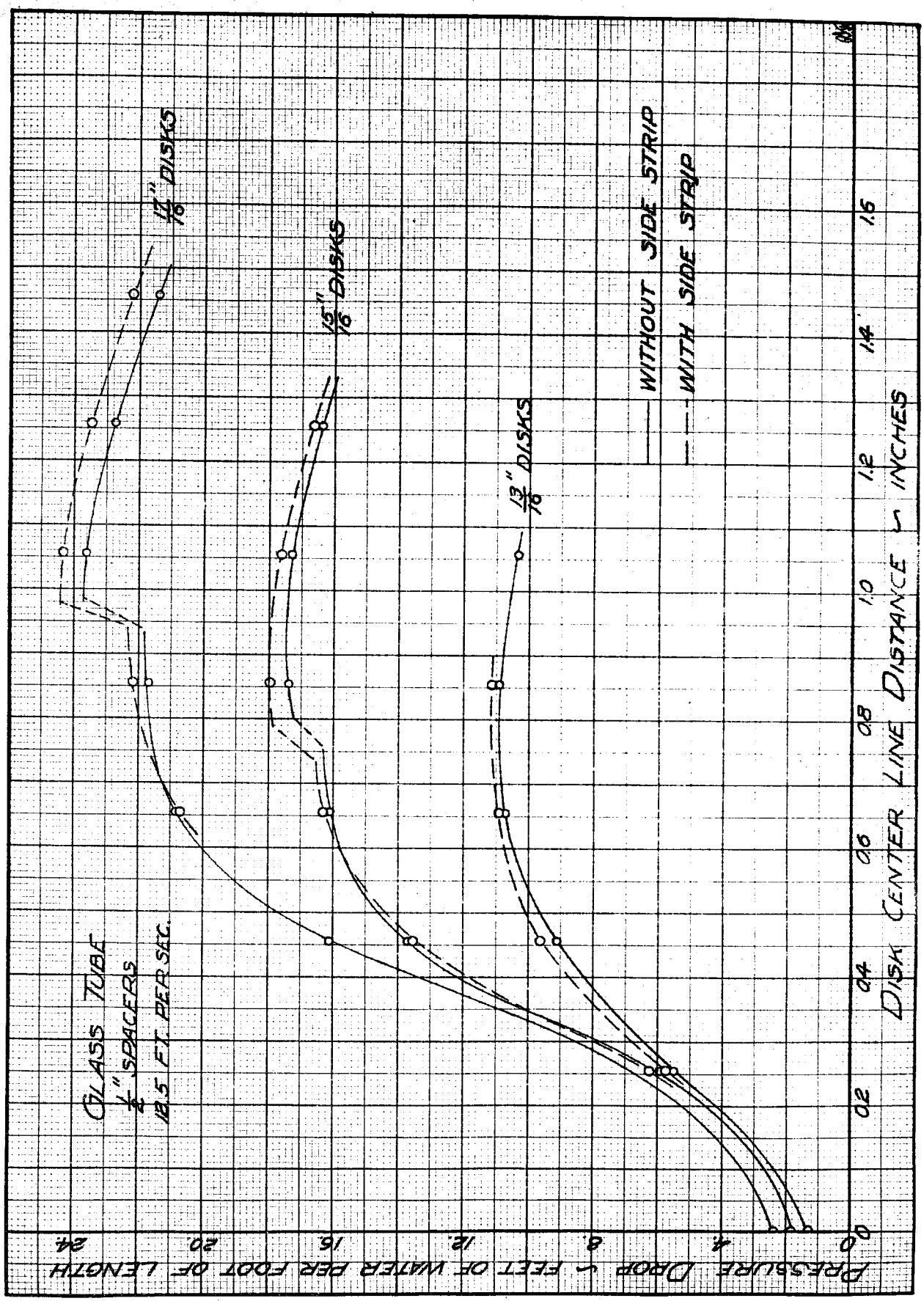

FIG. 8 EFFECT OF THE SIDE STRIP ON PRESSURE DROP.

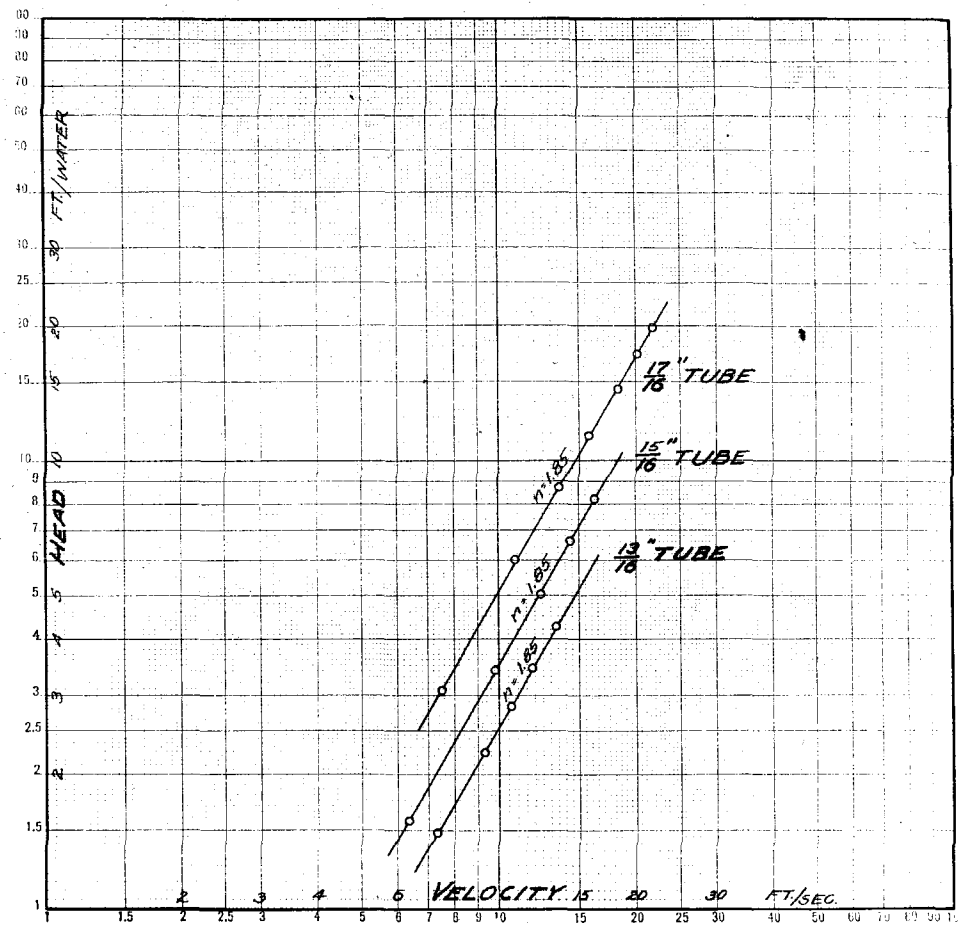

FIG. 9. HEAD VERSUS VELOCITY FOR ANNULAR SECTIONS.

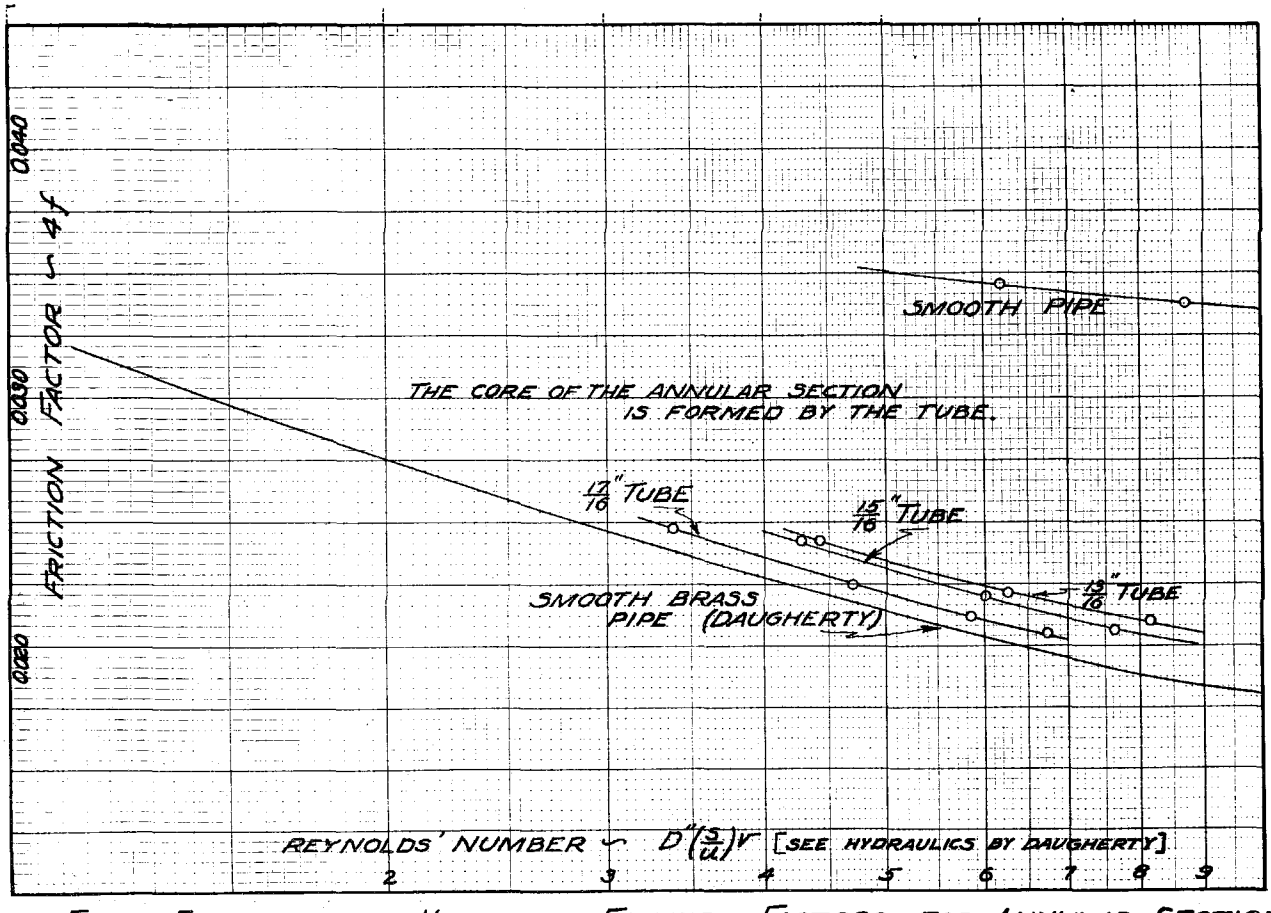

FIG. 10. EXPERIMENTAL VALUES OF FRICTION FACTORS FOR ANNULAR SECTIONS.

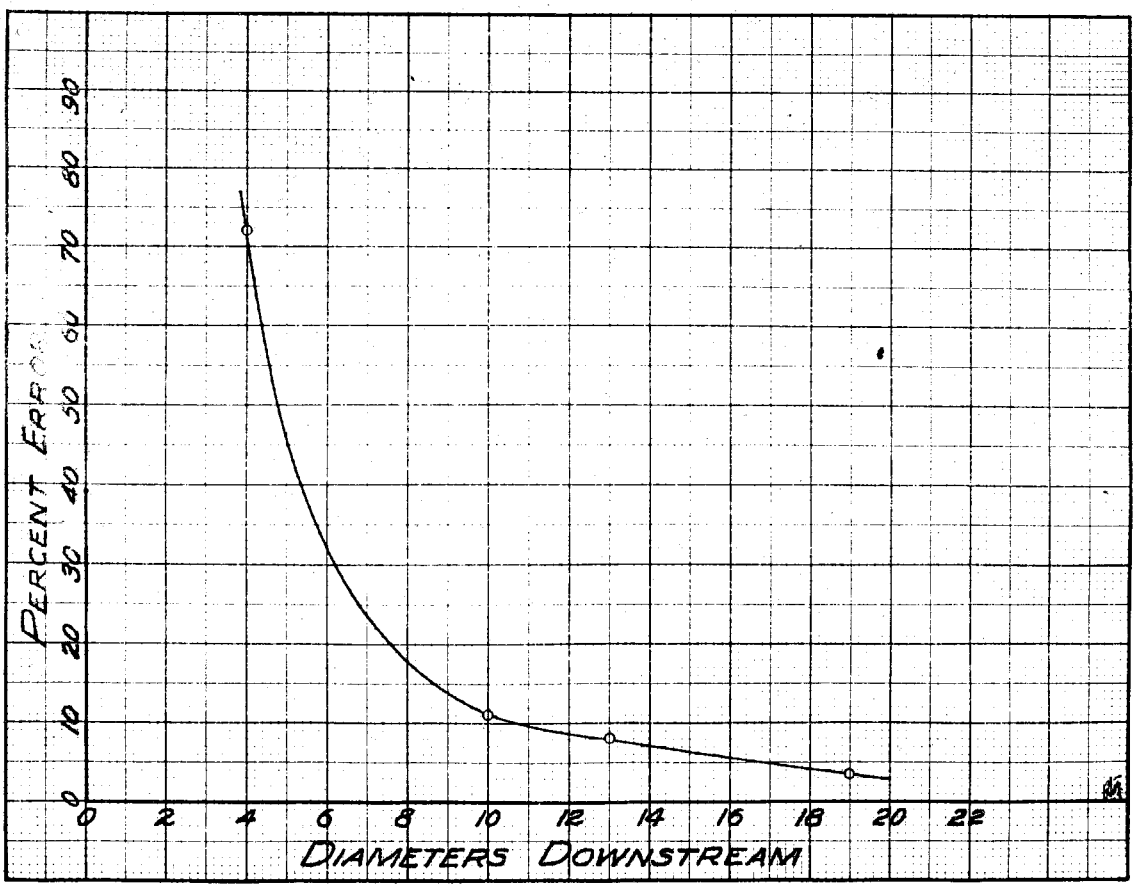

FIG. 11. ERRORS DUE TO POOR ENTRANCE CONDITIONS.

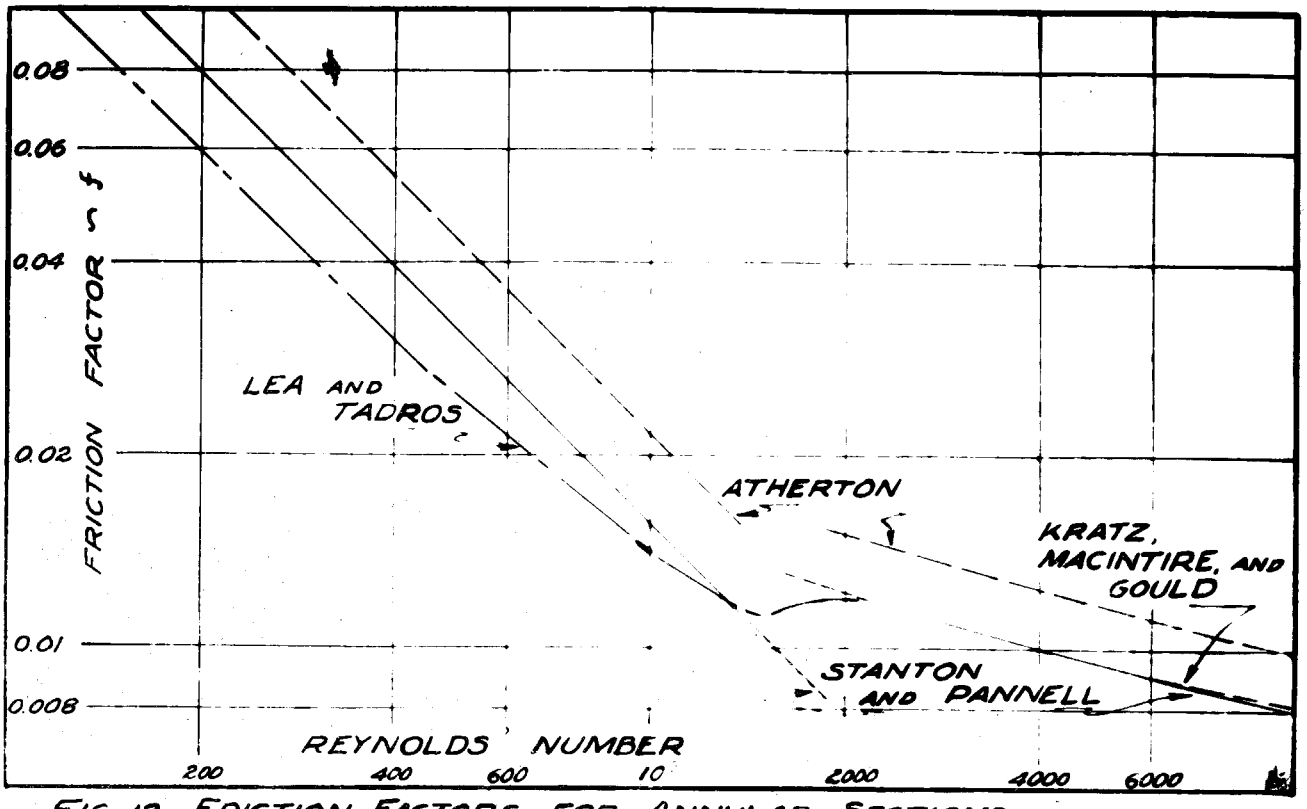

FIG. 12 FRICTION FACTORS FOR ANNULAR SECTIONS.

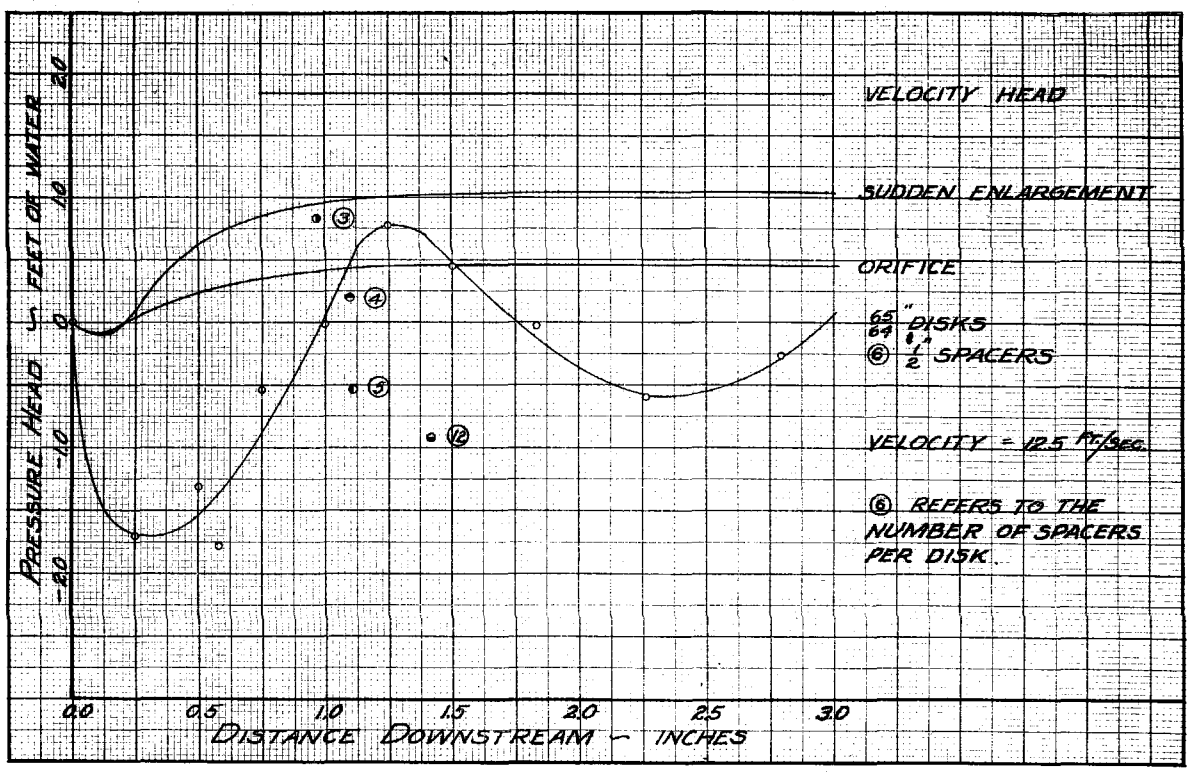

FIG. 13. PRESSURE HEAD AT POINTS DOWNSTREAM FROM THE LAST DISK.

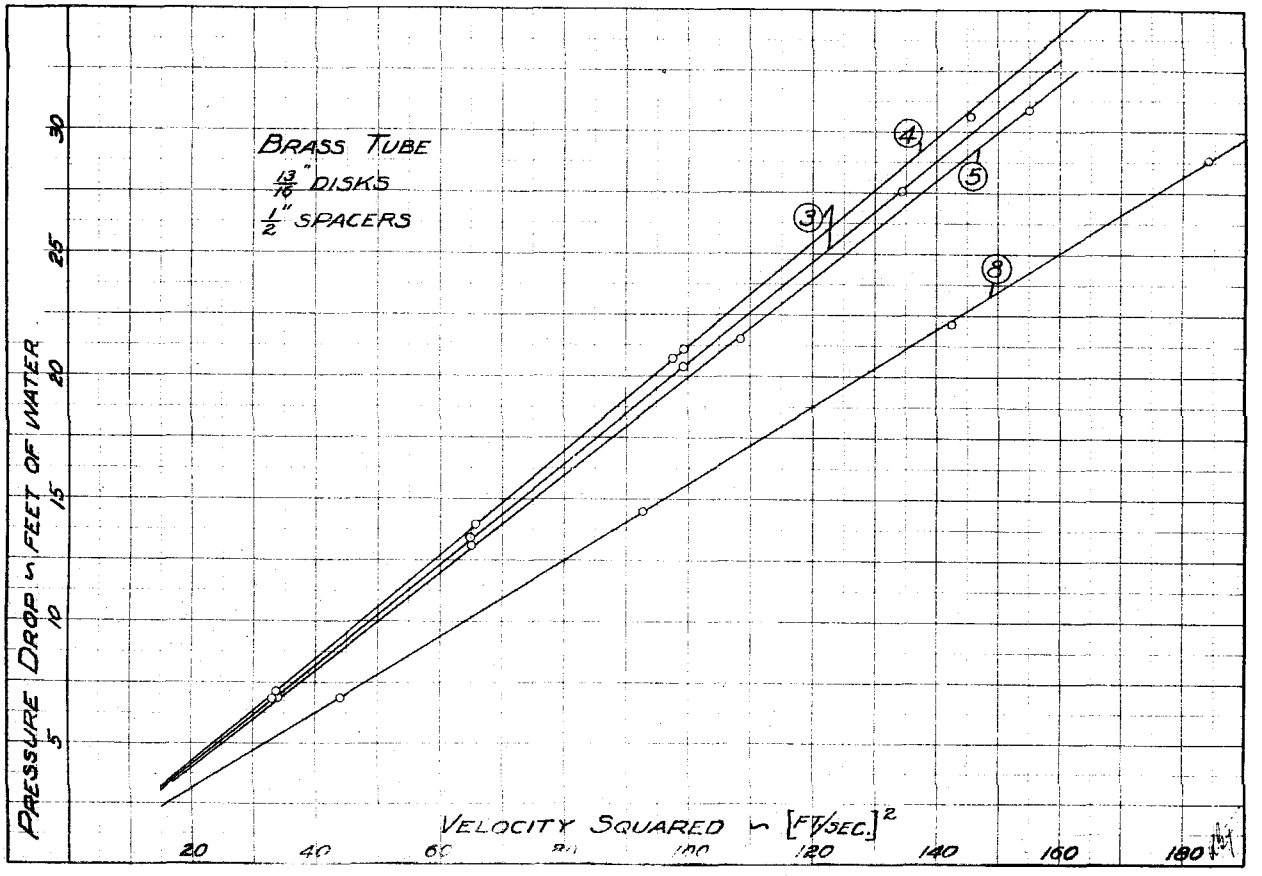

FIG. 14. TOTAL HEAD LOSS VERSUS VELOCITY SQUARED.

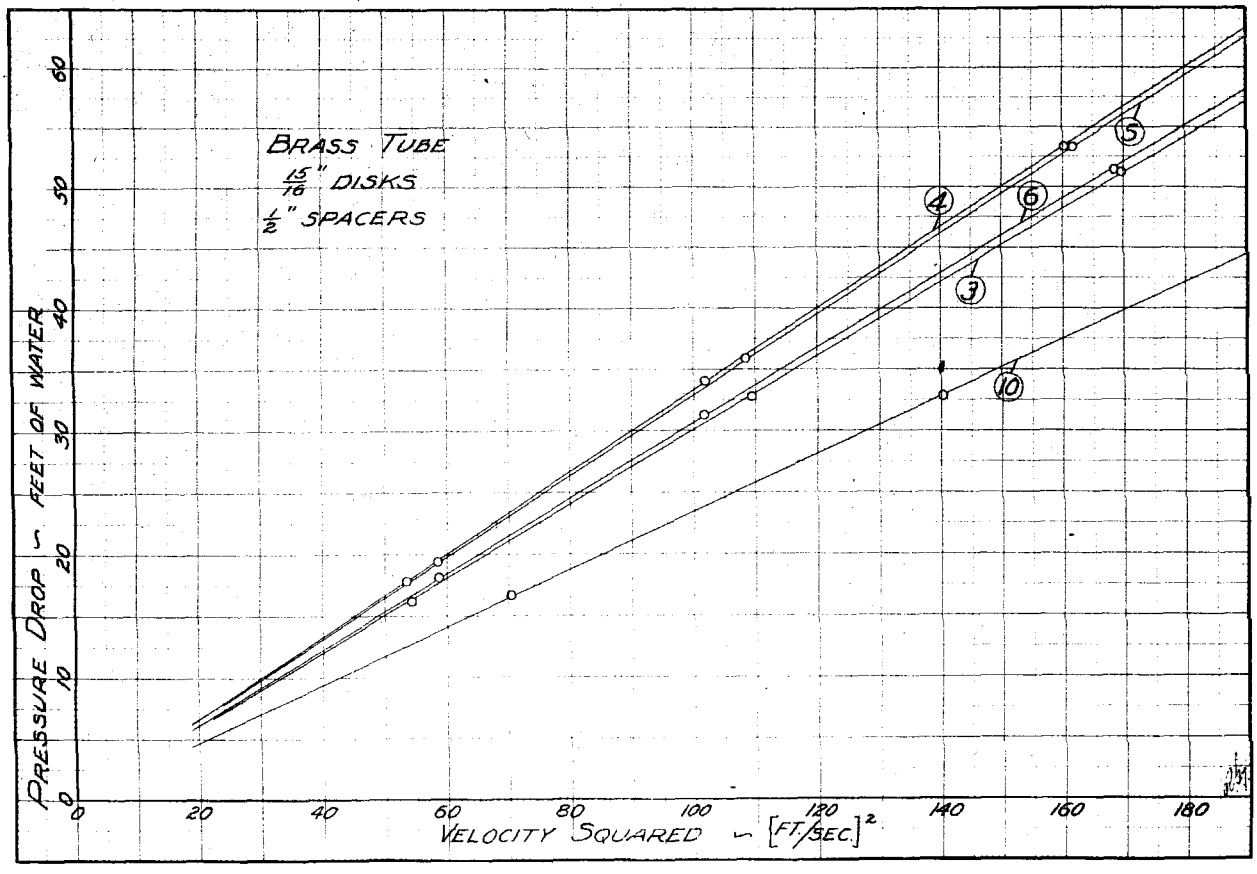

FIG. 15. TOTAL HEAD LOSS VERSUS VELOCITY SQUARED.

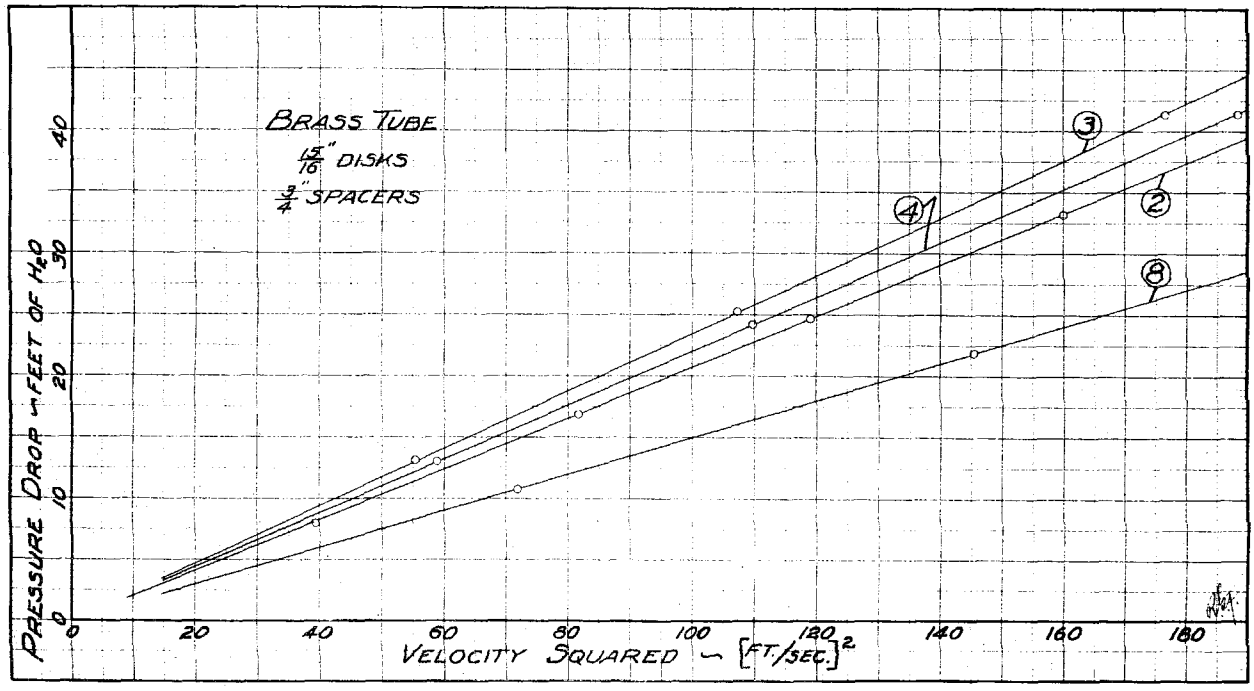

FIG. 16. TOTAL HEAD LOSS VERSUS VELOCITY SQUARED.

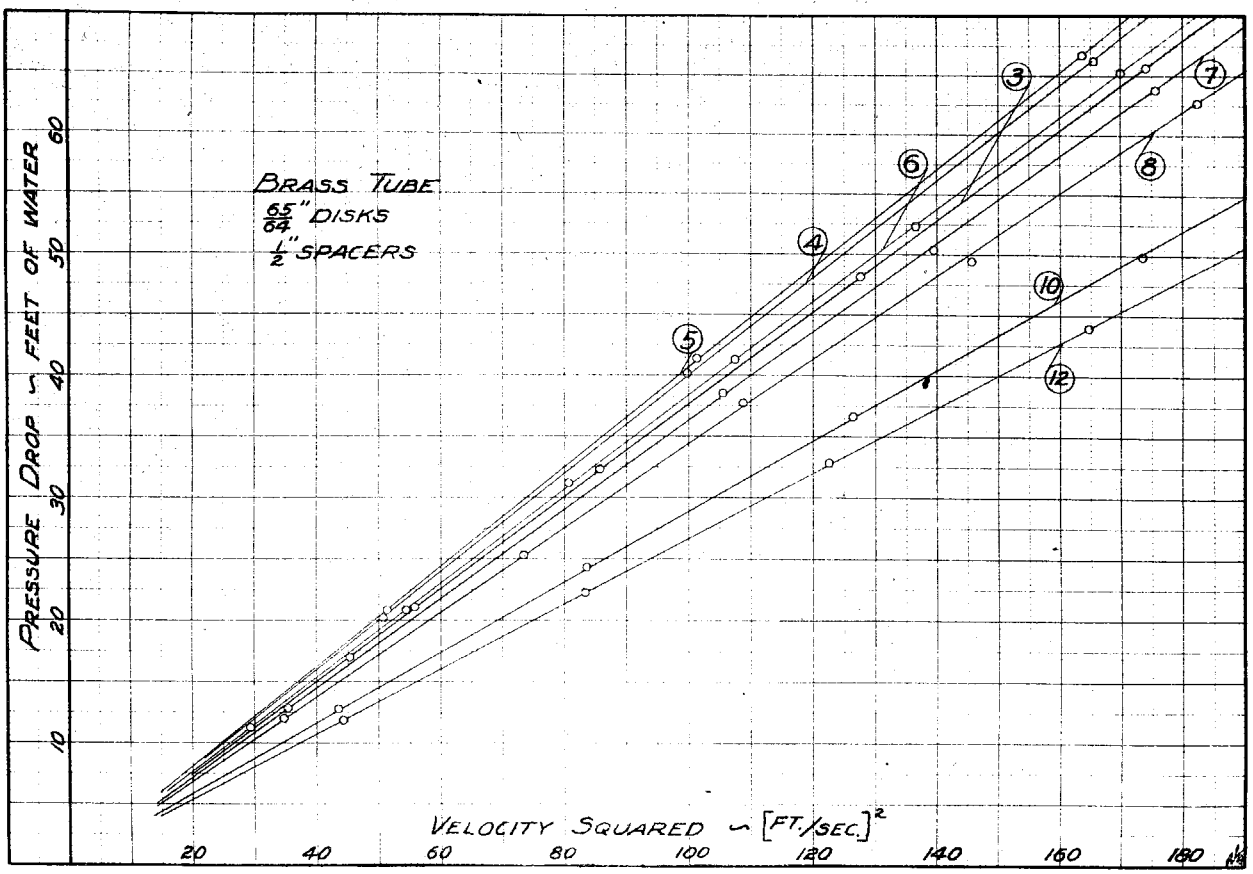

FIG. 17. TOTAL HEAD LOSS VERSUS VELOCITY SQUARED.

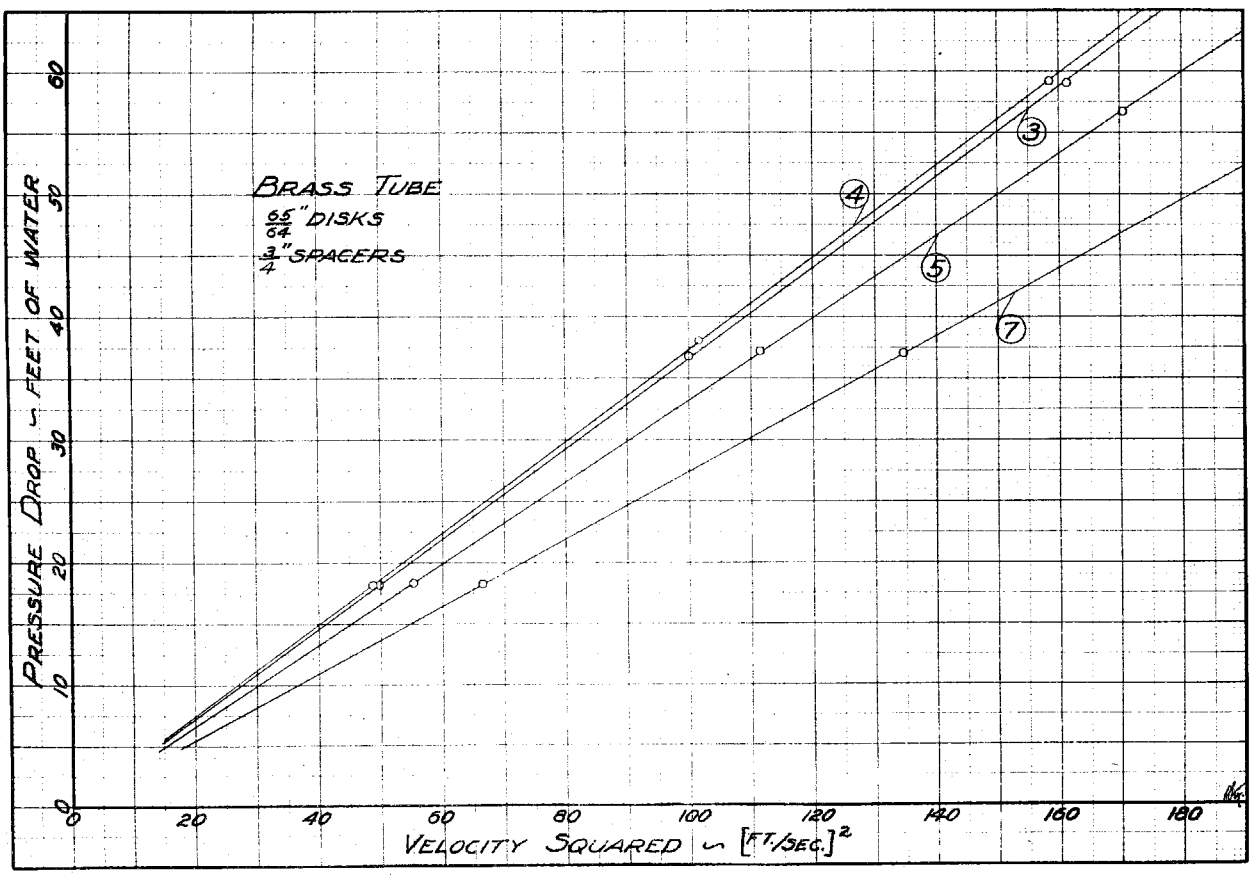

FIG. 18. TOTAL HEAD LOSS VERSUS VELOCITY SQUARED.

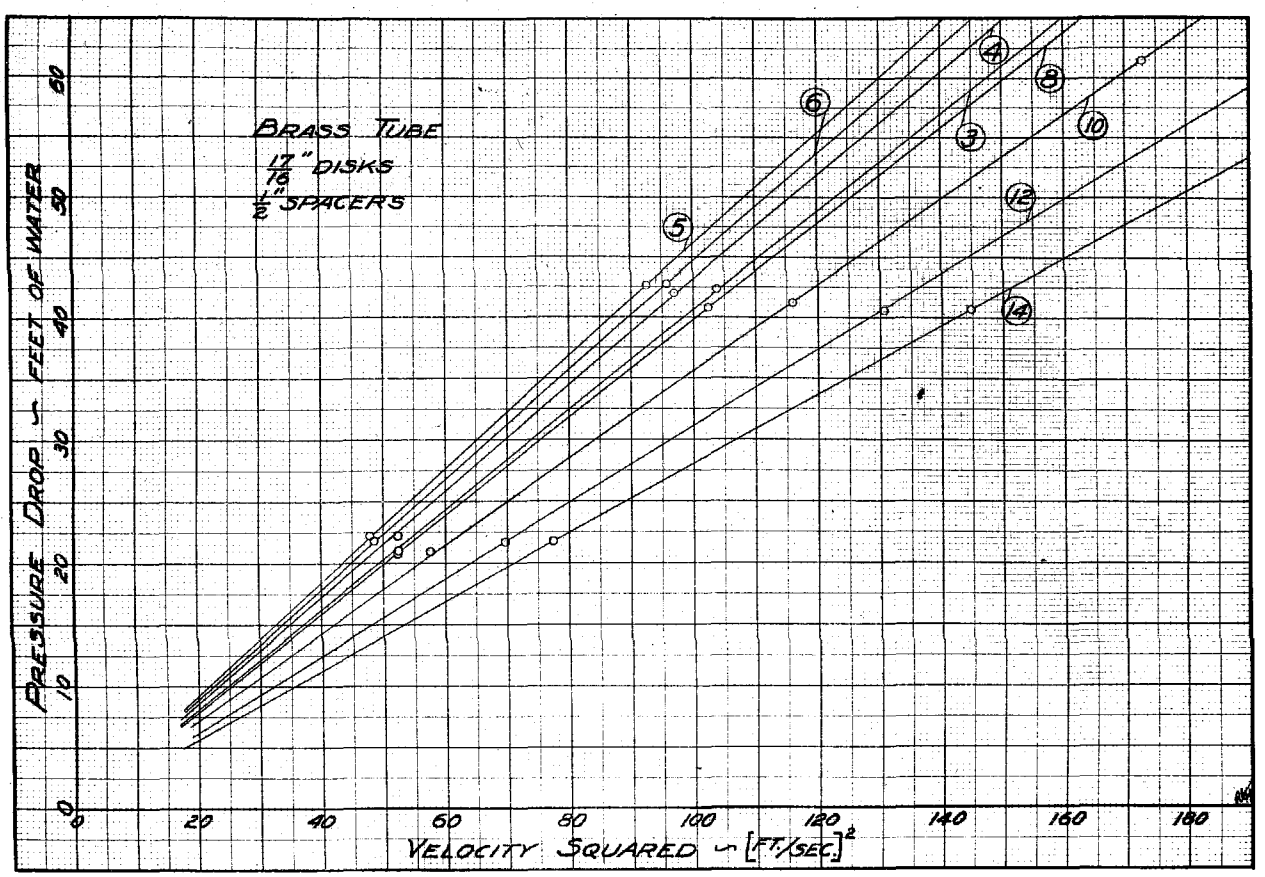

FIG. 19. TOTAL HEAD LOSS VERSUS VELOCITY SQUARED.

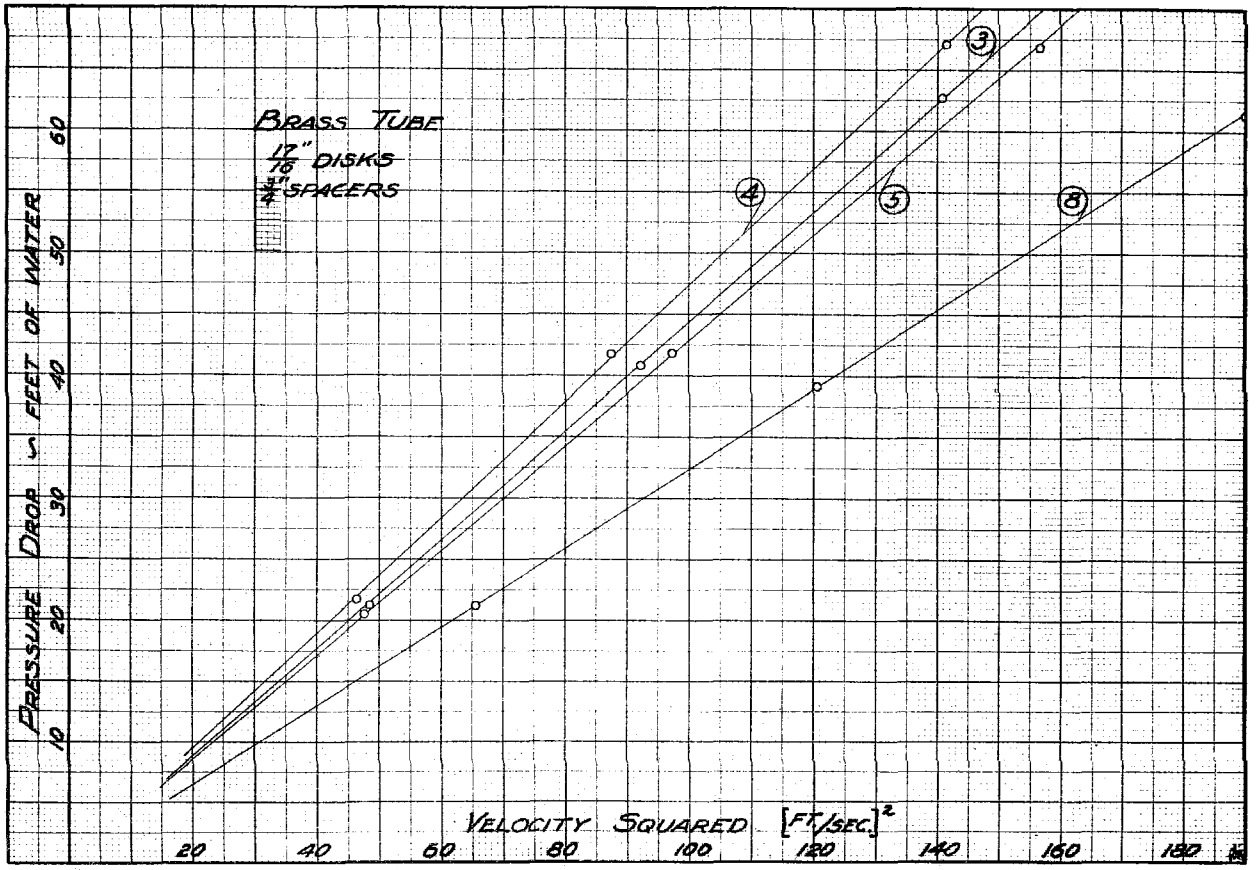

FIG. 20. TOTAL HEAD LOSS VERSUS VELOCITY SQUARED.

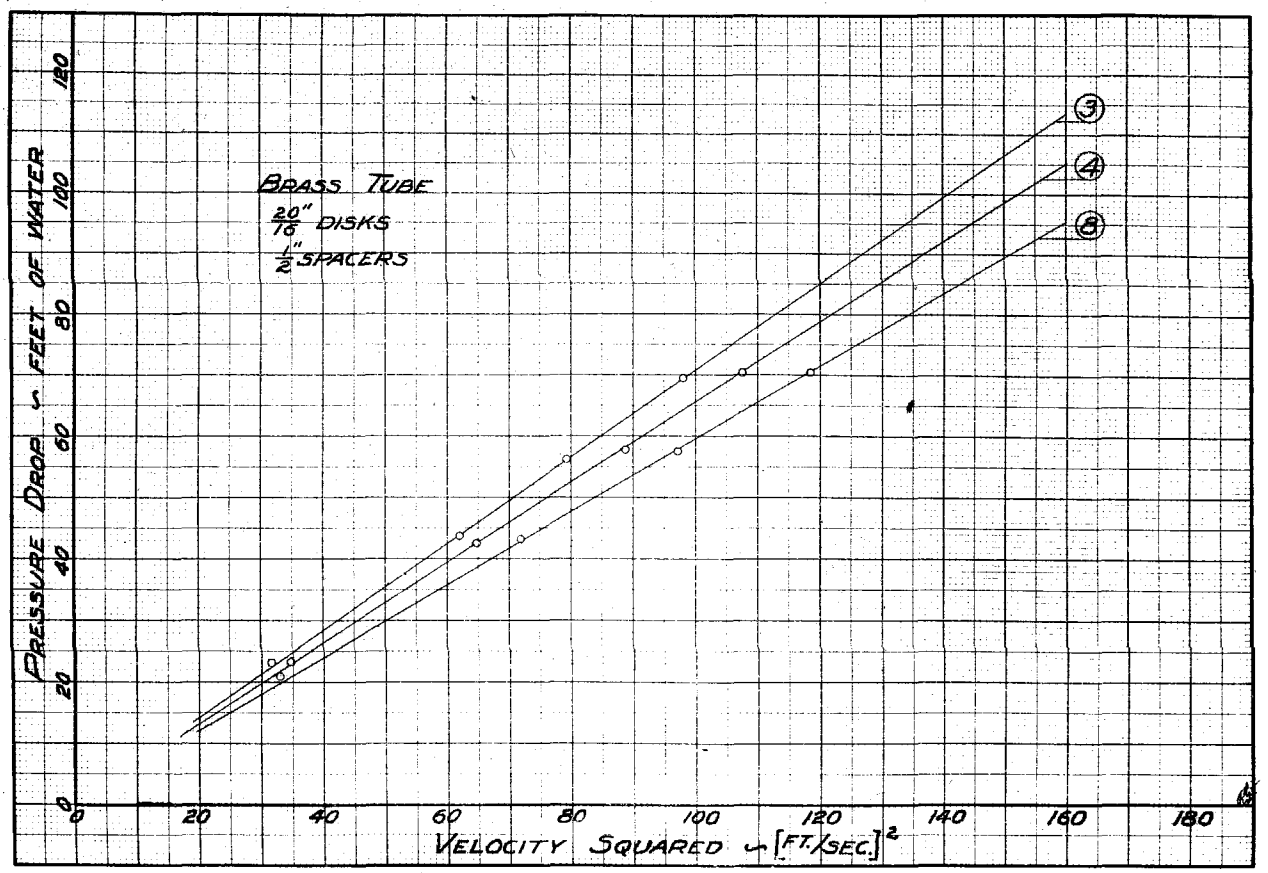

FIG. 21. TOTAL HEAD LOSS VERSUS VELOCITY SQUARED.

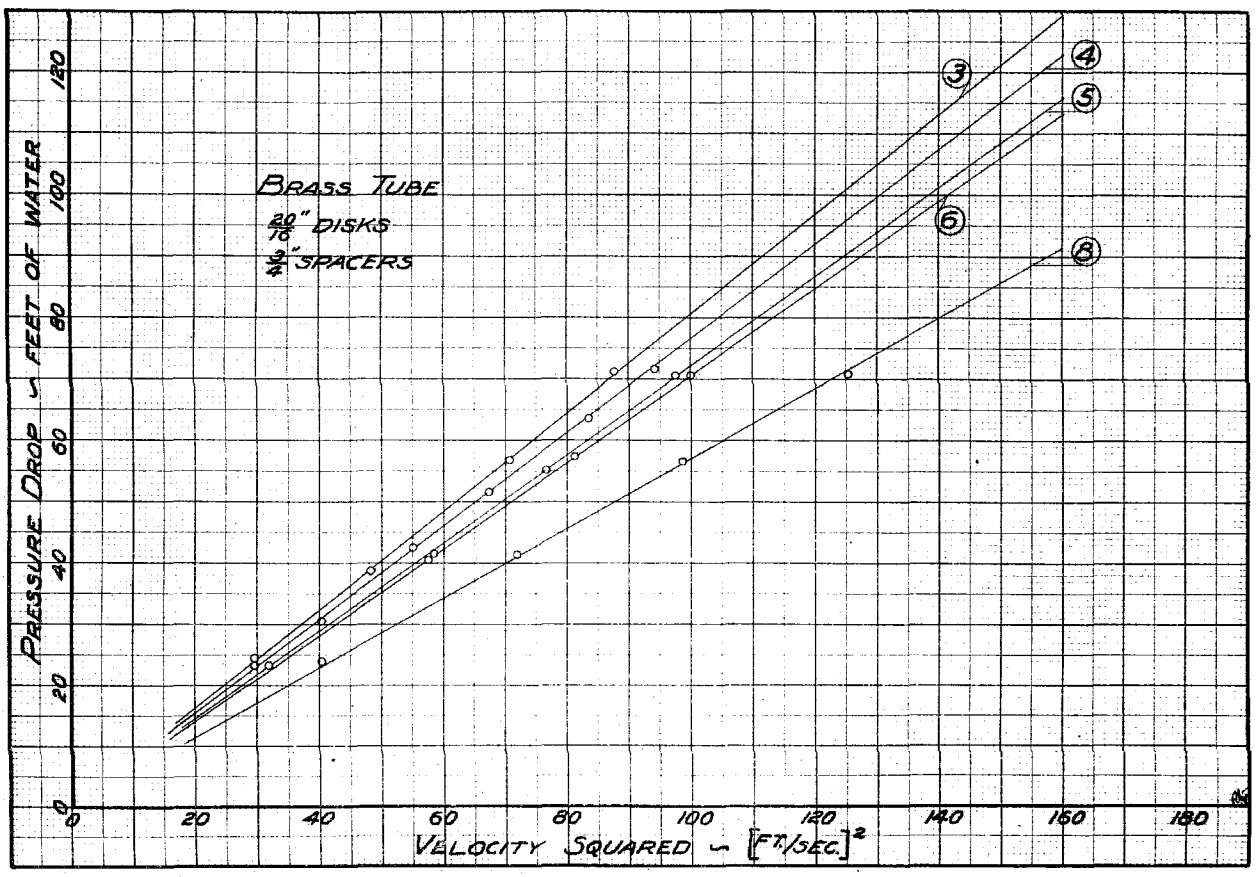

FIG. 22. TOTAL HEAD LOSS VERSUS VELOCITY SQUARED.

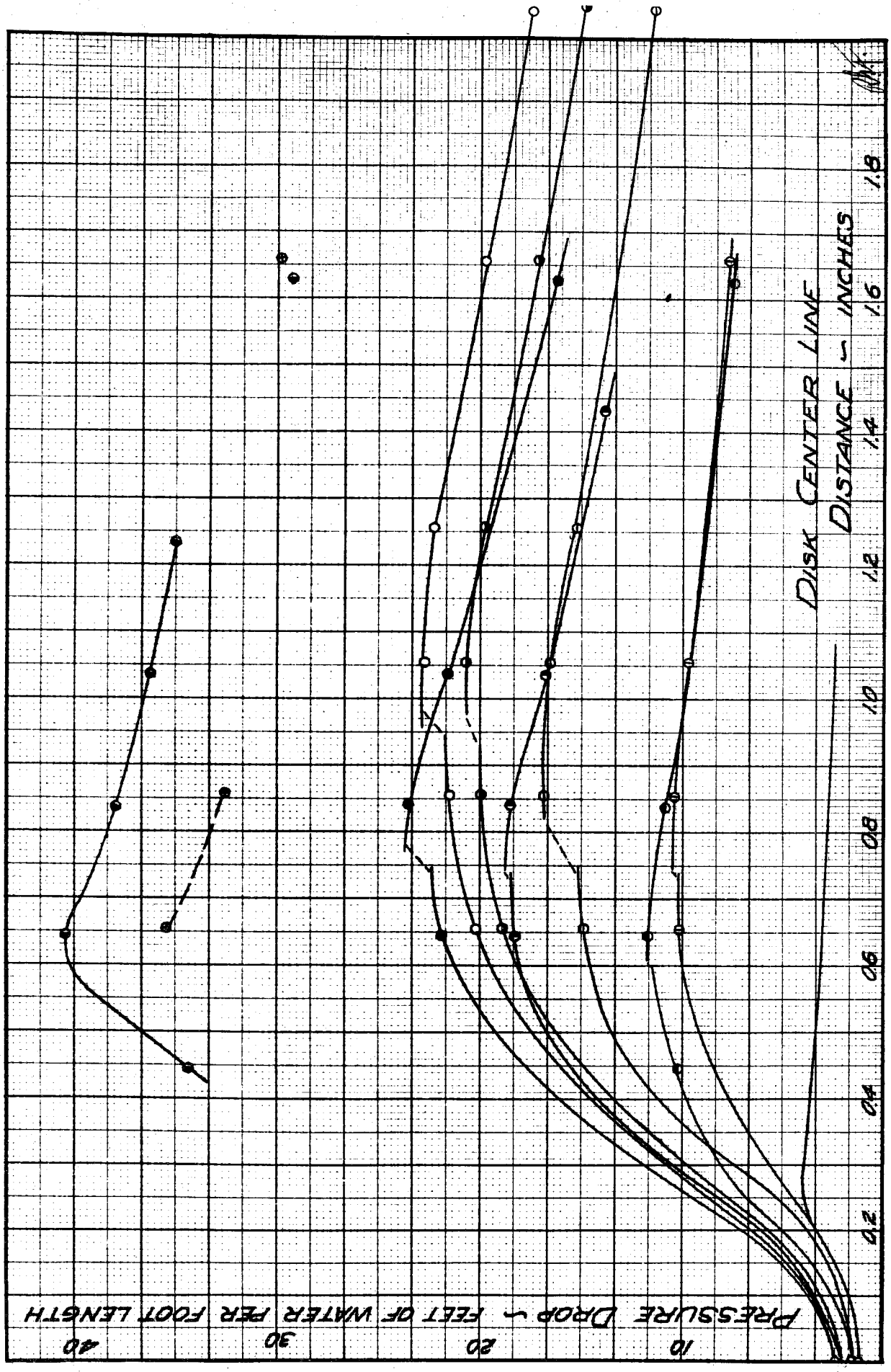

Fig. 23. Combined Experimental Results.

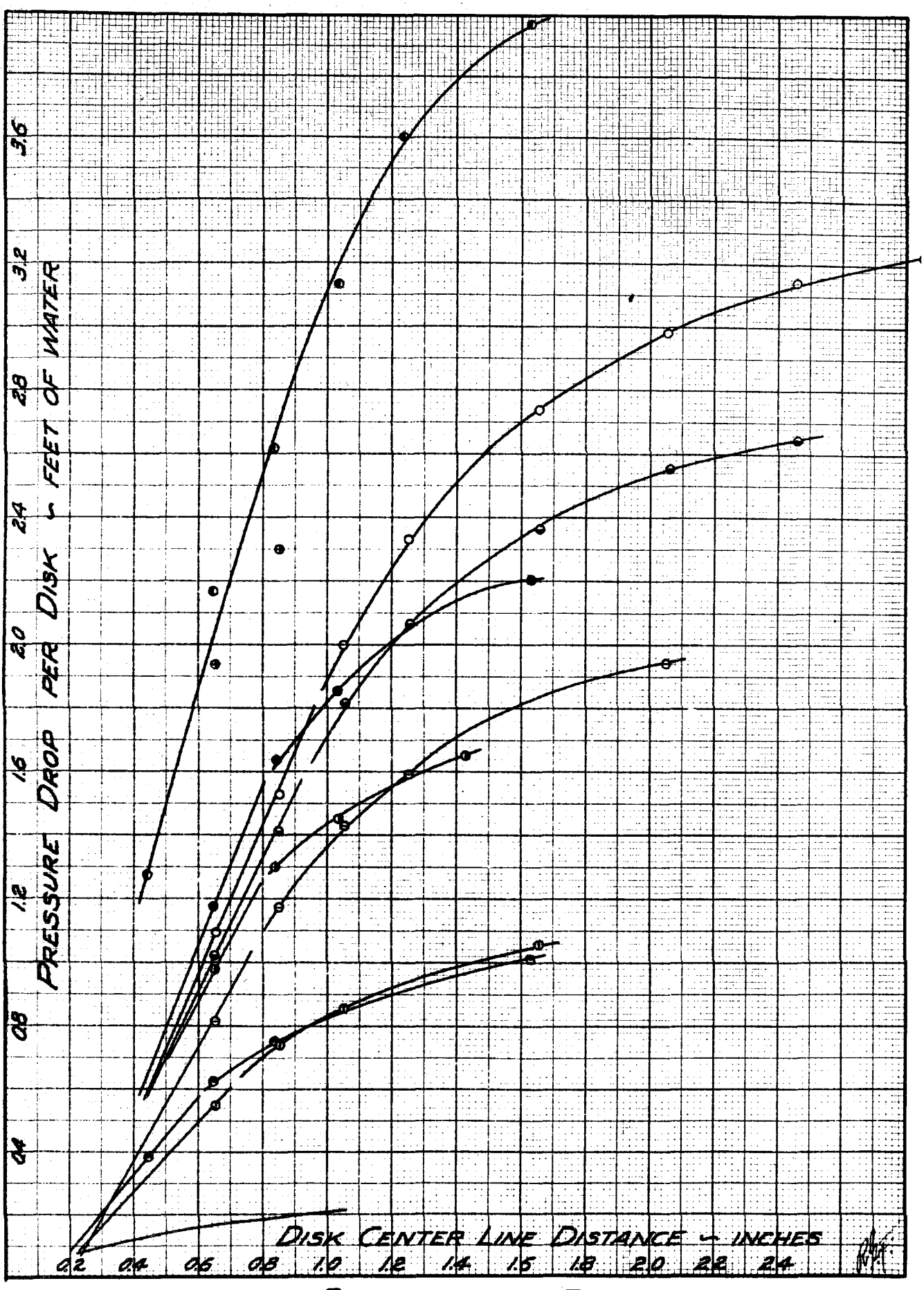

FIG. 24. COMBINED EXPERIMENTAL RESULTS.

◑	$\frac{13}{16}$" DISKS	$\frac{1}{2}$" SPACERS
⊖	$\frac{15}{16}$" DISKS	$\frac{1}{2}$" SPACERS
◓	$\frac{15}{16}$" DISKS	$\frac{3}{4}$" SPACERS
◒	$\frac{65}{64}$" DISKS	$\frac{1}{2}$" SPACERS
◑	$\frac{65}{64}$" DISKS	$\frac{3}{4}$" SPACERS
○	$\frac{17}{16}$" DISKS	$\frac{1}{2}$" SPACERS
●	$\frac{17}{16}$" DISKS	$\frac{3}{4}$" SPACERS
⊕	$\frac{20}{16}$" DISKS	$\frac{1}{2}$" SPACERS
◐	$\frac{20}{16}$" DISKS	$\frac{3}{4}$" SPACERS

FIG. 25(a). POINTS FOR FIGS. 23, 24, AND 27.

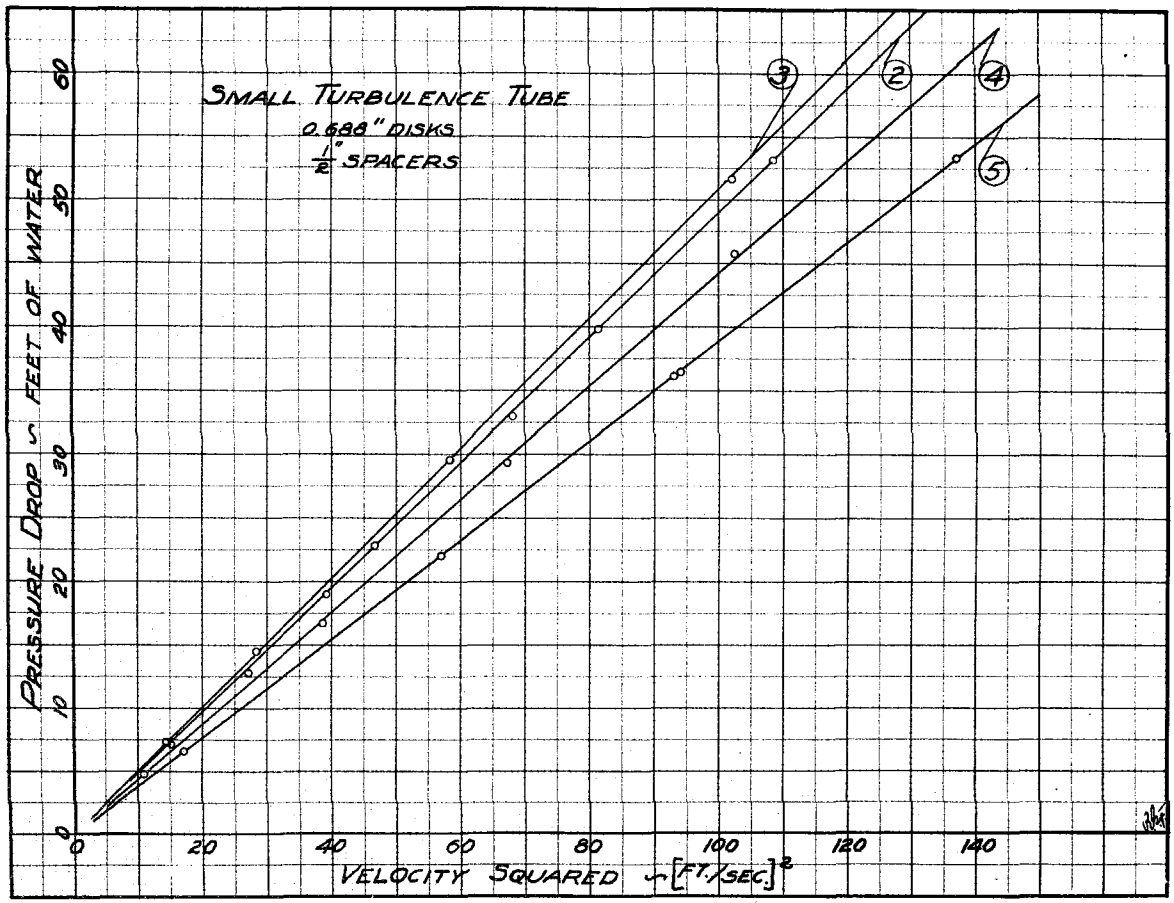

FIG. 25(b) TOTAL HEAD LOSS VERSUS VELOCITY SQUARED.

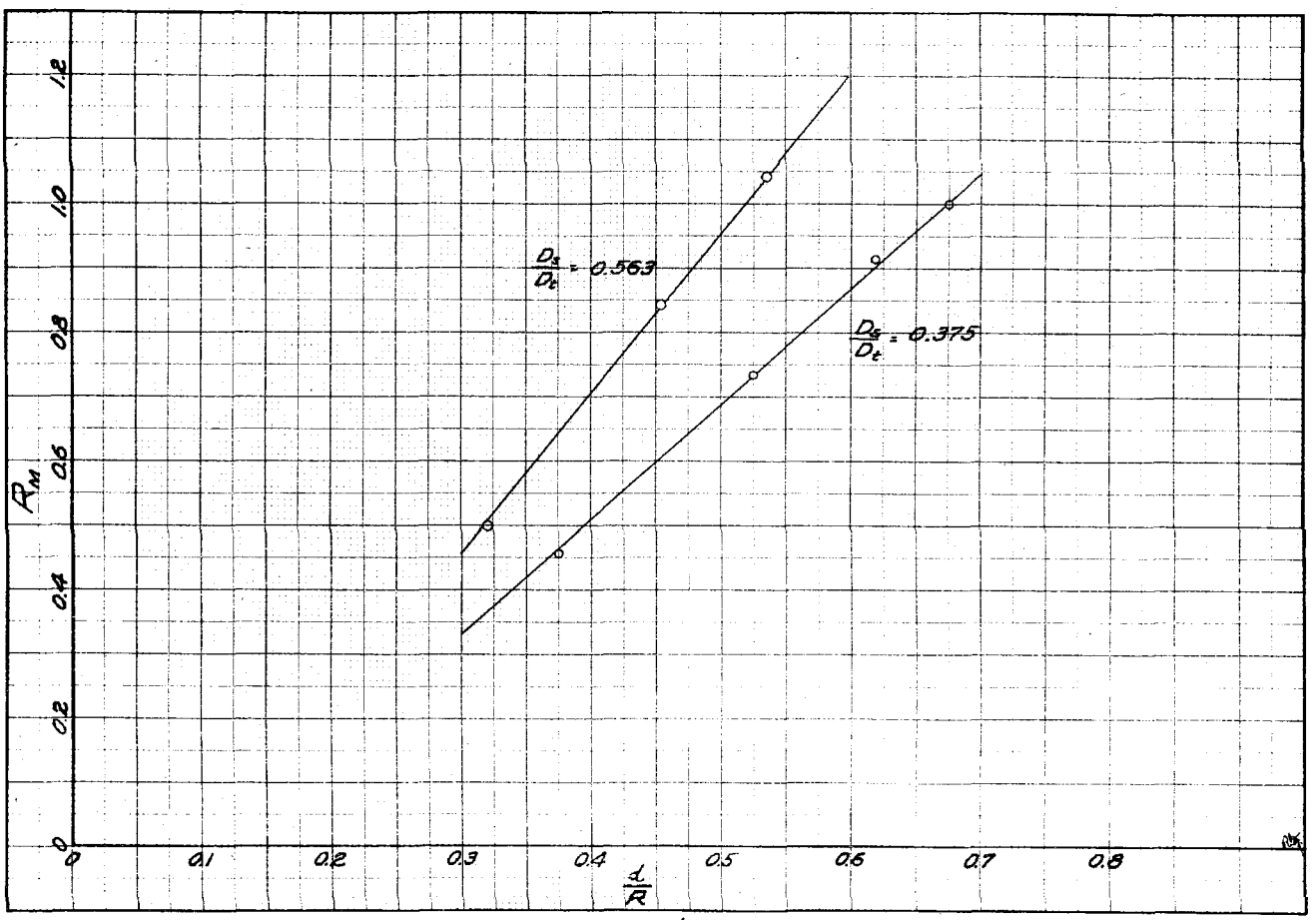

FIG. 26. R_M VERSUS $\frac{d}{R}$ FOR GIVEN SPACER SIZES.

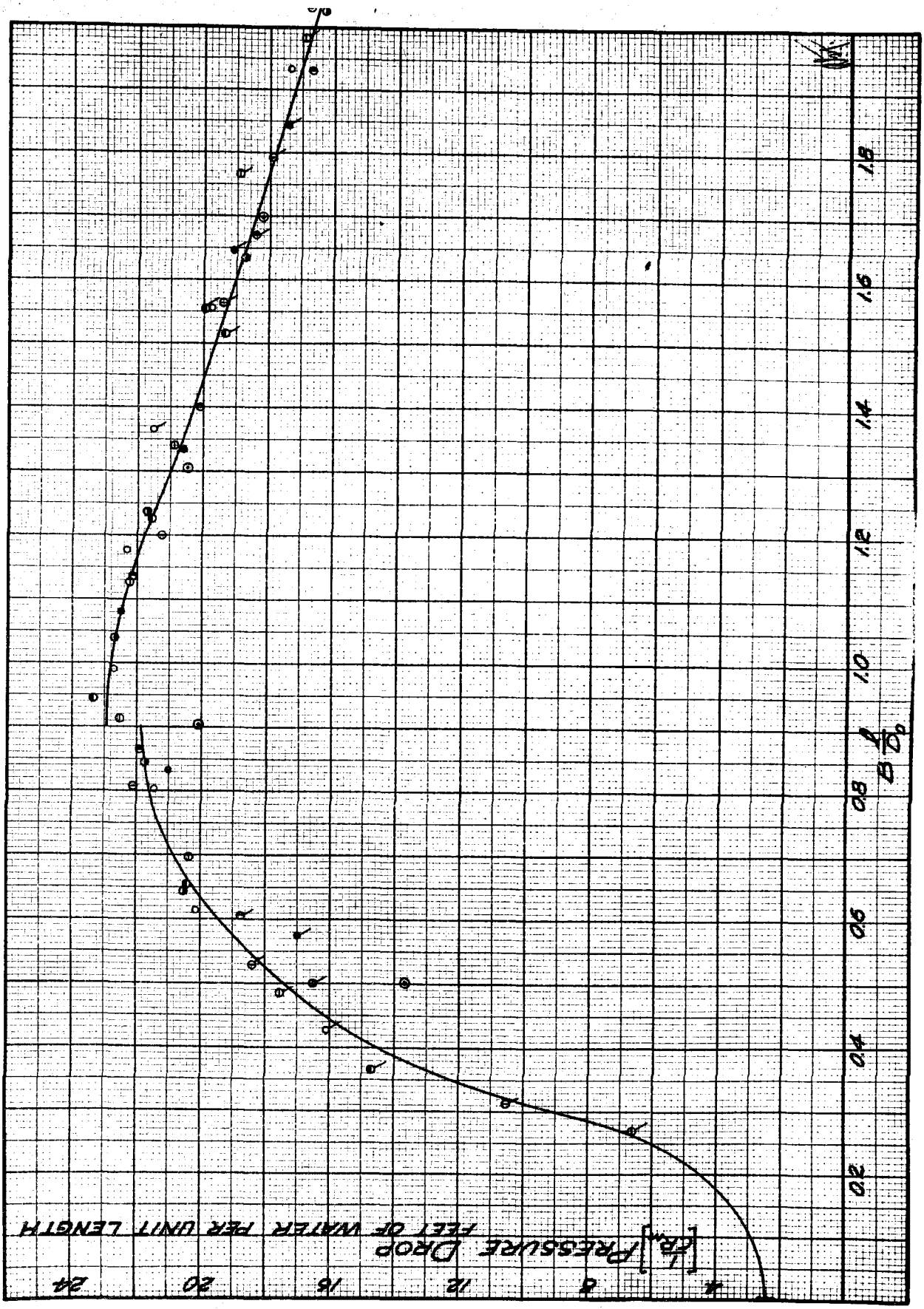

FIG. 27. COMBINED EXPERIMENTAL RESULTS WITH CORRECTION FACTORS.

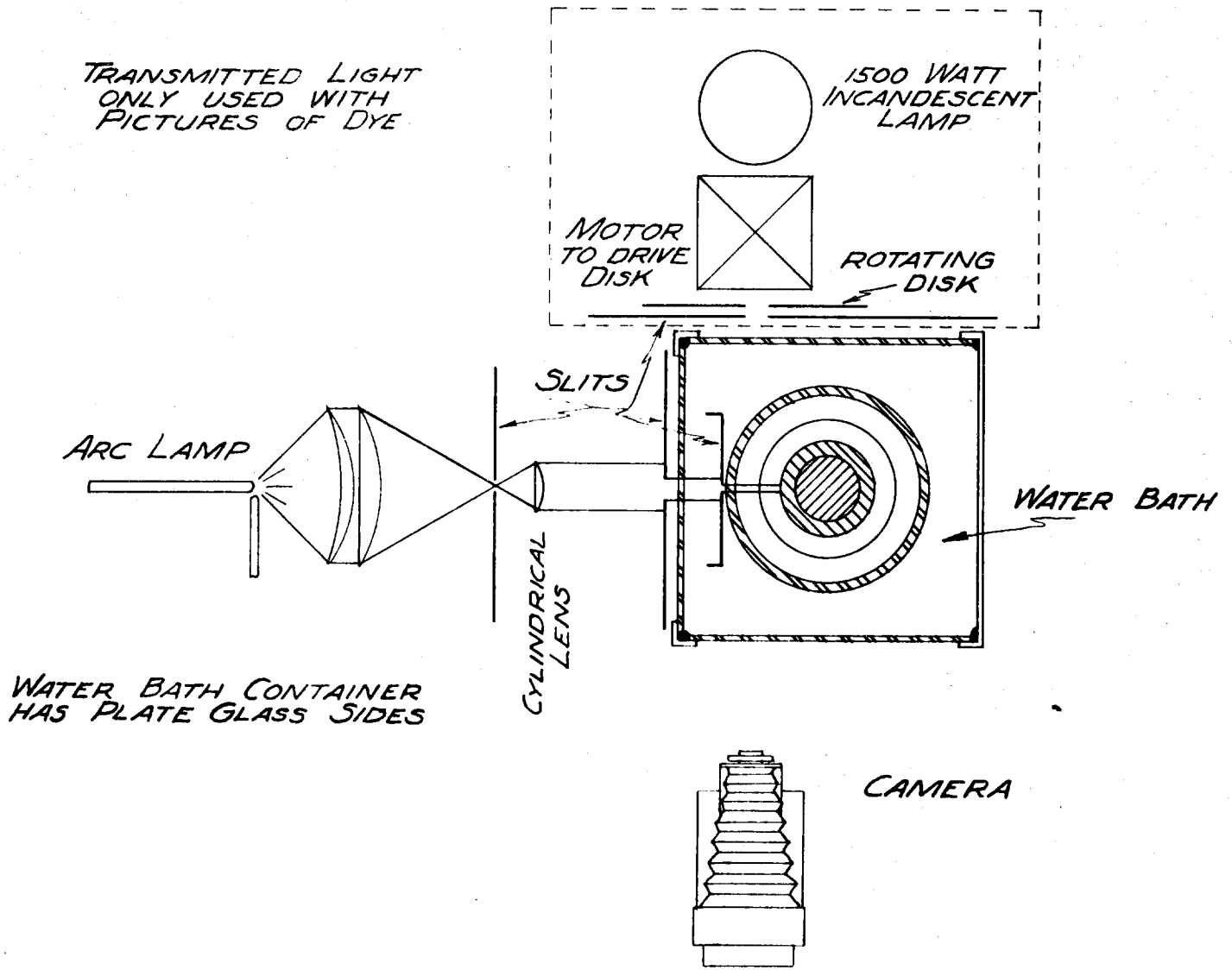

FIG. 28. APPARATUS FOR PHOTOGRAPHIC STUDIES.

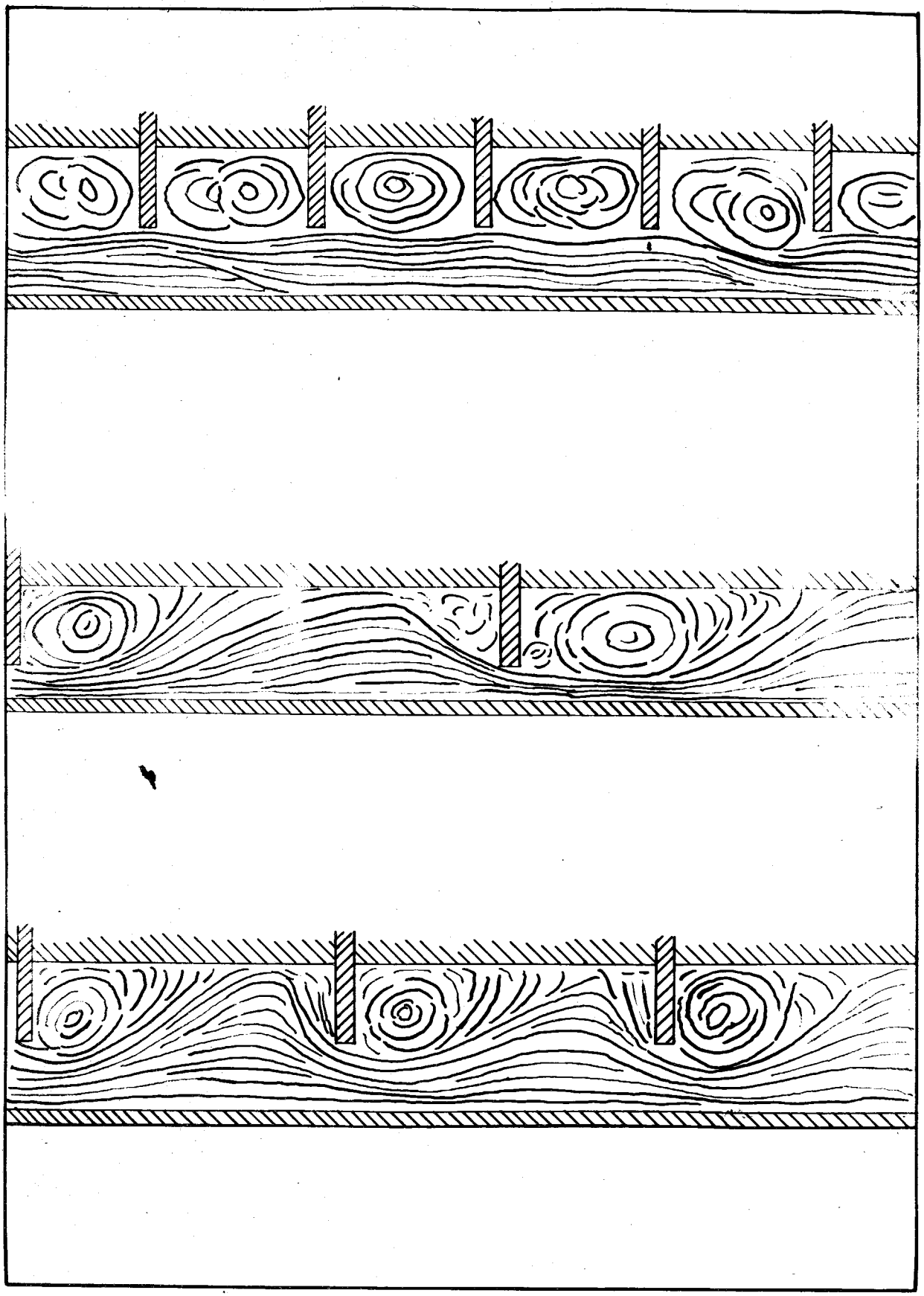

FIG. 23. GENERAL TYPES OF FLOW.

INDEX OF PHOTOGRAPHS

DOWNSTREAM CONDITIONS

Picture No.	Distribution		Page
93A	1-20/16" disk	½" spacers	71
94B	1-17/16" disk	"	72
95A	1-15/16" disk	"	72
96A	65/64" disk	6-½" spacers	73
97A	65/64" disk (solid)	½" spacer	73

19

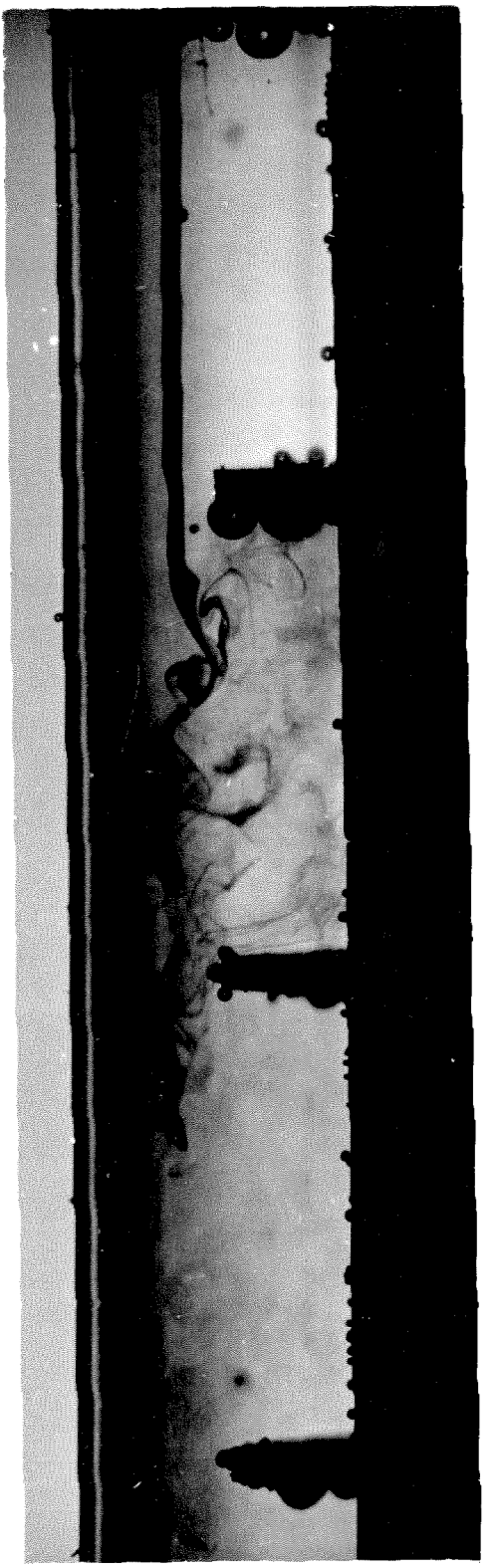

21

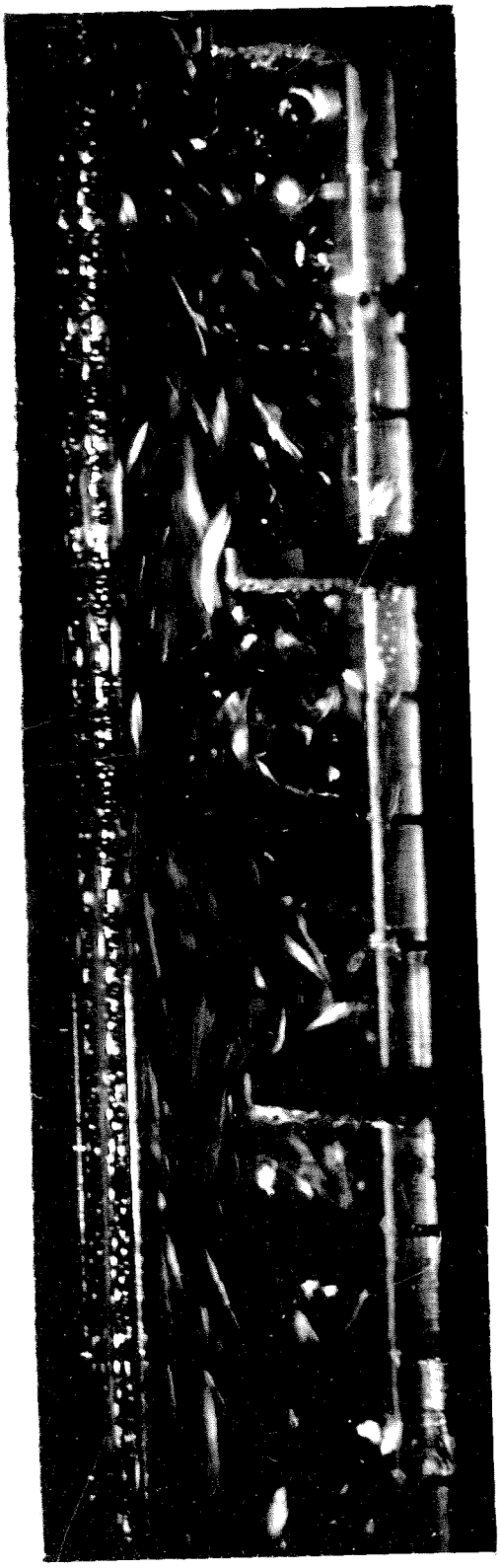

34

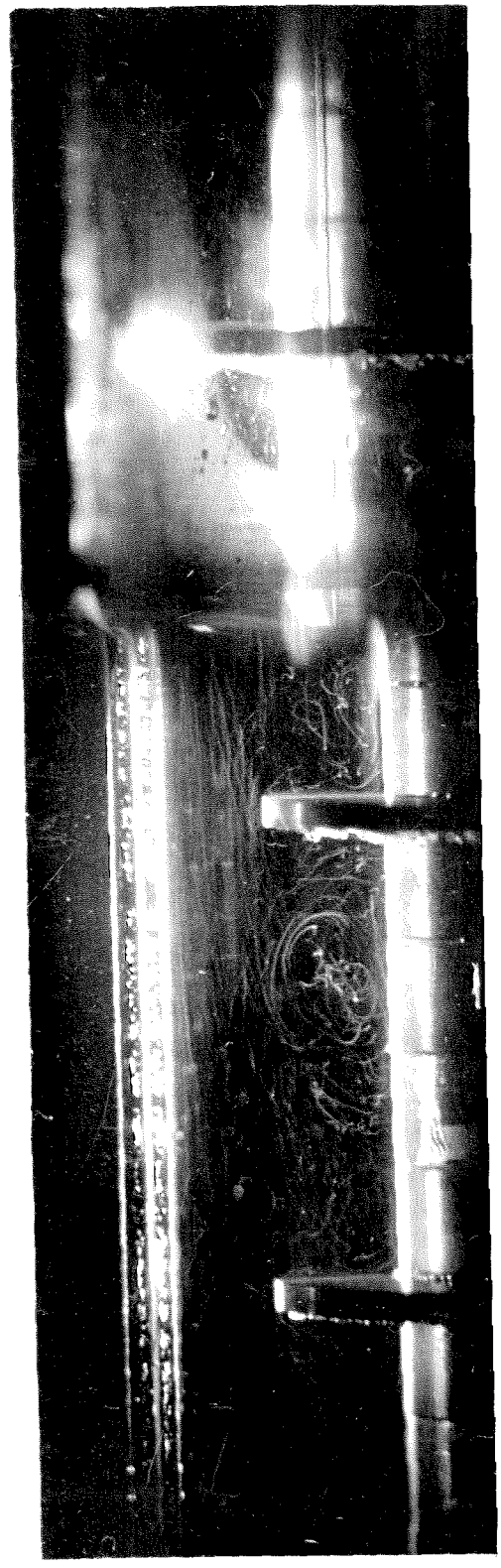

35

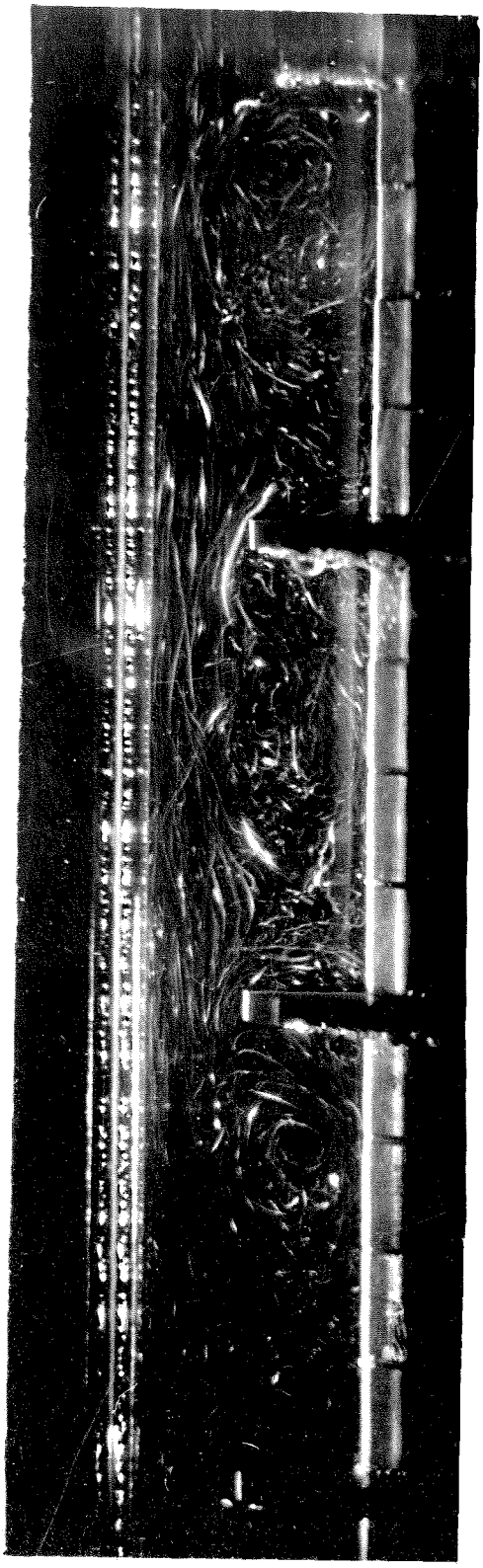

36B

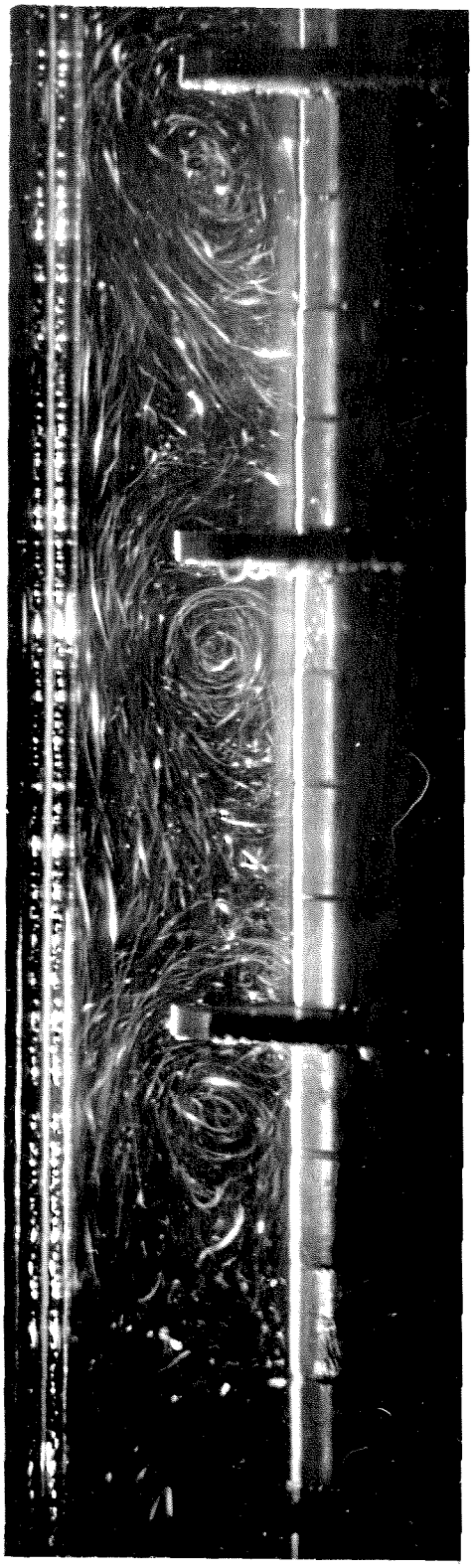

36A

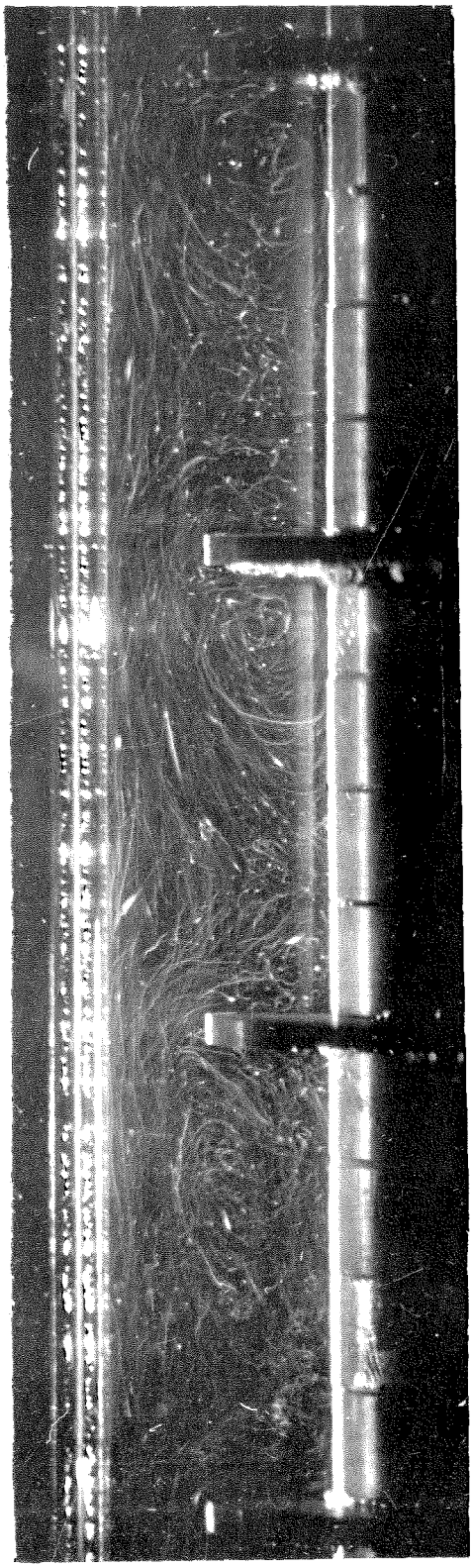

37

40 A

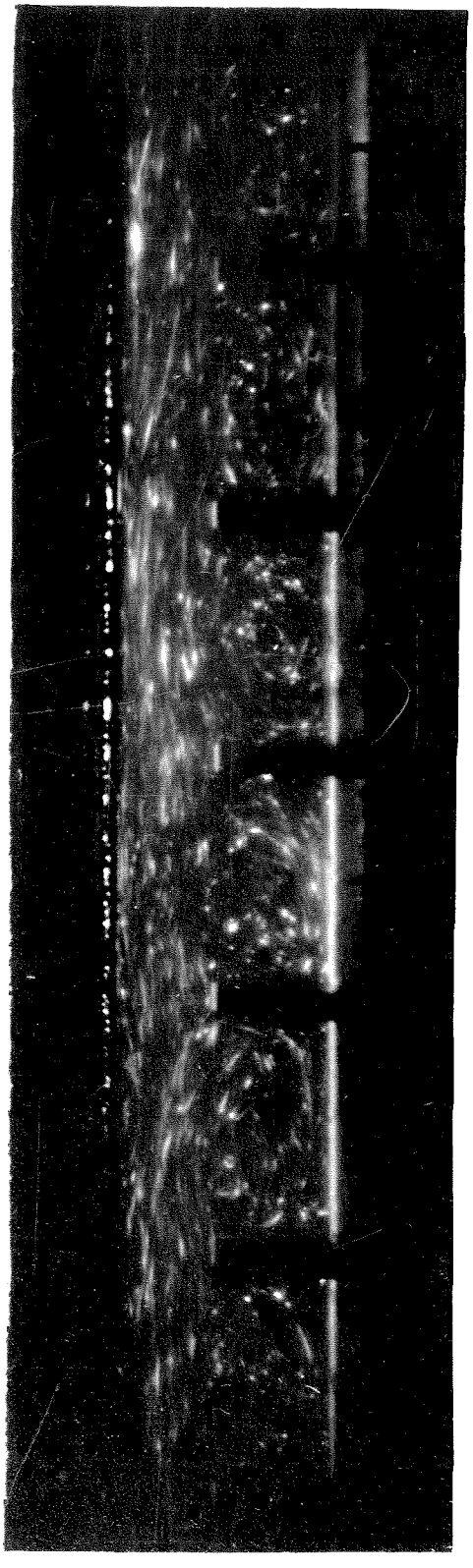

42 A

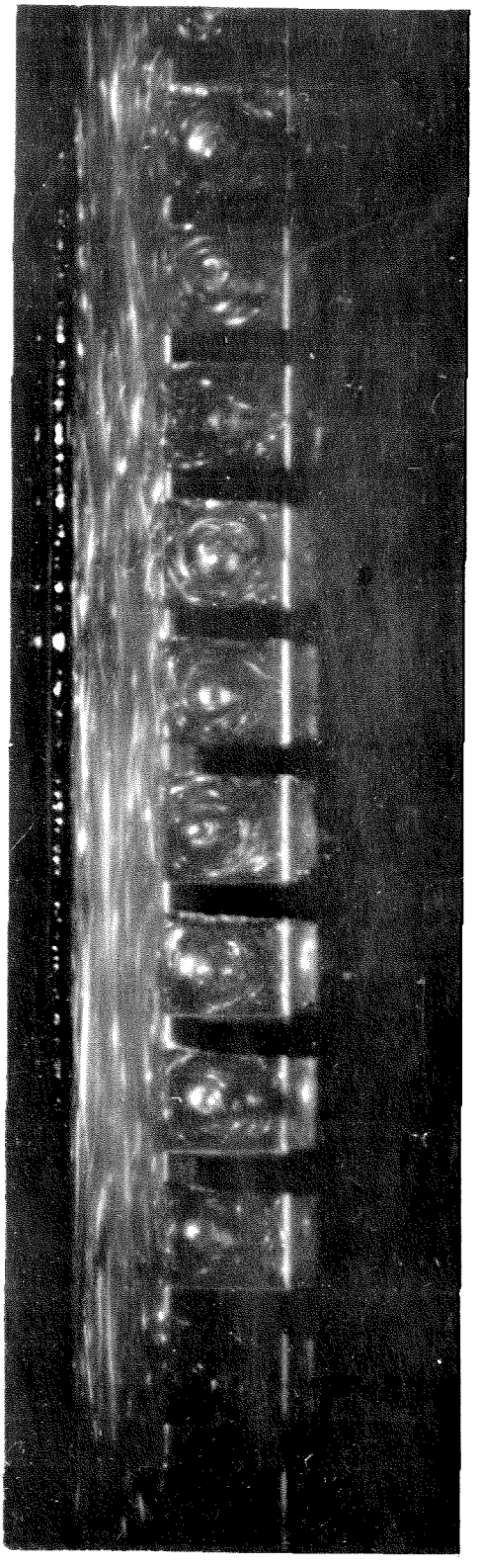

43 B

4-6 A

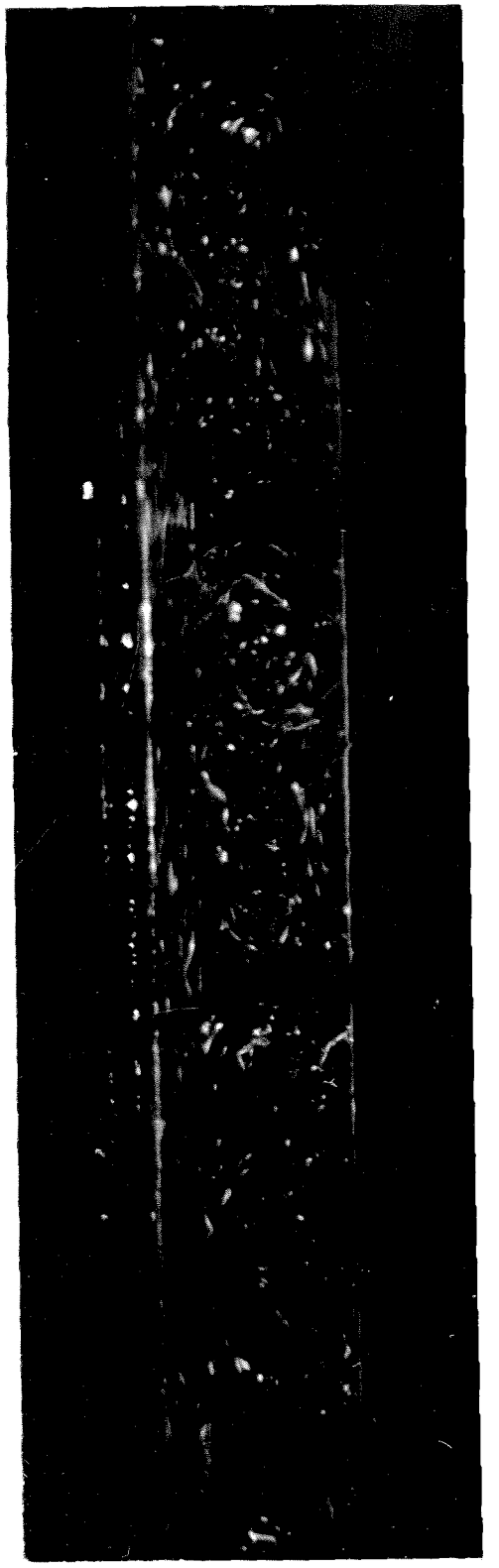

5 2A

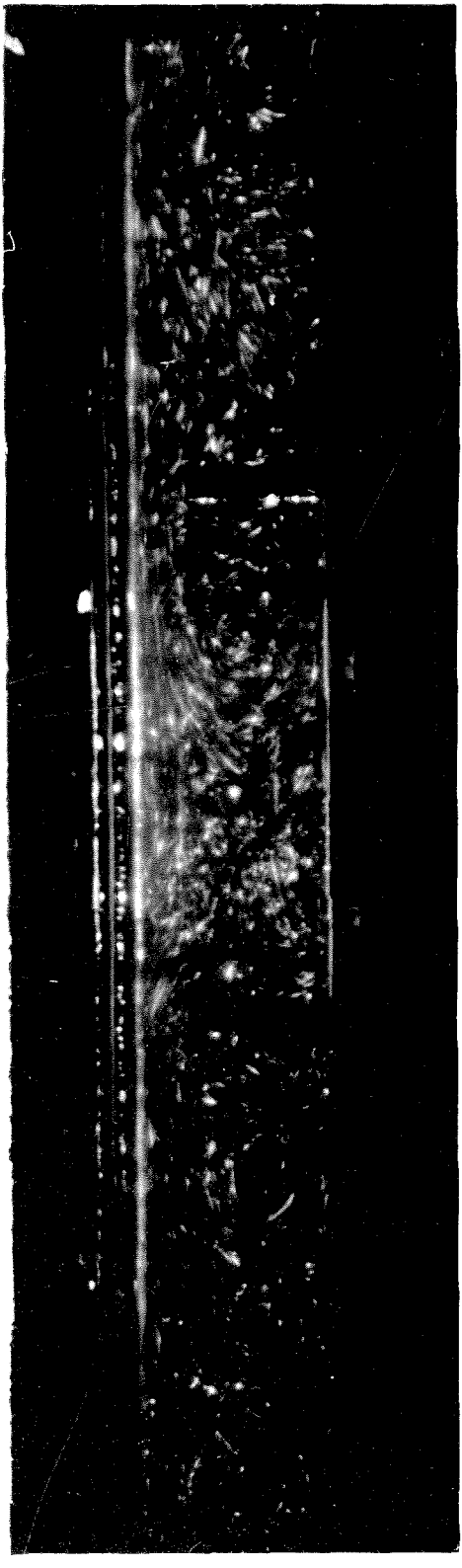

53 B

54 A

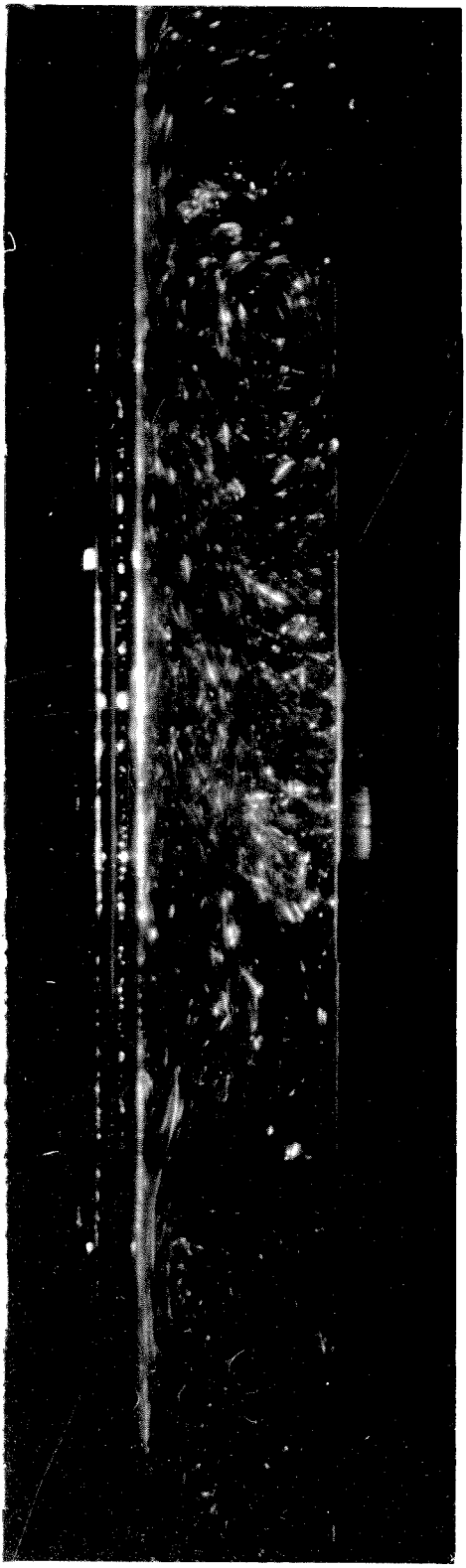

56 A

58 A

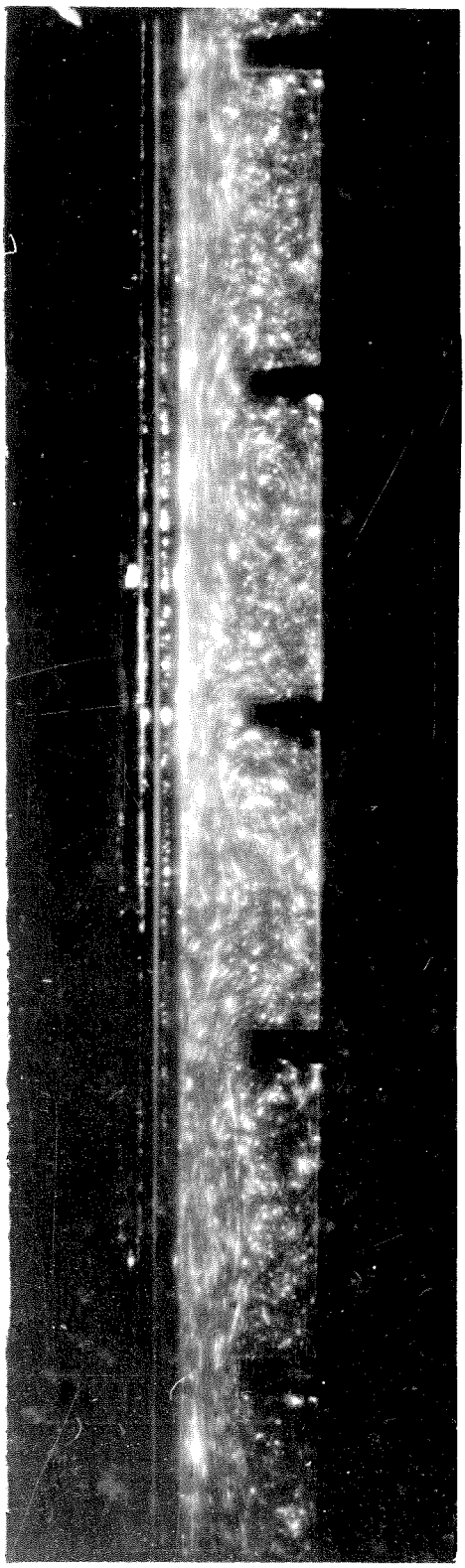

60 B

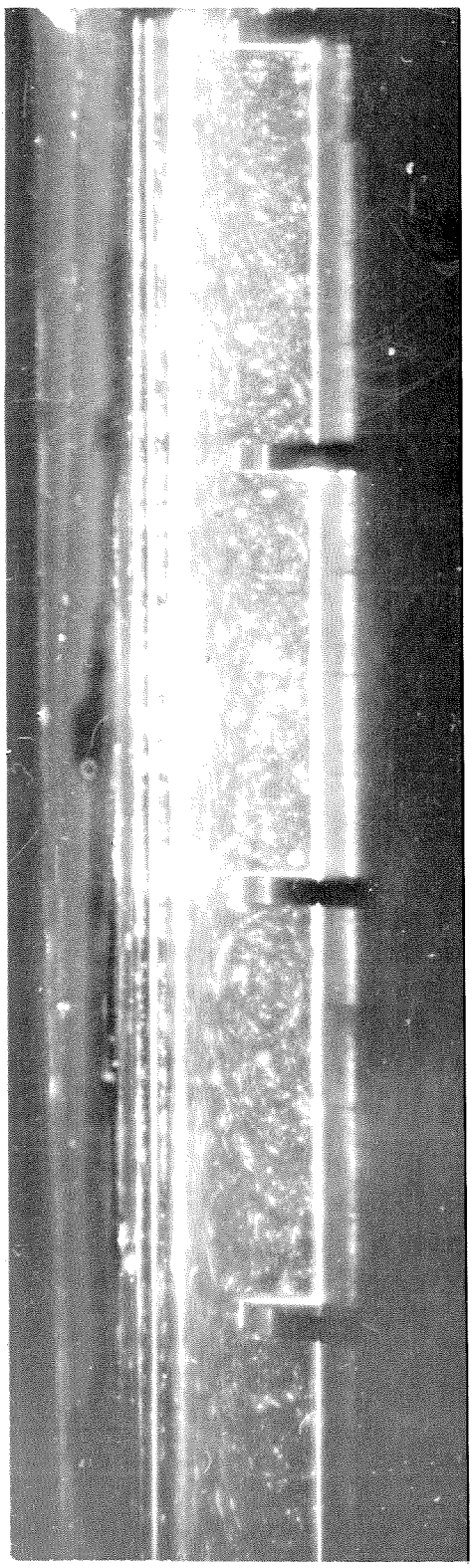

62 B

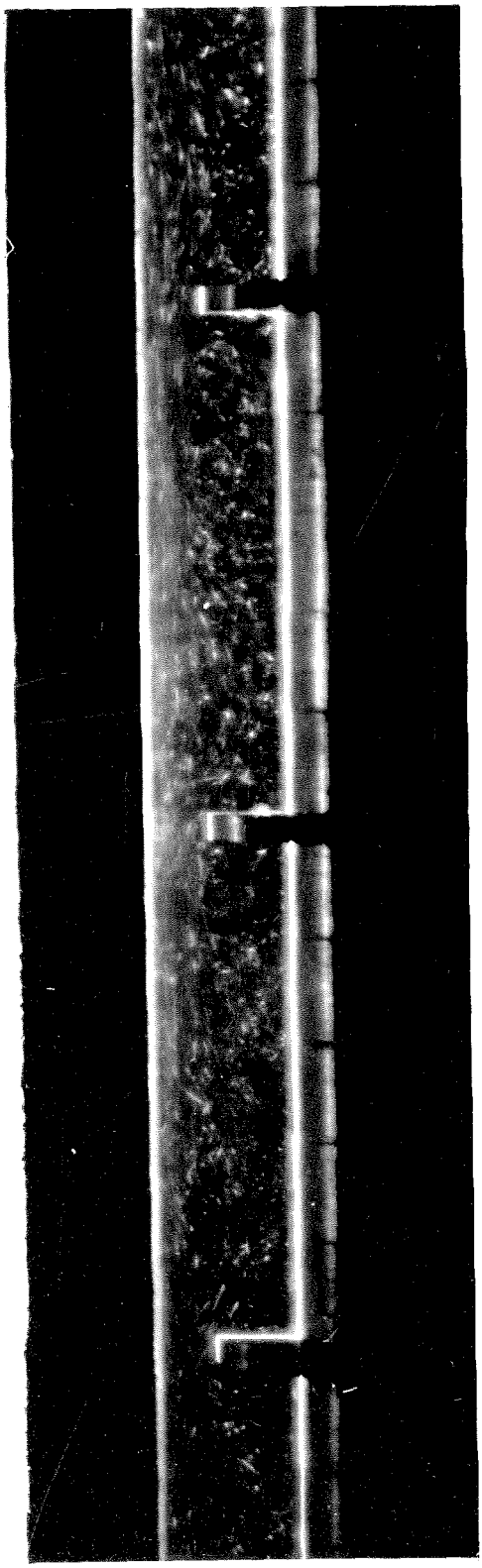

63B

64B

65 B

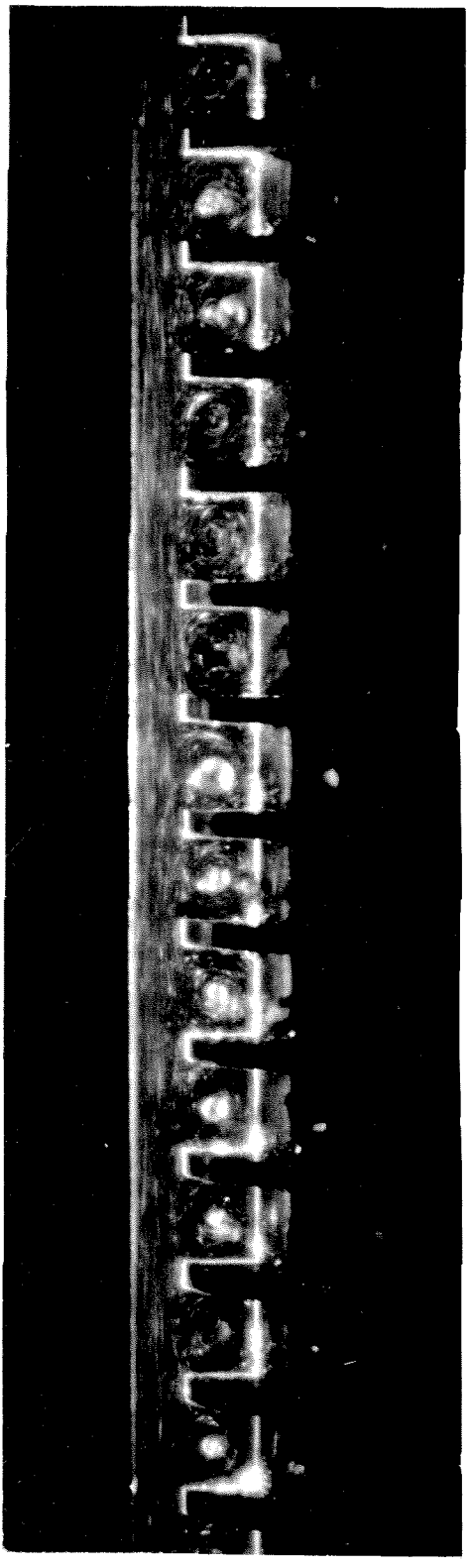

66 A

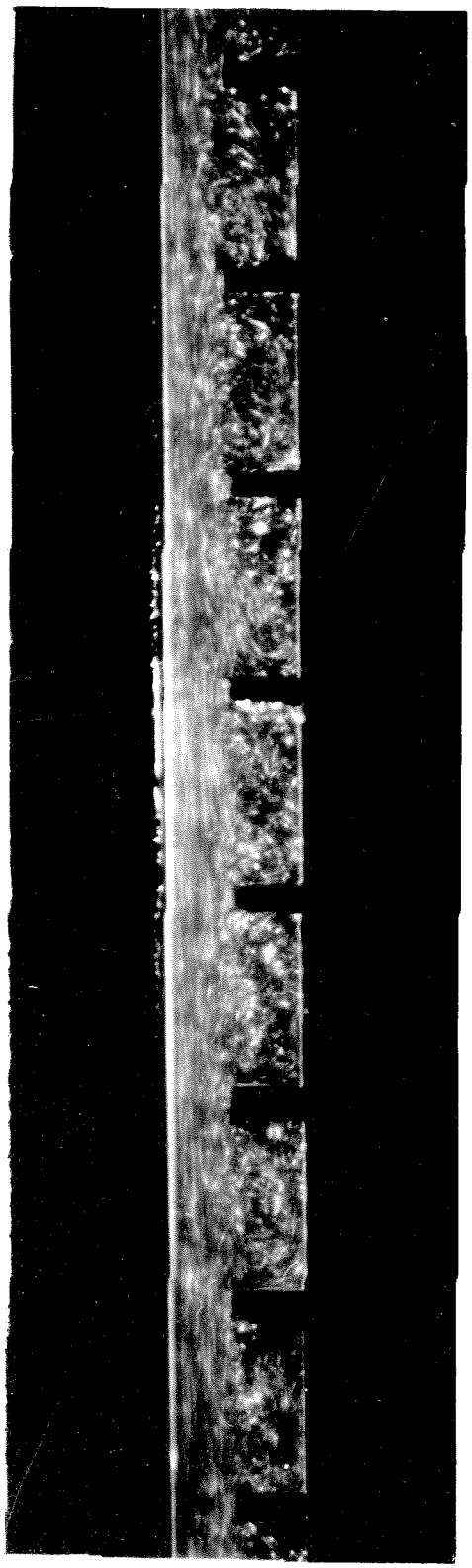

67A

68B

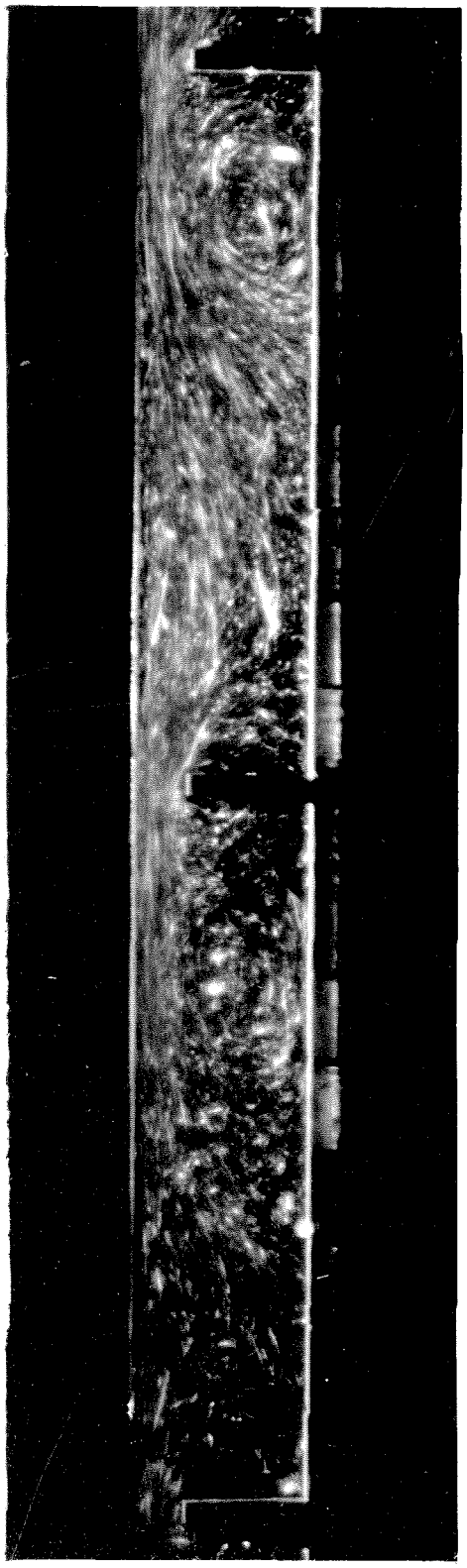

69B

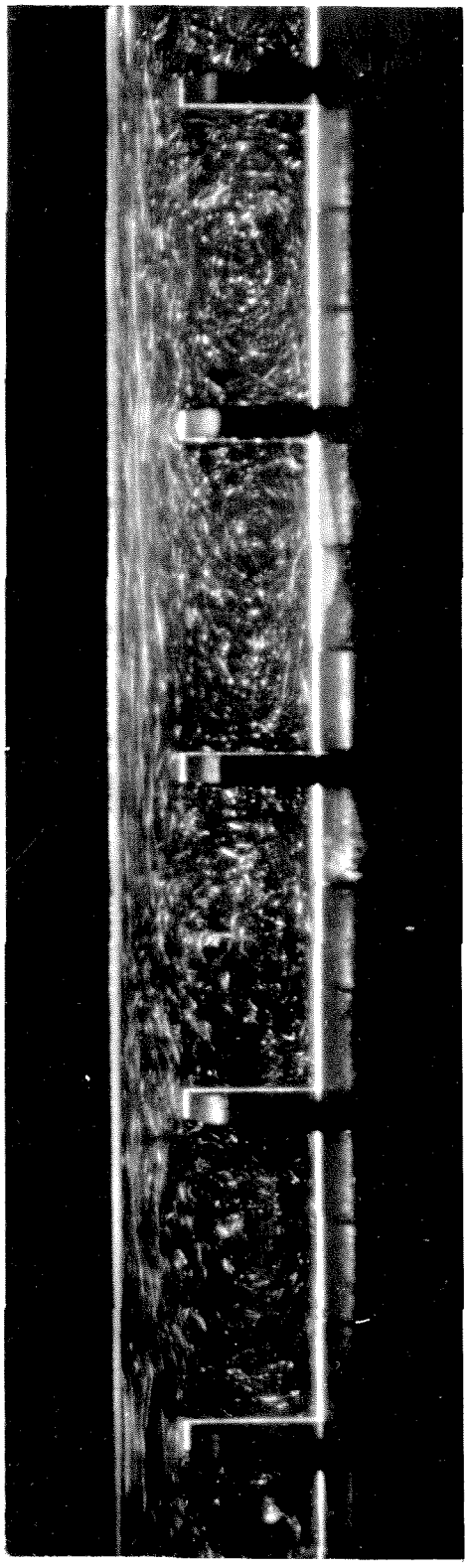

71B

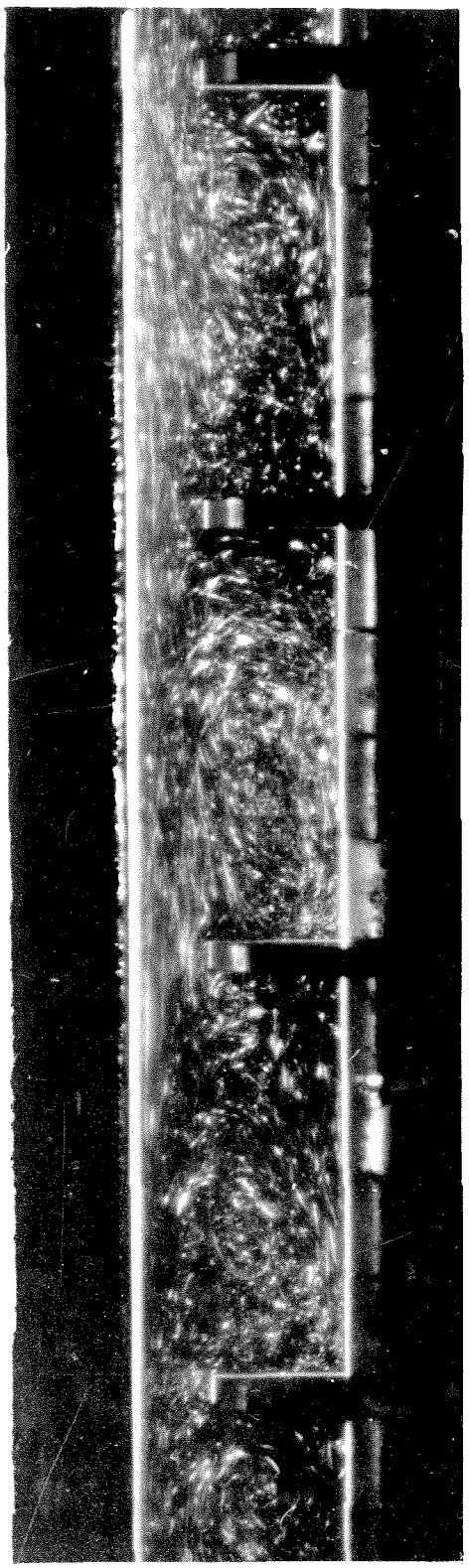

72 B

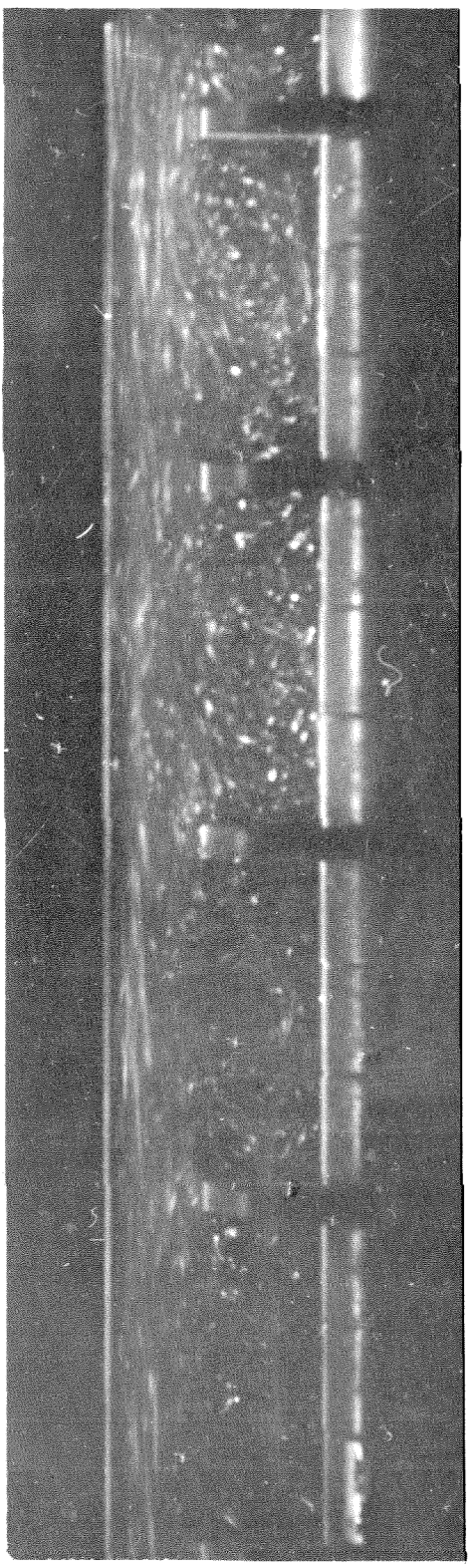

73 A

75A

76 B

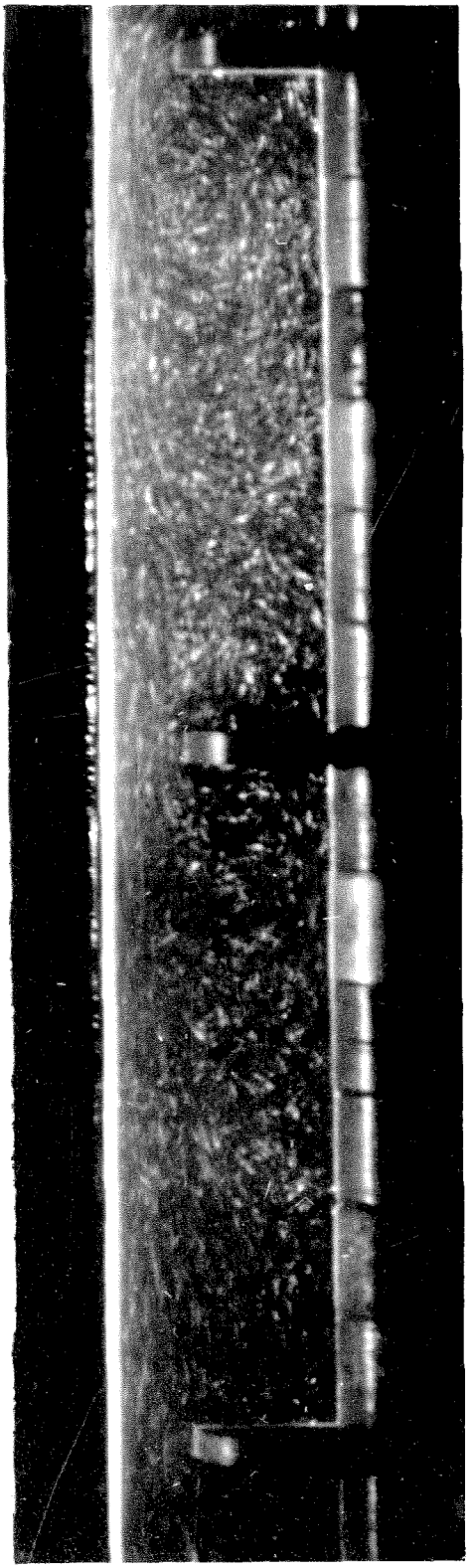

77 B

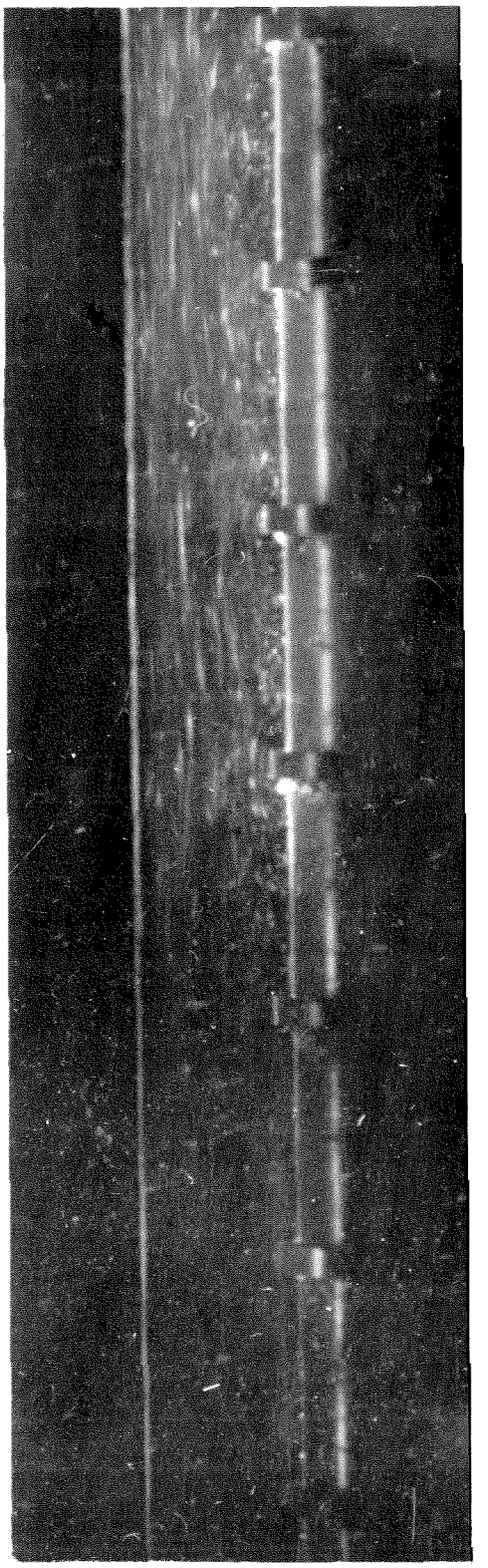

79 A

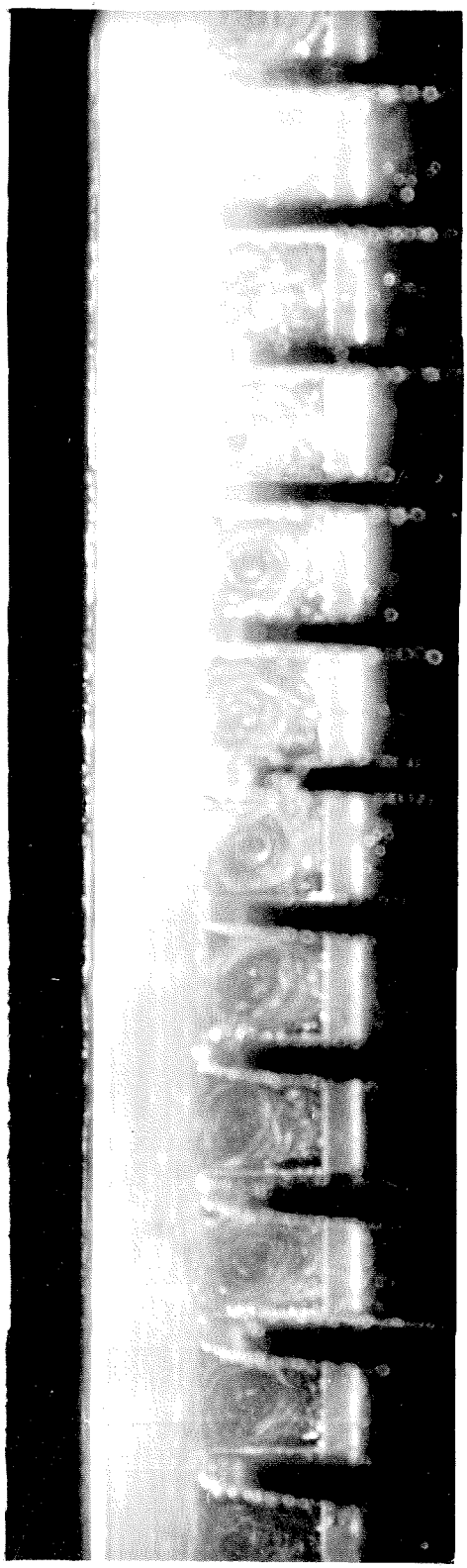

80A

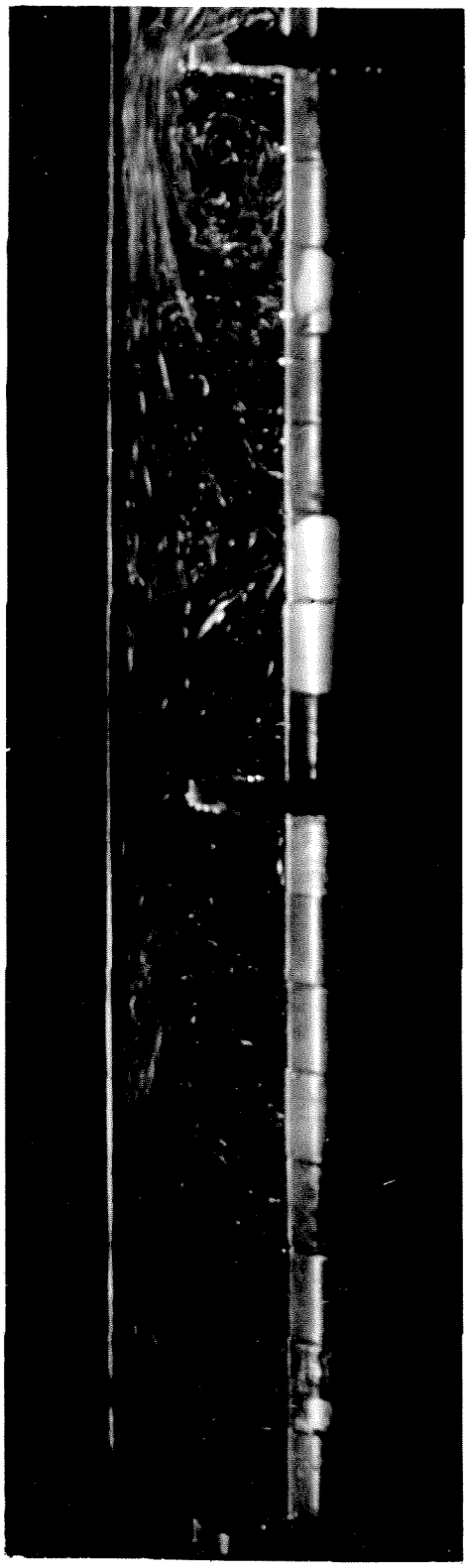

83A

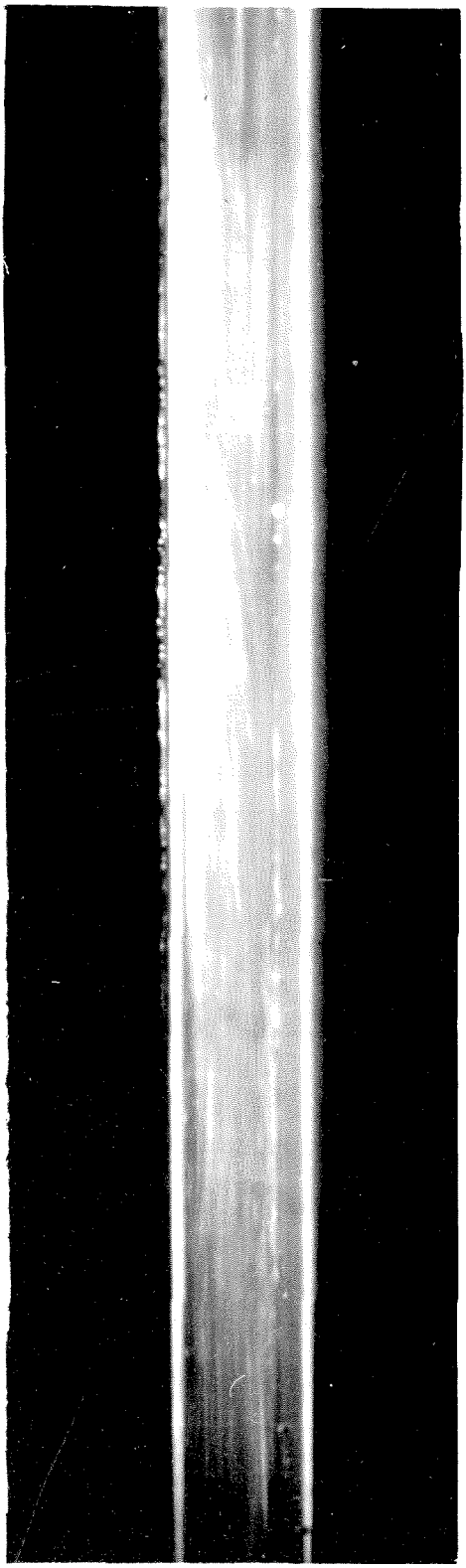

84A

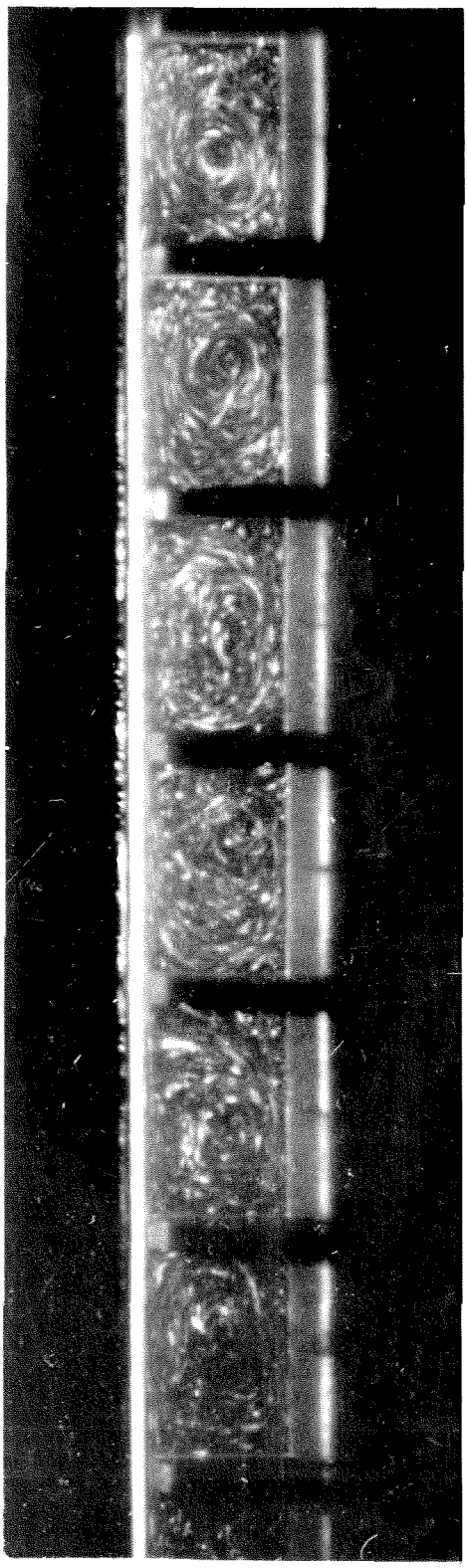

85B

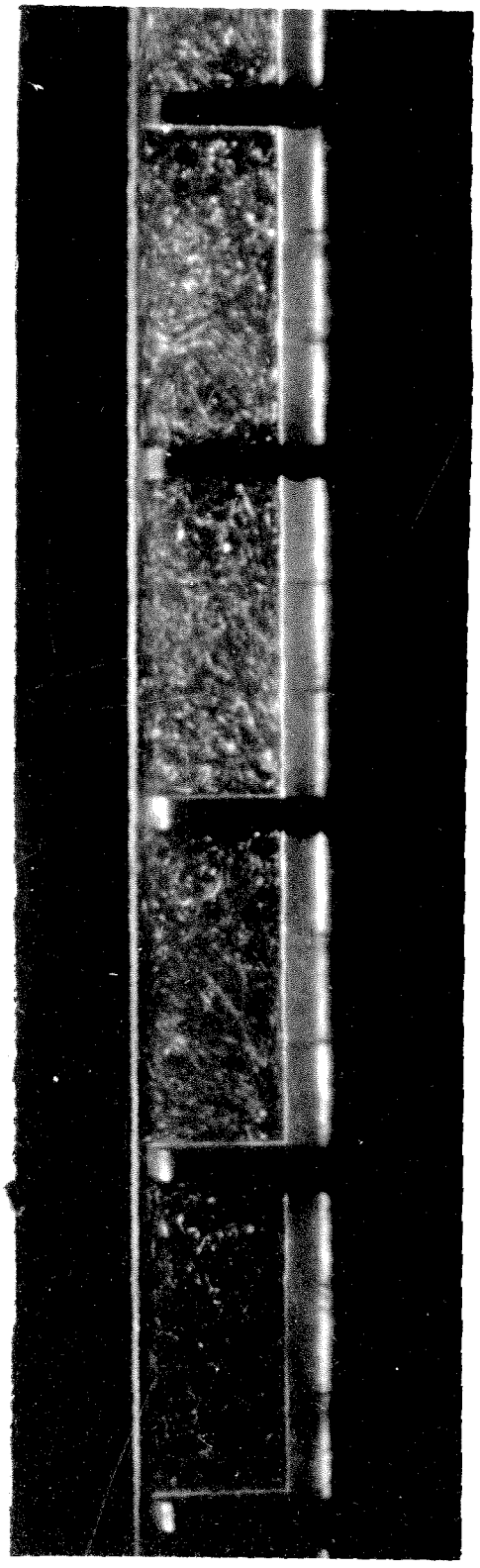

86 B

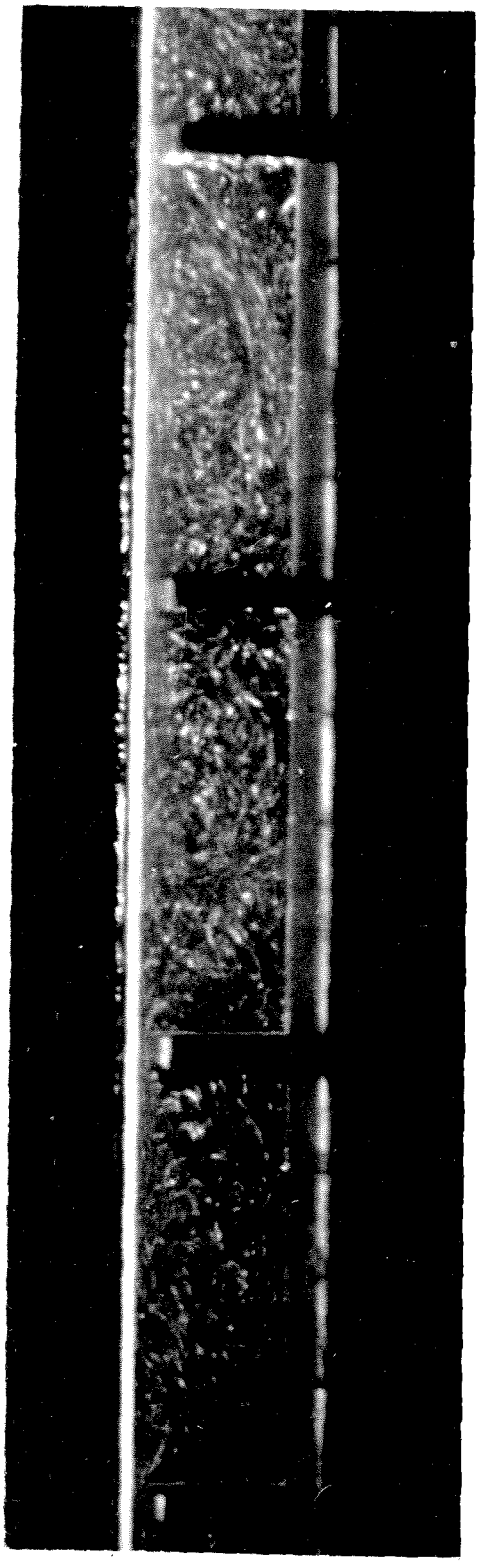

87 B

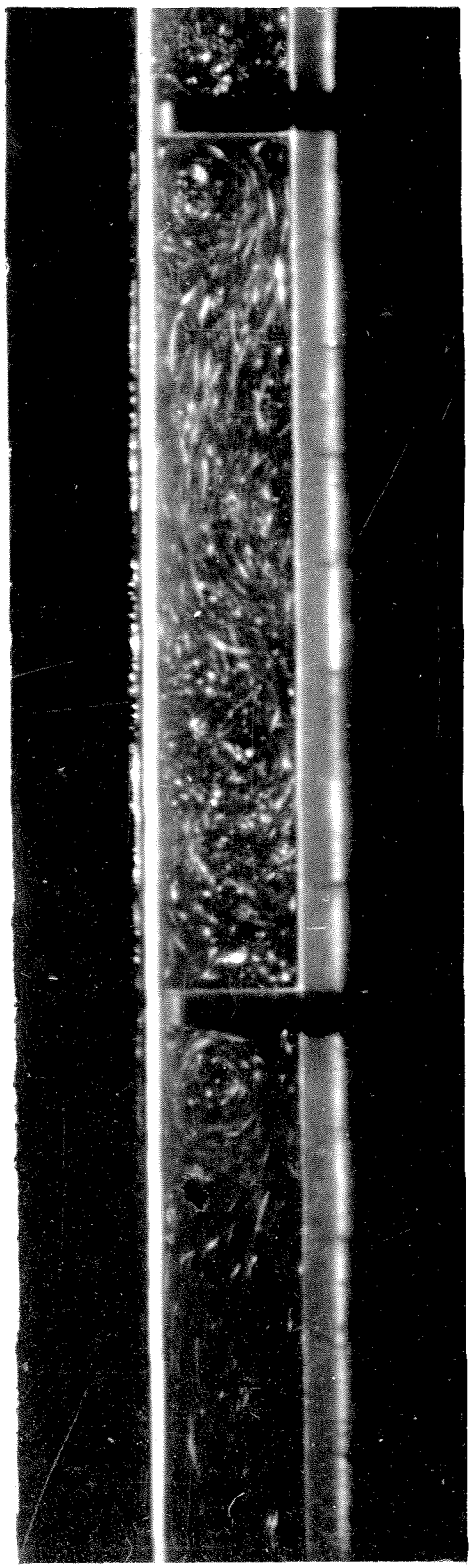

88A

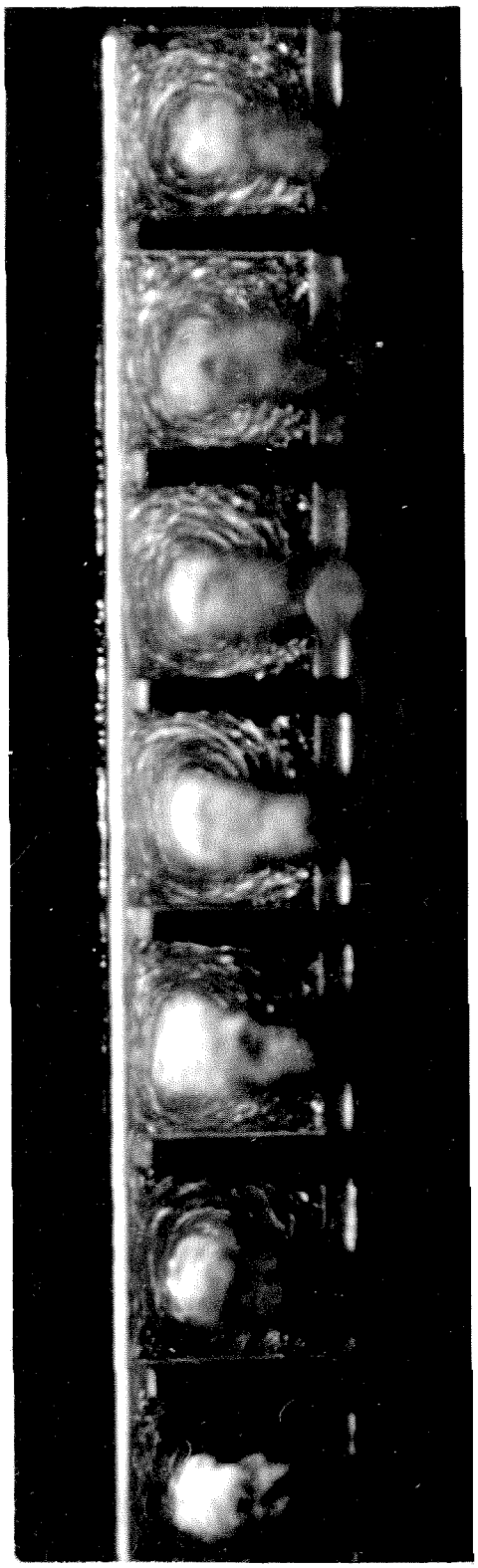

89B

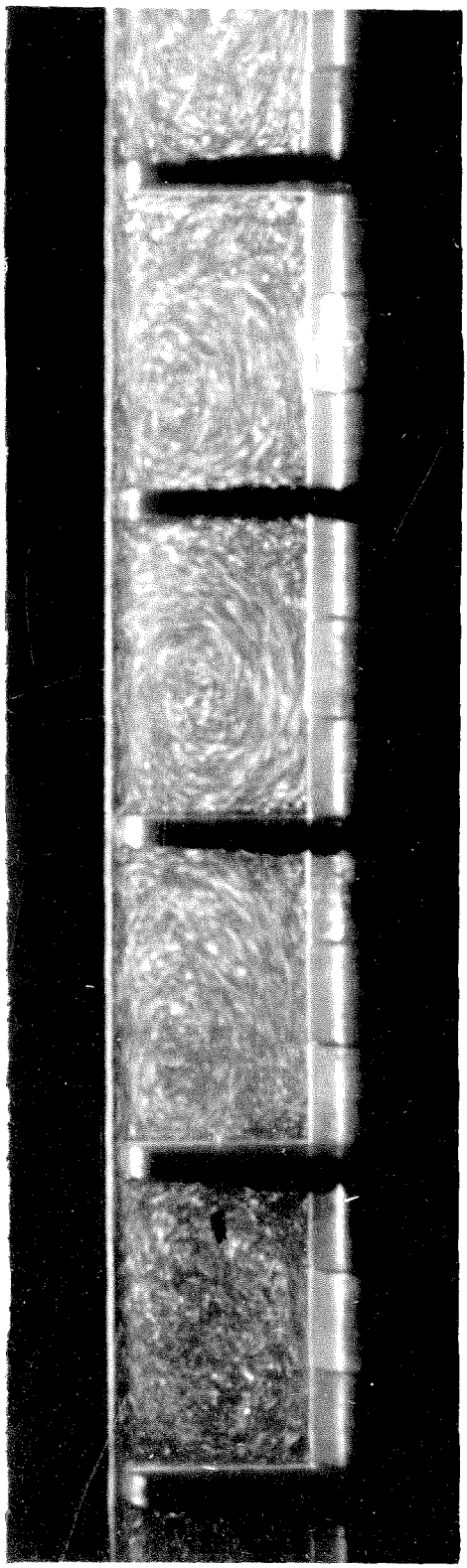

90 B

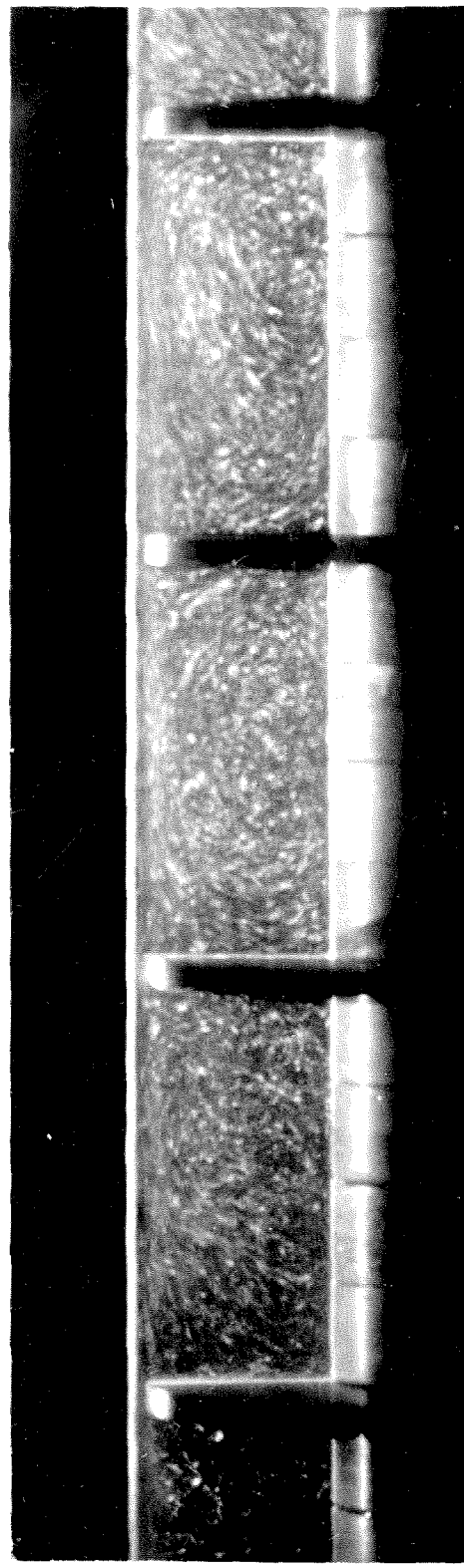

91 A

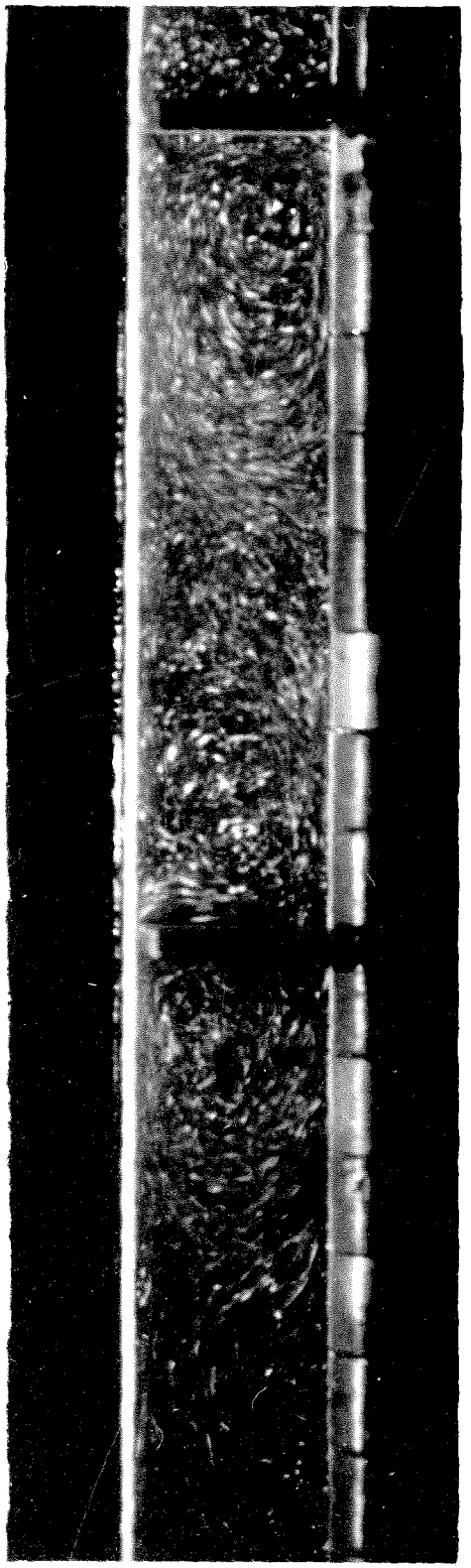

92 A

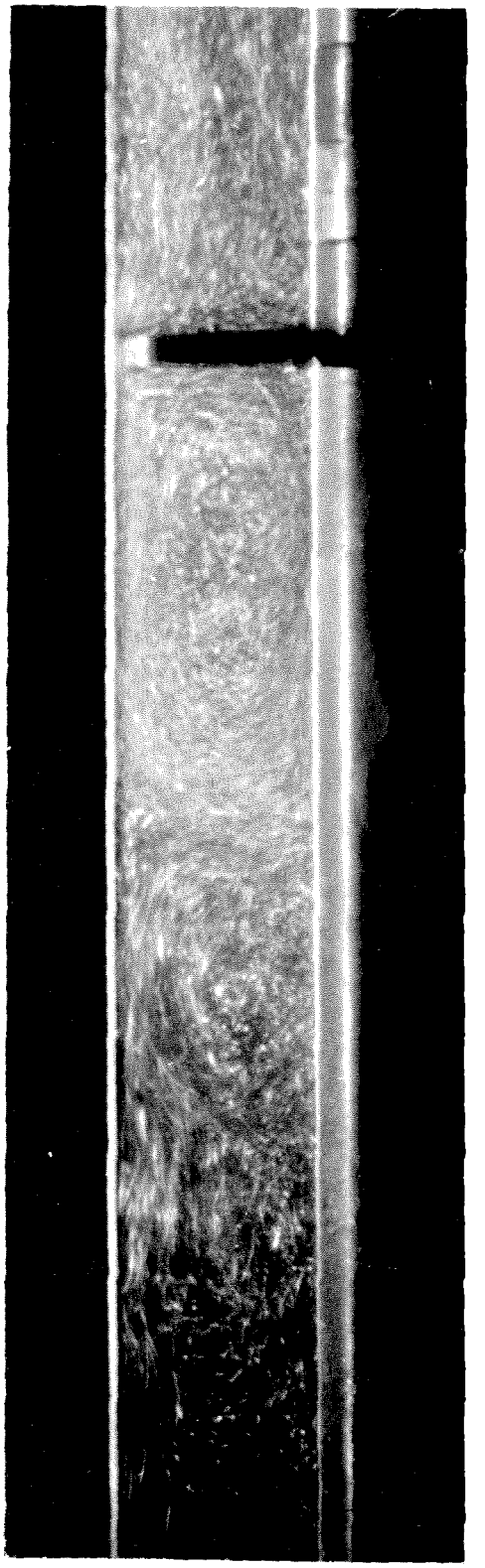

93 A

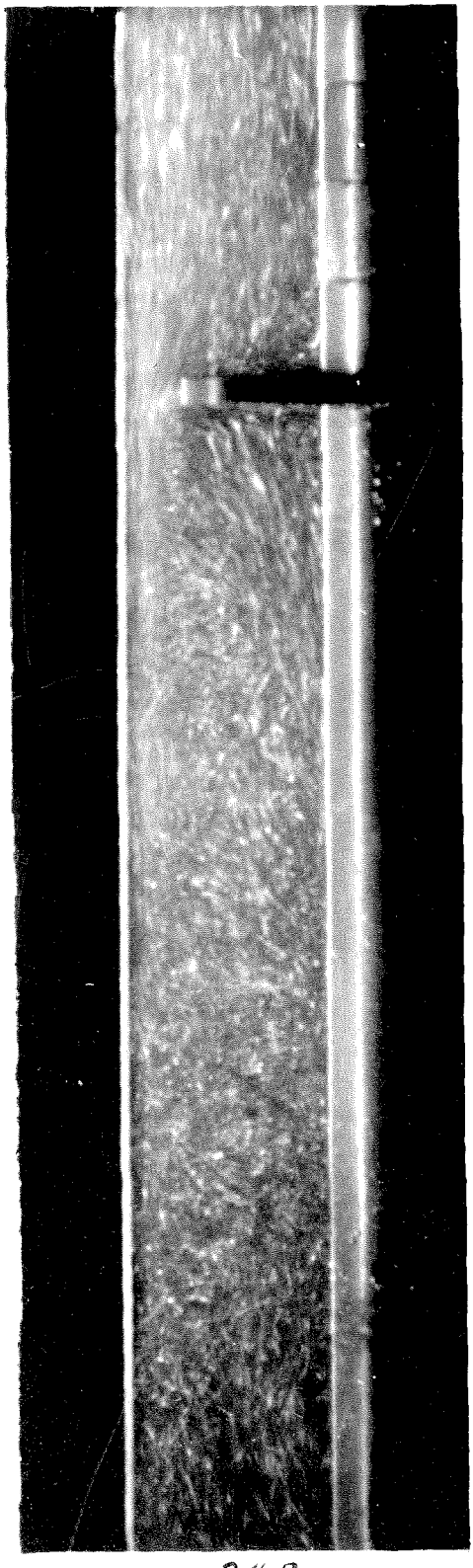

94B

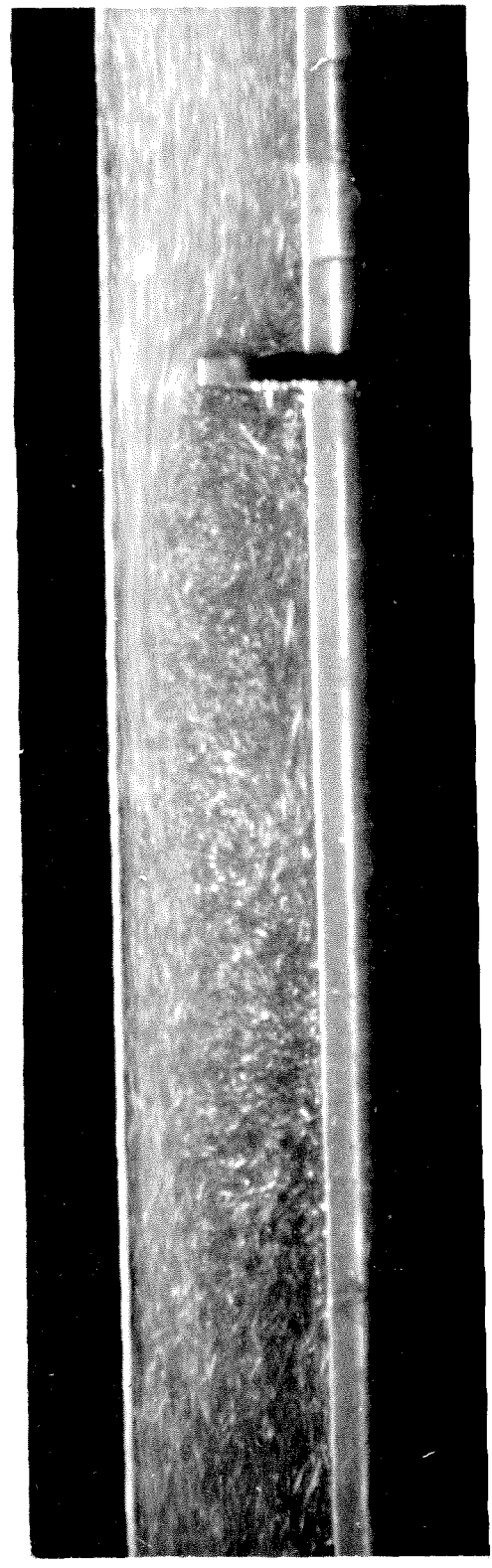

95A

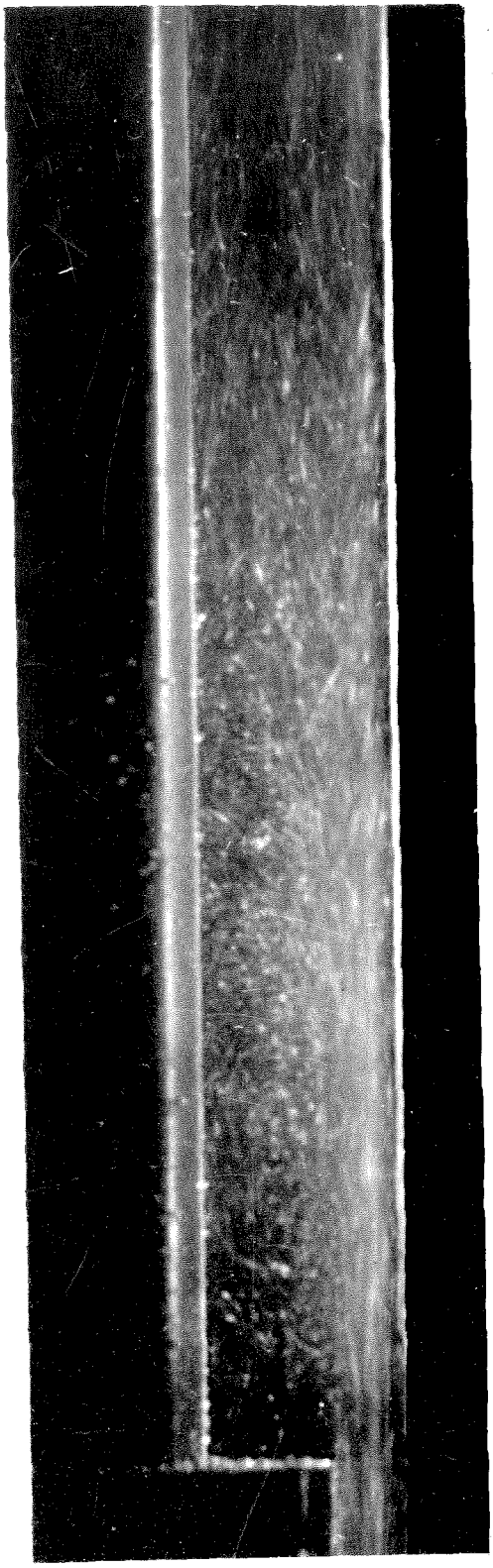

96 A

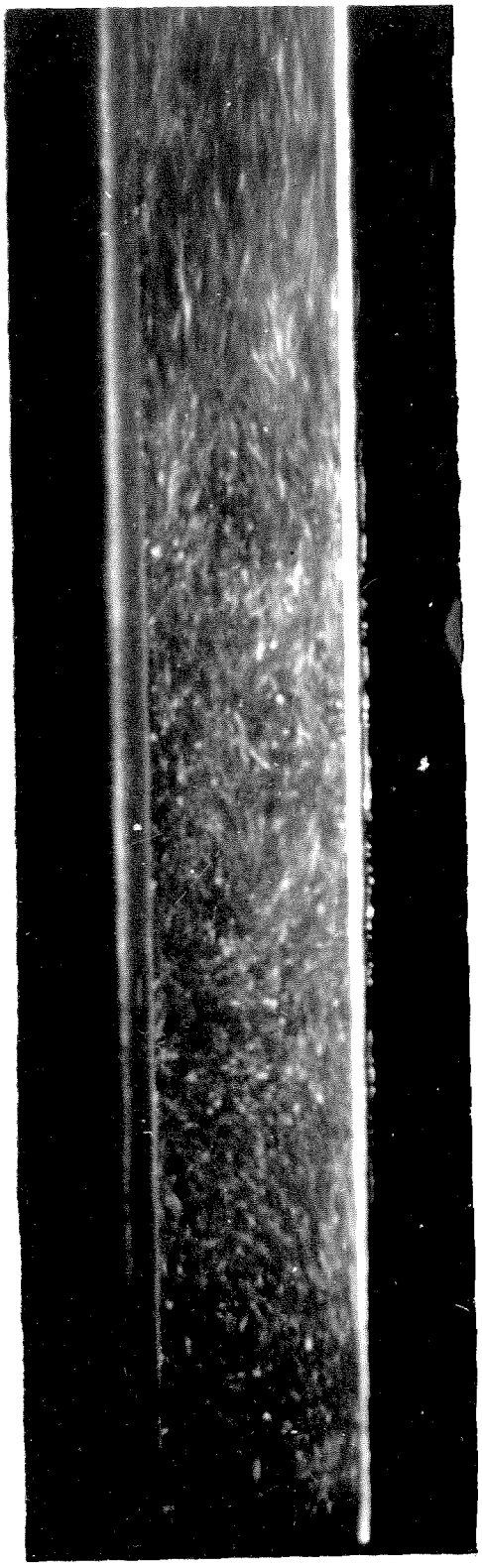

97 B

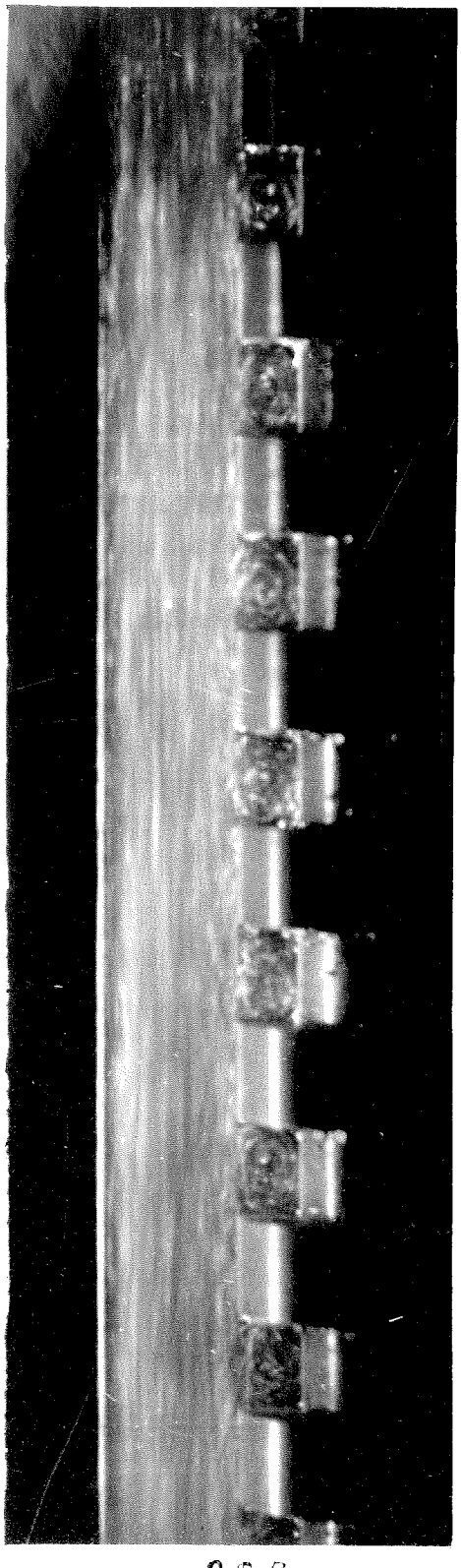

98 B

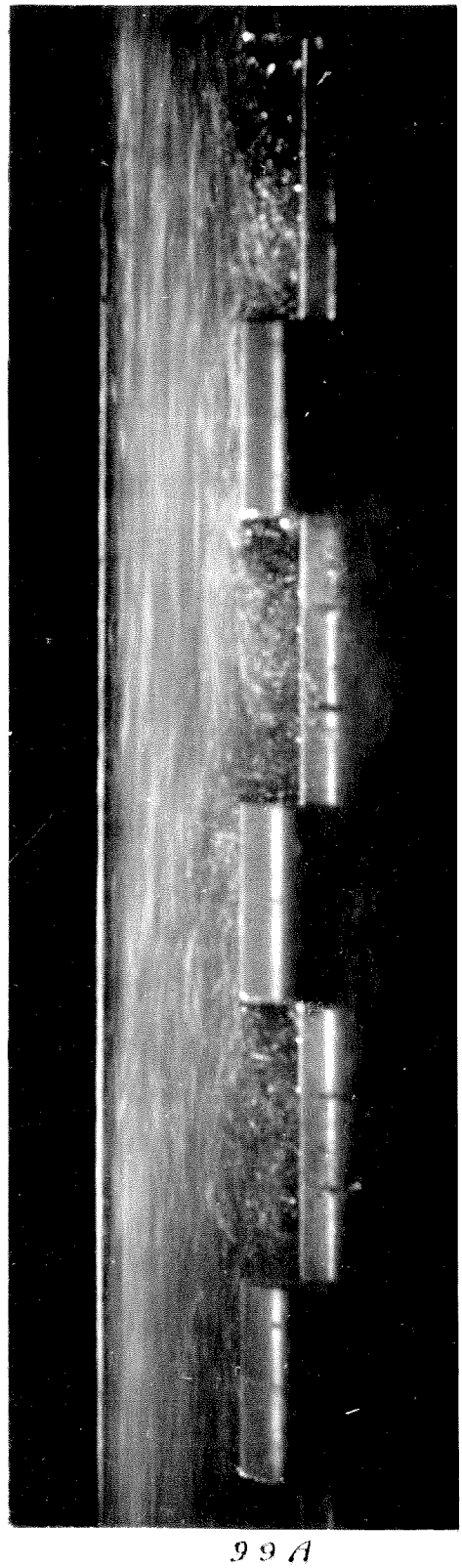

99 A

TABLE I (a)

Run Number	Disk Diameter	Spacer Diameter	Number of Spacers	Original Readings		Velocities		Total Head	Effective Length
				Flow	Head		Squared Corrected		
	inches	inches		lbs./min.	cms. of Hg.	ft./sec.	$[ft./sec]^2$	ft. of water	feet.
7-D	0.812	0.50	3	132.4	16.43	5.81	33.0	6.8	3.05
				183.8	32.52	8.07	67.4	13.4	
				262.1	66.58	11.54	134.2	27.5	
				226.8	49.54	9.96	99.3	20.4	
9-I	0.812	0.50	4	133.8	17.34	5.88	33.7	7.2	3.06
				185.2	33.88	8.14	65.8	14.0	
				226.8	51.03	9.96	99.3	21.1	
				225.2	50.20	9.88	97.7	20.7	
				274.0	74.13	12.03	145.8	30.6	
11-C	0.812	0.50	5	134.1	16.63	5.89	33.9	6.9	3.08
				184.2	31.72	8.10	65.0	13.1	
				236.7	52.24	10.40	108.5	21.5	
				282.0	74.90	12.39	155.0	30.9	
59-C	0.812	0.50	8	152.2	16.73	6.69	44.0	6.9	3.04
				219.3	35.13	9.63	92.7	14.5	
				270.5	53.54	11.89	142.5	22.1	
				307.3	69.76	13.49	184.0	28.8	
13-E	0.937	0.50	3	136.2	39.40	7.45	54.4	16.2	3.06
				191.5	79.4+	10.48	109.3	32.8	
				237.8	124.00	13.00	169.9	51.1	
15-D	0.937	0.50	4	135.2	43.19	7.40	53.6	17.8	3.06
				185.3	82.41	10.12	01.9	34.0	
				231.0	129.20	12.63	160.1	53.3	
17-J	0.937	0.50	5	141.1	47.12	7.72	58.5	19.5	3.08
				190.9	86.98	10.43	108.3	35.9	
				232.0	129.21	12.69	161.7	53.3	
18-E	0.937	0.50	6	141.6	43.97	7.74	58.7	18.1	3.03
				185.3	75.90	10.12	101.9	31.3	
				236.7	124.79	12.95	168.5	51.4	

TABLE I (b).

Run Number	Disk Diameter	Spacer Diameter	Number of Spacers	Original Readings		Velocities		Total Head	Effective Length
				Flow	Head		Squared Corrected		
	inches	inches		lbs./min.	cms. of Hg.	ft./sec.	$[ft./sec]^2$	ft. of water	feet.
57	0.937	0.50	10	154.8	40.40	8.46	70.5	16.7	3.09
				216.4	79.41	11.43	140.1	32.7	
				255.8	111.53	13.99	197.0	46.0	
49-B	1.015	0.50	3	104.2	41.15	6.74	45.4	17.0	3.06
				142.6	78.39	9.26	85.8	32.3	
				172.9	116.45	11.30	127.7	48.1	
				201.0	159.21	13.19	174.0	65.7	
				114.9	50.88	7.44	55.4	21.0	
50-B	1.015	0.50	4	109.8	48.81	7.11	50.6	20.1	3.07
				153.2	97.27	9.99	99.8	40.1	
				196.3	160.75	12.87	165.6	66.2	
51-B	1.015	0.50	5	110.6	50.72	7.15	51.1	20.9	2.99
				154.3	100.32	10.06	101.2	41.4	
				195.4	161.80	12.80	163.8	66.7	
52-C	1.015	0.50	6	83.3	27.35	5.39	29.1	11.3	2.93
				113.5	50.45	7.36	54.2	20.8	
				138.1	75.44	8.97	80.5	31.1	
				159.1	100.14	10.37	107.5	41.3	
				179.2	126.80	11.70	136.9	52.3	
				199.2	158.18	13.04	170.0	65.3	
53	1.015	0.50	7	91.8	31.14	5.92	35.1	12.8	3.02
					62.23				
				157.3	93.41	10.27	105.5	38.5	
				180.5	122.05	11.81	139.5	50.4	
				202.2	154.78	13.25	175.6	63.7	
54	1.015	0.50	8	91.3	29.12	5.90	34.8	12.0	3.04
				131.8	61.22	8.56	73.3	25.3	
				160.0	91.33	10.42	108.6	37.7	
				184.2	119.85	12.07	145.7	49.4	
				206.0	151.87	13.50	182.3	62.6	

TABLE I(c).

Run Number	Disk Diameter	Spacer Diameter	Number of Spacers	Original Readings		Velocities		Total Head	Effective Length
				Flow	Head		Squared Corrected		
	inches	inches		lbs/min.	cms. of Hg.	ft/sec.	$[ft/sec.]^2$	ft. of water	feet.
55	1.015	0.50	10	101.8	31.00	6.59	43.4	12.8	2.92
				140.6	59.05	9.15	83.7	24.4	
				172.0	88.80	11.23	126.1	36.6	
				200.8	120.70	13.18	173.7	49.8	
56-A	1.015	0.50	12	102.8	28.70	6.64	44.1	11.8	3.08
				104.2	53.90	9.13	83.4	22.2	
				169.7	79.80	11.07	122.5	32.9	
				196.1	106.15	12.84	164.9	43.8	
35-D	1.062	0.50	3	97.4	51.02	7.37	52.4	21.0	3.05
				136.2	102.87	10.31	103.9	42.4	
				172.8	167.41	13.08	169.9	69.0	
37-E	1.062	0.50	4	97.4	53.59	7.37	52.4	22.1	3.06
				131.6	101.96	9.96	96.9	42.0	
				168.2	167.82	12.73	160.3	69.1	
40-B	1.062	0.50	5	93.3	53.60	7.06	47.9	22.1	3.07
				128.5	103.52	9.73	92.3	42.7	
				163.3	168.00	12.37	151.1	69.3	
42-B	1.062	0.50	6	93.8	52.79	7.10	48.6	21.8	3.03
				130.8	103.84	9.90	95.8	42.8	
				165.9	167.54	12.55	155.7	69.1	
58	1.062	0.50	8	97.0	50.41	7.34	52.0	20.8	3.04
				135.2	98.89	10.23	102.3	40.8	
				173.0	163.00	13.10	170.1	67.2	
60	1.062	0.50	10	103.3	50.82	7.72	57.6	21.0	3.09
				143.7	99.84	10.88	116.0	41.2	
				174.1	149.19	13.19	172.6	61.5	
61	1.062	0.50	12	111.9	52.50	8.47	69.7	21.7	3.07
				152.2	98.52	11.52	130.6	40.6	
				185.3	145.93	14.02	195.8	61.6	

TABLE I(d).

Run Number	Disk Diameter	Spacer Diameter	Number of Spacers	Original Readings		Velocities		Total Head	Effective Length
				Flow	Head		Squared Corrected		
	inches	inches		lbs/min.	cms. of Hg.	ft/sec.	$[ft/sec.]^2$	ft. of water	feet.
62	1.062	0.50	14	117.6	52.70	8.90	77.1	21.7	3.10
				160.0	98.61	12.11	144.7	40.7	
				189.7	138.14	14.36		57.0	
73	1.249	0.50	1	25.8	61.31	5.83	34.0	25.3	
				38.0	120.91	8.59	73.8	49.8	
				46.3	172.20	10.45	109.2	70.9	
67	1.249	0.50	2	25.0	54.59	5.50	30.3	22.5	
				35.4	102.26	7.84	61.4	42.2	
				41.8	138.74	9.28	86.1	57.1	
				46.7	171.23	10.37	107.5	70.5	
68	1.249	0.50	3	25.4	56.64	5.61	31.4	23.3	3.06
				35.6	106.35	7.88	62.0	43.8	
				40.1	137.00	8.90	79.2	56.4	
				44.6	169.09	9.90	98.0	69.7	
69	1.249	0.50	4	26.6	56.71	5.84	34.1	23.4	3.06
				36.4	103.19	8.06	64.9	42.5	
				42.5	140.42	9.43	88.9	57.8	
				46.7	170.24	10.37	107.5	70.1	
72	1.249	0.50	8	25.3	51.09	5.72	32.7	21.1	3.04
				37.5	105.12	8.48	71.9	43.3	
				43.6	138.71	9.86	97.2	57.1	
				47.9	170.37	10.87	118.2	70.2	
B-19-B	0.937	0.75	2	114.6	19.45	6.27	39.3	8.0	3.06
				165.2	40.94	9.04	81.7	16.9	
				199.4	59.87	10.91	119.0	24.7	
				231.2	80.62	12.65	160.0	33.2	
				252.8	101.00	13.83	191.3	41.7	
B-13-B	0.937	0.75	3	137.0	31.81	7.50	55.1	13.1	3.05
				189.3	61.31	10.37	107.1	23.2	
				242.2	100.37	13.25	176.6	41.4	

TABLE I (e).

Run Number	Disk Diameter	Spacer Diameter	Number of Spacers	Original Readings		Velocities		Total Head	Effective Length
				Flow	Head		Squared Corrected		
	inches	inches		lbs./min.	cms. of Hg.	ft./sec.	[ft./sec.]^2	ft. of water	feet.
B-15-B	0.937	0.75	4	141.8	31.62	7.75	58.9	13.0	3.08
				191.9	58.74	10.49	109.8	24.2	
				251.0	100.42	13.68	188.5	41.4	
B-24	0.937	0.75	8	156.2	26.28	8.55	72.0	10.8	2.98
				220.2	52.73	12.04	145.3	21.8	
				269.5	79.30	14.74		32.7	
B-49-B	1.015	0.75	3	108.9	43.88	7.05	49.7	18.1	3.06
				153.4	89.28	10.00	100.0	36.8	
				193.9	143.15	12.70	161.3	59.0	
B-50-B	1.015	0.75	4	107.8	44.19	6.98	48.7	18.2	3.08
				154.4	92.14	10.07	101.4	38.0	
				192.2	143.46	12.59	158.5	59.2	
B-51-B	1.015	0.75	5	114.7	44.70	7.42	55.1	18.4	3.02
				161.8	90.34	10.55	111.3	37.2	
				199.3	137.50	13.06	170.6	56.7	
B-53-B	1.015	0.75	7	125.7	44.30	8.15	66.4	18.3	2.98
				177.6	89.79	11.60	134.6	37.0	
				212.5	129.35	13.93	194.0	53.4	
B-35-C	1.062	0.75	3	93.8	51.69	7.10	48.5	21.3	3.07
				128.2	99.31	9.71	92.1	40.9	
				157.9	152.00	11.95	140.7	62.7	
B-37-B	1.062	0.75	4	91.5	52.23	6.93	46.3	21.6	3.08
				125.2	101.38	9.48	87.5	41.8	
				158.0	162.55	11.97	141.2	67.0	
B-40-B	1.062	0.75	5	92.8	49.76	7.03	47.6	20.5	3.02
				131.8	101.40	9.97	97.1	41.8	
				166.1	161.98	12.58	156.7	66.6	
B-58	1.062	0.75	8	108.4	51.45	8.21	65.4	21.2	2.98
				146.3	95.10	11.09	120.6	39.2	
				182.6	148.59	13.82	190.0	61.2	

TABLE I (f).

Run Number	Disk Diameter	Spacer Diameter	Number of Spacers	Original Readings		Velocities		Total Head	Effective Length
				Flow	Head		Squared Corrected		
	inches	inches		lbs./min.	cms. of Hg.	ft./sec.	[ft./sec.]^2	ft. of water	feet.
B-67	1.249	0.75	2		170.28				3.05
					115.62				
B-68	1.249	0.75	3	24.0	58.96	5.43	29.4	24.3	3.05
				31.0	94.21	6.96	48.4	38.8	
				37.7	138.32	8.41	70.7	56.9	
				41.9	172.92	9.35	87.4	71.1	
B-69	1.249	0.75	4	24.6	56.33	5.47	29.9	23.2	3.08
				33.3	102.85	7.42	55.0	42.4	
				43.8	174.03	9.70	94.1	71.7	
				28.6	74.32	6.35	40.3	30.6	
				37.2	125.50	8.21	67.4	51.7	
				41.3	154.90	9.14	83.4	63.8	
B-70	1.249	0.75	5	25.2	56.30	5.65	31.9	23.2	3.02
				34.2	100.31	7.64	58.4	41.3	
				39.6	134.19	8.77	76.9	55.3	
				44.5	171.31	9.88	97.6	70.5	
B-71	1.249	0.75	6	24.4	54.22	5.47	29.9	22.4	3.08
				33.9	98.87	7.57	57.3	40.7	
				40.3	138.92	9.00	81.0	57.1	
				45.1	172.18	10.00	100.0	70.9	
B-72	1.249	0.75	8	28.4	58.10	6.33	40.1	24.0	2.98
				38.0	100.58	8.48	71.9	41.4	
				44.9	138.26	9.94	98.8	56.9	
				50.4	172.18	11.19	125.2	70.9	

Upper Limit of First Type			Lower Limit of Second Type		
				Spacers	
Disk	Picture	Spacers	Picture	Number	Size
15/16"	73 A	3	36 A	4	1/2"
65/84"	72 B	4	76 A	5	1/2"
17/16"	52 A	4	53 B	5	1/2"
17/16"	60 B	3	61 A	4	3/4"

Table II. Limits of Characteristic Flow Types.